THE

LONDON, EDINBURGH, AND DUBLIN

PHILOSOPHICAL MAGAZINE

AND

JOURNAL OF SCIENCE.

[SEVENTH SERIES.]

DECEMBER 1934.

XCVII. *A Study of an Electrically-maintained Vibrating Reed and its Application to the Determination of Young's Modulus.*—Part II. *Experimental.*

By E. G. JAMES, *B.Sc., Ph.D., and* R. M. DAVIES, *M.Sc., F.Inst.P., University College of Wales, Aberystwyth* *.

CONTENTS.

I. INTRODUCTION.

IN the first part of this work it has been shown how to determine from electrical measurements and from measurements of amplitude, the apparent resonant pulsatance ω_r of a reed fixed at one end and set in forced, transverse vibration by the action of superposed steady and alternating magnetic fields on a small piece of stalloy

* Communicated by Professor Gwilym Owen, M.A., D.Sc.

fixed at the free end of the reed. It has also been shown that this apparent resonant pulsatance ω_r differs in general from the true resonant pulsatance ω_0, and that ω_0 can be determined by suitable extrapolation of ω_r. ω_0 is a known function of the dimensions, the density and the Young's Modulus of the reed, and the mass of the stalloy attachment (*v.* below, section V.); ω_0 can be determined as described above, and, since all the quantities on which ω_0 depends can be determined directly with the exception of Young's Modulus, it follows that an experiment of this type can be used for the determination of Young's Modulus.

For convenience and accuracy such an experiment is best performed with reeds or bars which have resonant frequencies in the frequency range commonly employed with a.c. bridges, using a telephone as detector; taking this frequency range as extending approximately from 500 to 1000 cycles per sec., and assuming a reasonable value for the mass of the stalloy attachment, it is easily calculated that a resonant frequency within this range will be obtained for the majority of substances by using a comparatively short bar with a length of the order of 2 to 3 cm., breadth of the order of $\frac{1}{2}$ cm., and thickness of the order of 0·1 cm. These figures show that the suggested method will be of particular utility in connexion with materials such as crystals, which are usually available only in the form of short bars.

In order to explore the possibilities of the method, and in order to check the main features of the theory given in the first part of the paper, it was decided to carry out a series of experiments with a phosphor-bronze bar, and the results obtained show that the method is capable of exceedingly good accuracy.

II. Experimental Arrangements.

(a) *The Vibrating Bar and its Driving Arrangement.*

This part of the apparatus is shown in plan in fig. 1 (*a*) and in section in fig. 1 (*b*).

In this figure A represents the phosphor-bronze bar, to the upper end of which is soldered a small square piece *c* of thin sheet-stalloy of the same width as the bar. B represents a steel block, of 1″ square section and $2\frac{1}{2}$″ long, with two adjacent faces, L and M, carefully ground

flat and perpendicular to one another. B′ represents a strip of steel, 1″ long, 7/16″ wide, and 3/16″ thick, which is also ground flat on two perpendicular faces. The bar A is clamped at its lower end between the ground faces of the block B and the strip B′, the strip

Fig. 1.

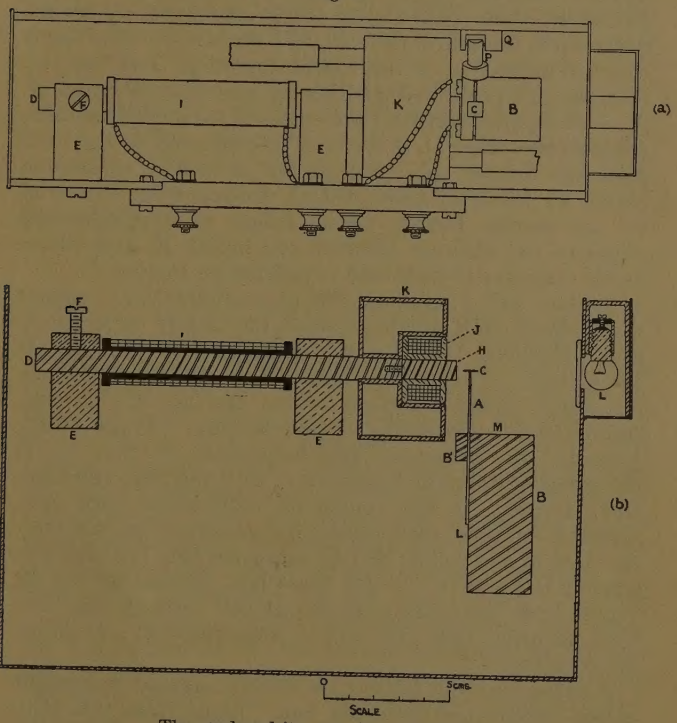

The reed and its associated apparatus.

being held in position by means of two screws passing into B on each side of the bar. The bar is carefully adjusted so that it is perpendicular to the upper face of B. This arrangement ensures that the lower end of the bar A is firmly clamped—a condition which must be complied with in work of this description. The steel block B is screwed in a vertical position to the inside

of a thick-walled brass box, in the side of which slots have been cut so that the block B can be moved vertically. This brass box is suspended rigidly in a water thermostat, the temperature of which is kept constant at 25° C. by means of a toluene regulator.

D represents a mild steel bar of circular cross-section and 3/8″ diameter, which is held horizontally by two brass blocks E, these two blocks being also fixed by means of screws to the side of the enclosing brass box. The bar D can be moved in a horizontal direction, and can be clamped in any desired position by means of the screw F. A small circular soft-iron pole-piece H, of slightly smaller cross-section than D, is screwed into the end of the mild steel bar nearest the reed. A coil of wire, I, containing about 30 turns of thick D.C.C. copper wire, is wound on an ebonite former whose length is approximately equal to the distance between the blocks E, and whose inside diameter is such that it just fits on the bar D.

Another coil, J, of about 300 turns of fine D.S.C. copper wire, wound on a wooden former, fits tightly on the soft-iron pole-piece H. The d.c. resistance of this coil is 128·4 ohms. This coil is connected in one arm of the a.c. resistance bridge described below, and the a.c. flowing through it sets the reed in forced vibration. As previously indicated the resistance and inductance of this coil is measured at different frequencies, with the reed vibrating and damped. In the course of preliminary work considerable trouble was caused by variation in the temperature of the coil J, and to overcome this the coil was surrounded with a circular brass box represented by K. Water from the thermostat is pumped through this box, thus ensuring that the coil is maintained at a constant temperature.

A small four-volt bulb, L, is fixed in a small watertight recess outside the enclosing box. Light from this bulb passes through a small glass window in the side of the box, and is reflected by the edge of the stalloy attachment C. A microscope fitted with a 12-mm. objective is rigidly clamped to a stone slab table, so that the microscope is vertically above the vibrating bar. When the microscope is focussed on the stalloy attachment the bright edge appears as a line when the bar is stationary and as a band of light when the reed is vibrating. The amplitude of vibration can be evaluated by measuring

the width of this band in a calibrated scale in the microscope eyepiece. Care must be taken that the position of the microscope relative to the coil is always the same, since change in the position of the microscope will alter the electrical constants of the coil J.

The motion of the reed can be damped when required by means of the arrangement shown at P and Q in fig. 1 (*a*). A short ebonite rod, P, fitted at one end with a small length of rubber tubing, is hinged in a recess in a block of ebonite, Q, which is stuck to the side of the box. When the rod is lifted by means of a piece of string, the rubber presses lightly against the side of the bar A, and thus stops the vibration. It does this without changing the equilibrium position of the bar, which is, of course, necessary in finding the impedance when the bar is damped.

(b) *The a.c. Generator.*

The a.c. required for these experiments is produced by a valve oscillator, followed by a tuned anode amplifier.

In the course of the experiments, the output from the generator is fed into two a.c. bridges—the bridge described below for the measurement of the impedance of the coil J and the frequency bridge. These two bridges naturally impose different loads on the generator, and in order that the frequency measured by the frequency bridge should agree with that used in the impedance bridge, it is clearly essential that the frequency of the generator output should remain constant between the load limits represented by the two bridges. At first a simple valve oscillator without amplifier was used, but it soon became evident that such a generator did not give the necessary constancy of frequency ; this oscillator was then fitted with a tuned-anode amplifier, and exhaustive tests with a variable artificial load showed that the frequency remained constant within load limits which were wider than those used in the experiments.

It is essential also that the output from the generator should be reasonably free from harmonics, partly because of the disturbing effects of such harmonics on the reed and partly because of the difficulty of balancing the frequency bridge with an impure source. On this account a tuned anode arrangement was chosen for the amplifier,

because of its natural filtering action as regards harmonics ; iron was also excluded from all circuits carrying a.c. These precautions resulted in an output which gave almost perfect silence in the frequency bridge detector at balance ; this showed that the output was practically free from harmonics.

The details of the oscillator are shown in fig. 2.

The oscillator valve V_1 is an Osram H.L. 610 valve. The oscillatory circuit consists of an inductance A and a variable capacitance C_1. The inductance A consists of two coils in series, each coil being of $3\frac{1}{2}$″ inside diameter, and winding section 1″ deep and $1\frac{1}{2}$″ wide, wound with 1500 turns of No. 28 D.C.C. copper wire. The capacitance C_1 consists of a number of mica condensers, giving a

Fig. 2.

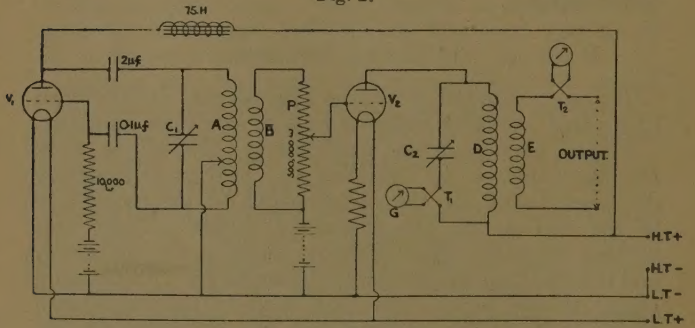

The valve-oscillator circuit.

variation of capacitance from 0 to 0·1 μF. in steps of 0·001 μF., together with a variable air condenser of maximum capacitance 0·001 μF. connected in parallel. One end of the inductance is connected to the anode of the valve V_1 through a 2 μF. condenser, while the other end is connected to the grid by a 0·1 μF. mica condenser. The H.T. supply is provided by a battery of accumulators, the positive pole of which is connected to the anode through a 75 henry choke H. The centre point of A is connected to the negative H.T. lead, so that the arrangement functions as an auto-transformer.

A wire-wound resistance of 10,000 ohms is connected in series with a $1\frac{1}{2}$ volt battery, which supplies the necessary negative grid-bias to this valve.

The coil B, also of 1500 turns, is coupled magnetically to the coil A, while a potentiometer P of 500,000 ohms resistance is connected across its extremities. The movable contact of this potentiometer is connected to the grid of the amplifying valve V_2—a Marconi L.S. 5 valve. As the filament voltage of this valve is $4\frac{1}{2}$ volts a fixed resistance is placed in one of the L.T. leads so as to reduce the filament voltage to this amount.

Another tuned circuit, consisting of an inductance D and a capacitance C_2 is placed in the anode lead of the valve V_2. The inductance D consists of two coils of copper wire similar to A, while the capacitance C_2 consists similarly of a number of mica condensers. A vacuo thermo-junction T_1 of 4 ohms heater resistance is connected in the capacitance branch of the circuit C_2D; the current through this vacuo thermo-junction will clearly be the a.c. flowing in C_2D, and it may be measured by means of a Tinsley Portable Galvanometer connected across the " couple " terminals of T_1.

The frequency of the oscillator can be altered by varying the capacitance C_1, and the circuit C_2D can be tuned to the oscillator frequency by varying the capacitance C_2, resonance being shown by maximum current in the galvanometer connected to vacuo thermo-junction T_1.

Power is taken from the generator to the bridges by means of the coil E, of about 1500 turns of copper wire, which is coupled magnetically to the coil D, and in order to avoid undesirable coupling, the coils D and E are enclosed in an earthed, thick-walled copper box.

Another vacuo thermo-junction T_2, of heater resistance 3 ohms, is connected in one of the output leads from the coil E, and serves to measure the output current from the generator. The galvanometer used with this vacuo thermo-junction is the one used with T_1, a double-pole double-throw switch being used to connect the galvanometer to the appropriate vacuo thermo-junction.

The output current is best varied by altering the position of the movable contact on the potentiometer P. This increases or diminishes the alternating p.d. on the grid of the valve V_2 without altering the load on V_1, and it therefore allows the output current to be altered without variation in the frequency of the oscillator.

(c) *The Bridge for measuring the Resistance and Inductance of the Coil J.*

The bridge used for measuring the resistance and inductance of the coil is the Rayleigh bridge, and is shown diagrammatically in fig. 3.

Two equal non-inductive calibrated resistances, P and Q, form two ratio arms, AD and DC, of the bridge ABCD. The third arm, BC, contains a variable inductance, L, whose resistance is S. A variable calibrated non-inductive resistance, R_1, is connected in series with the coil J of fig. 1, making the fourth arm, AB, of the bridge. B and D are connected to the output terminals

Fig. 3.

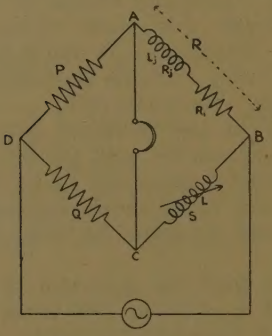

The Rayleigh bridge.

of the oscillator, while the detector is connected between A and C.

If R_j and L_j are the resistance and inductance respectively of the coil J, and S and L the resistance and inductance respectively of the variable inductor,

then if $P=Q$,

at balance

$$R_j+R_1=S \quad \text{or} \quad R_j=S-R_1,$$

and $L_j=L$.

The resistance of the variable inductor is about 600 ohms, and for maximum sensitivity P and Q should be of about the same magnitude. The values actually used were $P=Q=300$ ohms.

The detector used is a pair of headphones of 100 ohms resistance, one of the phones being short-circuited.

In order to obtain very fine adjustment of the resistance R_1 a manganin slide wire resistance is connected in series with the resistance box. This resistance is shown in plan in fig. 4 (*a*), in elevation in fig. 4 (*b*), and a section through the slider is shown in fig. 4 (*c*).

A wooden scale, A, 40 cm. in length, is screwed to a wooden base, BB′. Two strips of ebonite, C, 1/16″ thick,

Fig. 4.

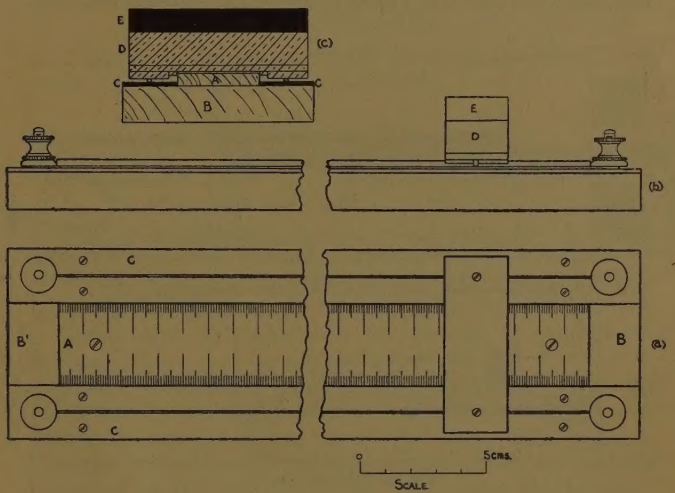

The variable resistance.

7/8″ wide, are screwed to the base on each side of the scale A. Two manganin No. 20 S.W.G. wires are stretched between two pairs of terminals, so that they rest on the ebonite strips. The two wires are connected at B′ by a piece of copper wire. The slider consists of two brass knife edges, soldered to a brass plate, 1″ wide, 0·1″ thick, and 2·7″ long; two rectangular strips of brass, 1″ long, 1/8″ wide, and 1/16″ thick, form the knife edges, and they are soldered to the plate, the distance between their inner edges being equal to the width of the scale. These strips act as guides to the slider

and prevent side play. The slider is weighted by means of a brass block D, $\frac{1}{2}''$ thick, while a block of ebonite, E, $\frac{3}{8}''$ thick, is screwed to the top of the brass block and acts as an insulating handle by means of which the slider is moved. The manganin wires are lubricated by means of liquid paraffin, so that when the slider is moved no crackling noises are heard in the telephone. The total variation of resistance given by the slider is 1·5 ohm.

The variable inductance is shown in fig. 5. It consists of a large fixed coil, A, and a small movable coil, B. The former of the coil A is a fibre cylinder $1\frac{3}{4}''$ outside diameter

Fig. 5.

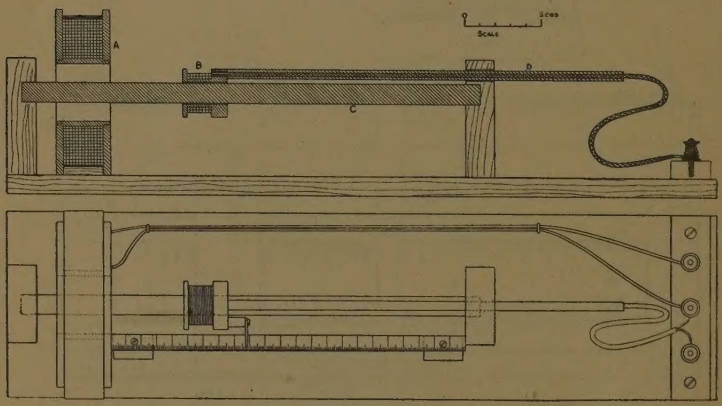

The variable inductor.

and $\frac{1}{8}''$ thick, with ebonite cheeks 3/16″ thick screwed on to it, the width of the winding space being 1″. The coil is fixed with its axis horizontally in a wooden block which is cut in the form of a semicircle, and a press-pahn strap holds the coil rigidly in this semicircular support. An ebonite rod, C, of circular cross-section and $\frac{1}{2}''$ diameter, passes through the centre of the coil and is fixed in two rectangular wooden supports. The small coil B just fits on the ebonite rod, and can be slid along the rod by means of a small ebonite tube, D, through which the leads pass. This ensures that the coupling between the large coil and the leads of the small coil does not vary when the small coil is moved. The terminals are fixed

at one end of the wooden base, so as to be as far away as possible from the coils. A wooden scale is fixed parallel to the ebonite rod C, and a pointer fixed to the movable coil B serves to indicate the position of the coil on the scale.

The two coils are connected in series, so that if

L_1=the inductance of the coil A,

L_2=the inductance of the coil B,

M=the mutual inductance between the coils.

Then the effective self-inductance of the inductor is

$$L=L_1+L_2\pm 2M,$$

and therefore, by reversing the leads of the coil B, the inductance can be made to vary from

$$L_1+L_2+2M \quad \text{to} \quad L_1+L_2-2M.$$

The total inductance (L_1+L_2) is arranged to be approximately equal to the inductance of the coil J of fig. 1 and so that the total variation covers the total change in inductance of the coil J near the resonant frequency of the vibrating bar. This is arranged by an initial approximate determination of the inductance by means of Anderson's bridge. The variable inductor is then carefully calibrated by means of Anderson's bridge.

During preliminary experiments, this variable inductor was wound with copper wire, and a drift in the measured damped resistance of the coil J was found to take place. This was traced to change in the resistance of the variable inductor, brought about by variation of room temperature. The inductor was therefore rewound with manganin wire.

In its present construction the fixed coil A consists of 1120 turns of No. 28 manganin wire, and the movable coil B of 432 turns of No. 28 manganin wire. The total resistance of the inductor is 601·31 ohms, and it gives a variation of inductance from 61·20 to 72·31 millihenries.

(d) *The Frequency Bridge.*

The frequency of the alternating current is measured by means of the frequency bridge described elsewhere by one of the authors (' Journal of Scientific Instruments,' vol. x. p. 274 (1933)).

Using the notation of this paper, the values of the various components of the bridge were as follows :—

$$K=0{\cdot}3337_8\ \mu F.\ ;\ M=10{\cdot}00_0\ mH.$$

$$R=100{\cdot}0_7\ \text{ohms}.$$

$$Q=299{\cdot}8_0\ \text{ohms}.$$

whence ω, the pulsatance at balance, is given by

$$\omega^2=\frac{1}{MK}\cdot\frac{S}{(Q+R+S)},$$

$$\omega^2=\frac{1}{10^{-2}\times 0{\cdot}3337_8\,.\,10^{-6}}\cdot\frac{S}{(399{\cdot}8_7+S)}. \quad . \quad (1a)$$

III. Description of the Method.

In order to investigate the apparent resonance pulsatance of the vibrating bar, measurements are taken of the amplitude of vibration of the bar and the resistance and inductance of the driving current coil J of fig. 1 at different pulsatances near the resonant pulsatance of the bar. The amplitude of vibration, the resistance, and the inductance of the coil J are then plotted against the pulsatance so that resonance curves are obtained.

Referring to fig. 1, the vibrating bar A is adjusted to a convenient length and the mild steel bar D arranged so that the distance between the pole-piece and the stalloy attachment is fairly small. Current from a two-volt battery is passed through the coil I, thus magnetizing the bar D ; the current is first of all arranged to be about 1·4 amps., and the bar is brought to its cyclic state by reversing the current several times by means of a reversing key.

Current from the a.c. generator is then passed through the Rayleigh bridge, of which the coil J constitutes one arm. The bridge is first of all approximately balanced ; the current through the bridge is then adjusted to a definite value, and the bridge is then accurately balanced. Observations are then taken of the resistance R_1 and the inductance L of J and the amplitude of vibration, ξ_m, of the bar.

The current from the generator is then switched by means of a double-pole double-throw switch from the Rayleigh bridge to the frequency bridge. A resistance is placed in series with this bridge, so that the load is

approximately equal to that of the Rayleigh bridge. The frequency bridge is then balanced, and the bridge used has the useful property of being a single adjustment bridge.

The frequency of the alternating current is then slightly altered and the above observations repeated.

Fig. 6(*a*).

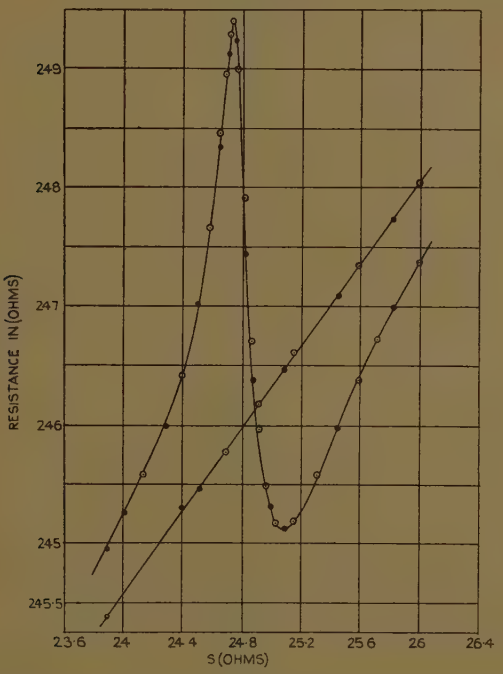

Graph of "damped" and "free" resistance against balancing resistance, S, of frequency bridge.

Readings are taken as the frequency of the alternating current is varied from a value below the resonant frequency of the bar to a value above the resonant frequency, and the whole set of observations are repeated as the frequency of the alternating current is decreased again to the original value.

It is important to secure a sufficient number of measurements in the region where R_m, L_m and the amplitude of vibration vary rapidly; for this purpose very small changes are made in the frequency near resonance, and the observations of resistance, inductance, and amplitude of vibration are plotted against S of equation (1 *a*) on squared paper as the series of observations is carried out. In this way it is ensured that the maximum and minimum values are not missed.

Fig. 6 (*b*).

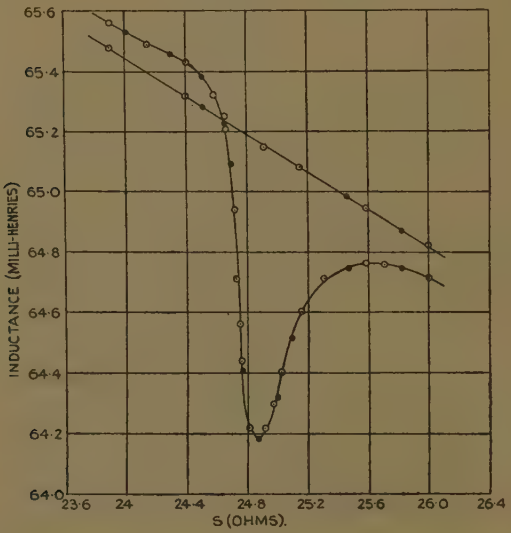

Graph of "damped" and "free" inductance against balancing resistance, S, of frequency bridge.

After every third or fourth observation the reed is damped as described above, and the damped resistance and inductance of the coil are measured.

A typical set of observations of resistance and inductance is shown in fig. 6. For this curve the steady magnetizing current was 1·43 amp., the alternating current 9 m.a. and the distance between pole-piece and stalloy attachment 0·165 mm. Fig. 6 (*a*) shows the "free" and "damped" resistance plotted against S—the balancing

resistance of the frequency bridge, whilst in fig. 6 (*b*) the "free" and "damped" inductance are plotted against S. Fig. 6 (*c*) shows the variation of the reactance ($L\omega$) with S; it has been obtained from curve (*b*) by multiplying each point on the curve by its corresponding pulsatance. This curve shows a variation of S from

Fig. 6 (*c*).

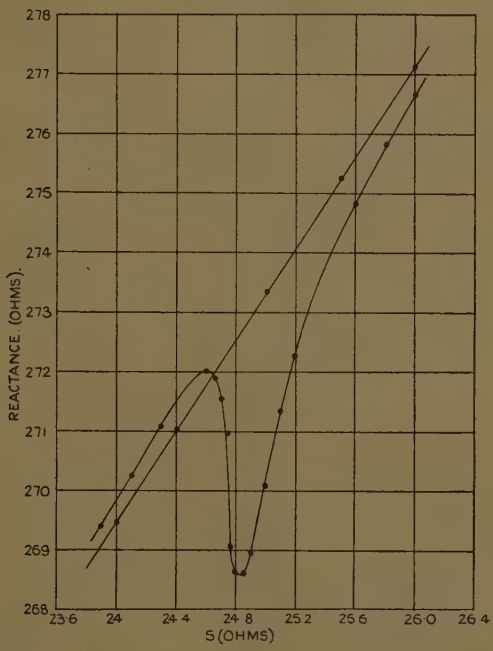

Graph of "damped" and "free" reactance against balancing resistance, S, of frequency bridge.

24 ohms to 26 ohms; this corresponds to a variation in the pulsatance from 4100 to 4275. It is seen that the damped resistance increases as the frequency increases, and the damped inductance decreases as the frequency increases; both the damped resistance and inductance are linear within the range of frequency taken.

Fig. 7 (*a* and *b*) shows the corresponding "motional" resistance and "motional" reactance plotted against the pulsatance ω. The general features of these curves are seen to agree with the theoretical curves of fig. 4 in the theoretical part of this work.

Fig. 7.

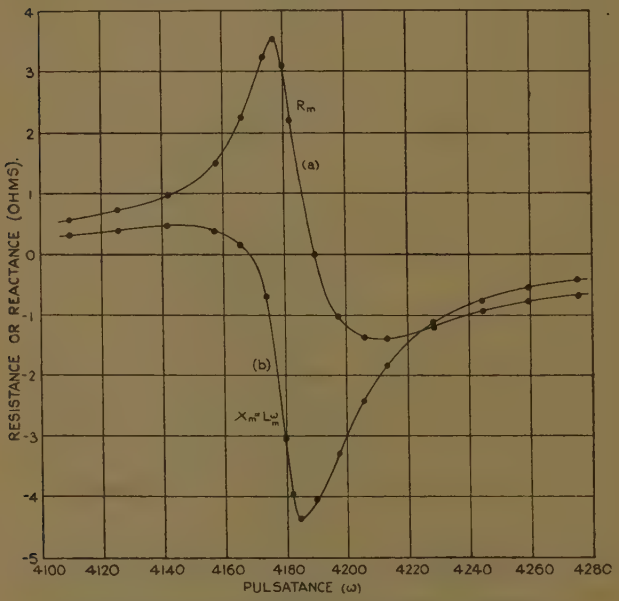

(*a*) Graph of motional resistance R_m against pulsatance ω.
(*b*) Graph of motional reactance X_m against pulsatance ω.

Accuracy of the Observations.

Fine adjustment of the resistance R_1 of the Rayleigh bridge is made by means of the manganin slide wire resistance shown in fig. 5. The total variation of resistance given by this slider is 1·5 ohm. When the bridge is balanced, a movement of the slider of $\frac{1}{2}$ cm. on each side of the balance point gives an appreciable increase in the intensity of sound in the telephone. A movement of 1 cm. on the slider corresponds to a variation in resistance of 0·04 ohm, and therefore the error in balancing the bridge for resistance is certainly less than 0·04 ohm.

The variable inductor, on the steepest part of the calibration curve, can be adjusted at balance, so that a movement of the pointer of 0·1 mm. on each side of the balance point gives an appreciable increase in the intensity of sound in the telephone. A movement of 1 mm. of the pointer corresponds to a variation of inductance (on the steepest part of the curve) of 0·14 millihenry; so that the error in measuring the inductance is about 0·014 millihenry, and is certainly less than 0·02 millihenry. When the gradient of the calibration curve is smaller the order of accuracy is better than this, since the error due to error in reading the position of the pointer is less.

In balancing the frequency bridge the slider of the manganin slide-wire resistance in series with S can be adjusted so that a movement of 1 mm. on each side of the balance point gives appreciable increase in the intensity of sound in the telephone. A movement of 2 mm. corresponds to a change of resistance of 0·008 ohm, and hence, when S=25 ohms, this corresponds to a variation in pulsatance of 1 in 6000. The value of the various resistances, however, are not known to better than 1 in 1000, and the actual frequency cannot therefore be determined to a greater accuracy than this.

The amplitude of vibration of the reed is measured by means of a calibrated scale in the microscope eyepiece. 1 division on this scale corresponds to 0·0106 mm. The amplitude can be evaluated to 0·1 of a scale division, so that the accuracy of measurements is 0·001 mm.

The distance d between the edge of the stalloy attachment and the pole-piece was measured by means of a microscope, using a $1\frac{1}{4}''$ objective. The pole-piece and edge of the stalloy attachment were illuminated by a lamp, and the distance evaluated by means of a calibrated scale in the microscope eyepiece.

In the measurements of the variation of the resistance and inductance with the frequency, what we are concerned with mostly is the variation of the motional resistance and inductance, *i. e.*, the difference between the "free" and "damped" resistance and inductance. As the steady magnetizing and driving currents are decreased and the distance between reed and pole-piece increased, the motional resistance and inductance decrease, and a limit to their measurement is reached when the maximum

variation in these quantities becomes comparable with the experimental error. The amplitude of vibration, however, can be measured more accurately, so that amplitude resonance curves can be obtained for smaller magnetizing and driving fields and greater distances between reed and pole-piece.

Figs. 8 (*a*) and 8 (*b*) show resistance and inductance curves, beyond which the variation is too small to be

Fig. 8 (*a*).

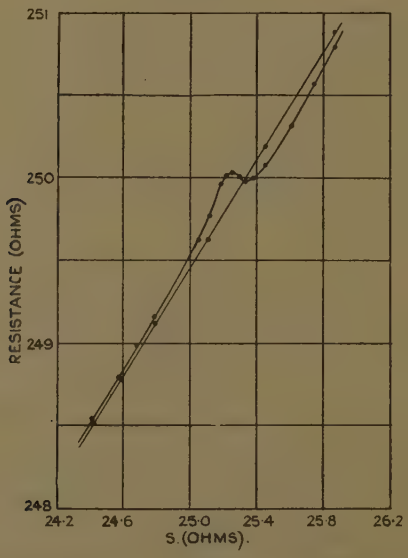

Graph of "free" and "damped" resistance against S—small amplitudes.

advantageously measured. For this curve the steady magnetizing current I_s was 0·38 amp., the alternating driving current $I_m = 18$ m.a., and the distance between reed and pole-piece $d = 0{\cdot}165$ mm.

The impedance Z is given by the equation

$$Z^2 = R^2 + (\omega L)^2.$$

The motional impedance is therefore determined from the motional resistance and the motional reactance. As shown in section II. *c* of Part I. the apparent resonant

pulsatance can only be determined electrically from the impedance-pulsatance curve; for the purpose of the present work it was therefore unnecessary to draw the resistance-pulsatance and reactance-pulsatance curves in each instance, and the following procedure was adopted.

Taking a value of S, the corresponding value of ω is determined from the formula

$$\omega^2 = \frac{1}{MK} \cdot \frac{S}{R+Q+S}.$$

From the graph of resistance against S, the difference between the free and damped resistance is found for this

Fig. 8 (*b*).

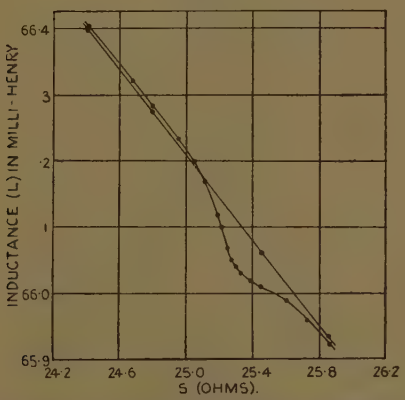

Graph of "free" and "damped" impedance against S—small amplitudes.

value of S; let this be denoted by R_m. For the same value of S the difference between the free and damped inductances are found; let this be denoted by L_m. This difference in inductance, multiplied by the corresponding value of the pulsatance, gives the motional reactance $\omega L_m = X_m$. The motional impedance for this value of S is then given by $Z_m = \sqrt{R_m^2 + X_m^2}$, and is evaluated, using the Davis-Grinstead slide rule.

This procedure is repeated for several values of S, and a curve connecting Z_m and ω is then obtained. The pulsatance at which this curve is a maximum gives the apparent resonant pulsatance of the bar.

IV. Results.

The various parameters which determine the apparent resonant pulsatance ω_r, and the shape of the amplitude-pulsatance and the impedance-pulsatance curves, are (*a*) the length, *l*, of the reed, (*b*) the steady magnetizing current, I_s, (*c*) the amplitude I_m of the driving current, and (*d*) the distance, *d*, between the reed and the pole-piece.

Three values of *l* have been taken; for each value the amplitude-pulsatance and the impedance-pulsatance

Fig. 9 (*a*).

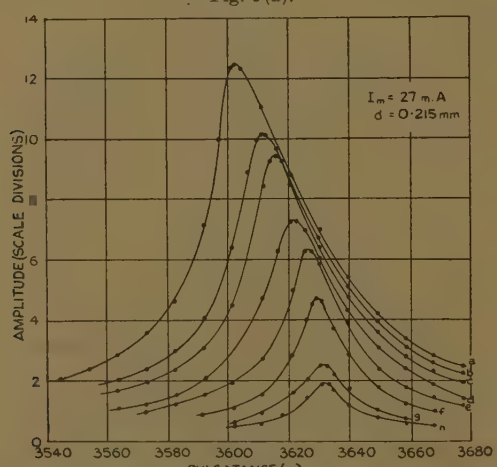

Typical family of amplitude-pulsatance curves—large amplitudes.

curves have been drawn, and ω_r has been determined for different values of I_m, I_s, and *d*.

Two typical series of experimental results are shown for a reed length, $l = 2{\cdot}59_4$ cm.; altogether some sixty resonance curves were taken for this reed length. Typical amplitude-pulsatance and impedance-pulsatance curves are given in figs. 9 (*a*), 9 (*b*), 10 (*a*), 10 (*b*). Each figure gives a family of curves for which I_m and *d* are constant and have the values marked on the diagram; thus, fig. 9 (*a*) shows a family of amplitude curves for which $I_m = 27$ m.a. and $d = 0{\cdot}215$ mm. Each individual curve

Fig. 9 (*b*).

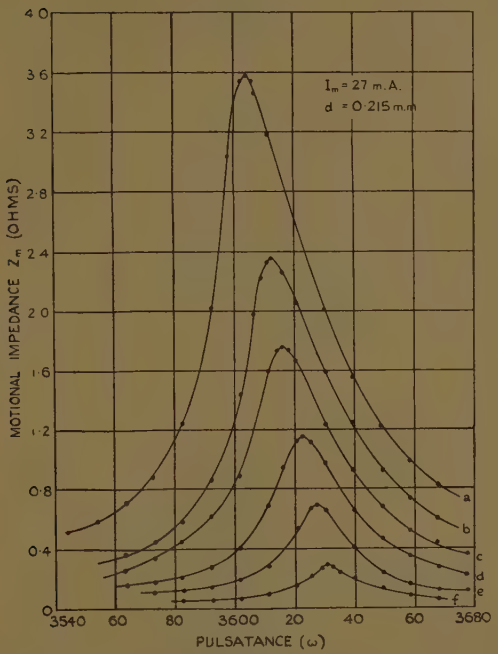

Typical family of motional impedance-pulsatance curves—large amplitudes.

Fig. 10 (*a*).

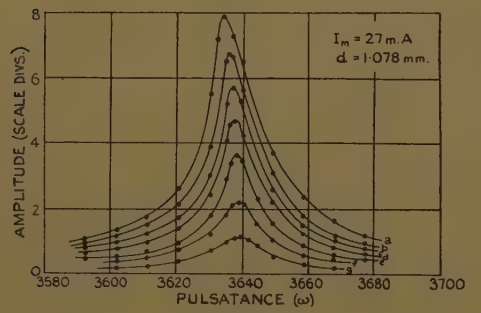

Typical family of amplitude-pulsatance curves—small amplitudes.

on a given diagram corresponds to a definite value of the steady current I_s; the values of I_s which give the curves labelled with the different letters are as follows :—

(*a*) I_s=1·43 a., (*b*) I_s=1·15 a., (*c*) I_s=0·96 a.,
(*d*) I_s=0·77 a., (*e*) I_s=0·57 a., (*f*) I_s=0·38 a.,
(*g*) I_s=0·18 a., (*h*) I_s=0·09 a.

The two main featues of the curves can be summarized as follows :—

(i.) For small amplitude of vibration the amplitude-pulsatance curves do not appear to be distorted.

(ii.) When the amplitude of vibration increases both curves appear to be distorted, the distortion taking

Fig. 10 (*b*).

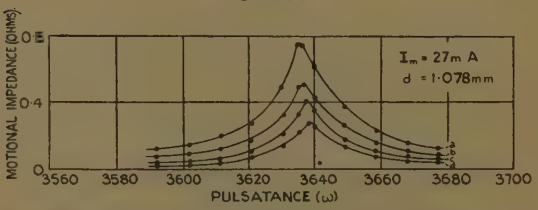

Typical family of motional impedance-pulsatance curves—small amplitudes.

the form of a bending over of the curves towards the region of small pulsatance.

Both features are in agreement with theory.

The pulsatances of maximum amplitude and maximum motional impedance may best be represented as shown in figs. 11 and 12.

In fig. 11 ω_r (obtained from figs. such as figs. 9 (*a*)–10 (*b*)) is plotted against the magnetizing current I_s, the distance d being constant for each individual curve; the values of ω derived from the amplitude-pulsatance curves are indicated by large black dots, whilst the values of ω_r derived from the impedance-pulsatance curves are indicated by smaller dots surrounded by a circle. In the three lowest curves in this figure the value of d is constant and equal to 0·215 mm., whilst the values

of the measuring current I_m for the three curves are (*a*) 27 m.a., (*b*) 18 m.a., and (*c*) 9 m.a. respectively; extrapolation of the three curves to zero I_s gives practically identical values for the apparent resonance-

Fig. 11.

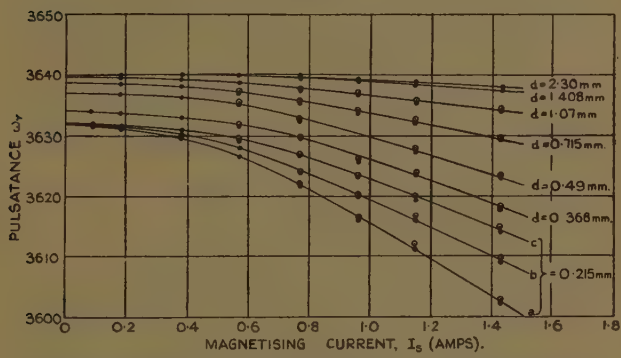

Graph of apparent resonance pulsatance ω_r, against magnetizing current.

Fig. 12.

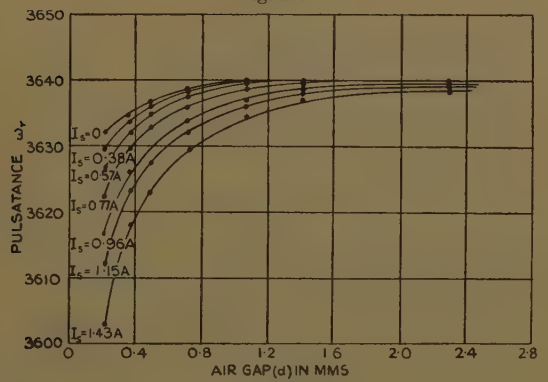

Graph of apparent resonance pulsatance (ωr) against air gap (d). Reed length = 2·59$_4$ cm.

pulsatance at zero I_s, and hence for the determination of ω_0 it is unnecessary to use more than one value of I_m. For the remaining values of d a single value of the driving

current I_m (27 m.a.) was used, and the remaining curves in this figure are for this value of I_m.

In fig. 12 ω_r is plotted against d, the magnetizing current I_s being constant for each individual curve.

From these figures it is seen that

(i.) The pulsatance of maximum amplitude practically coincides with the pulsatance of maximum impedance.

Fig. 13.

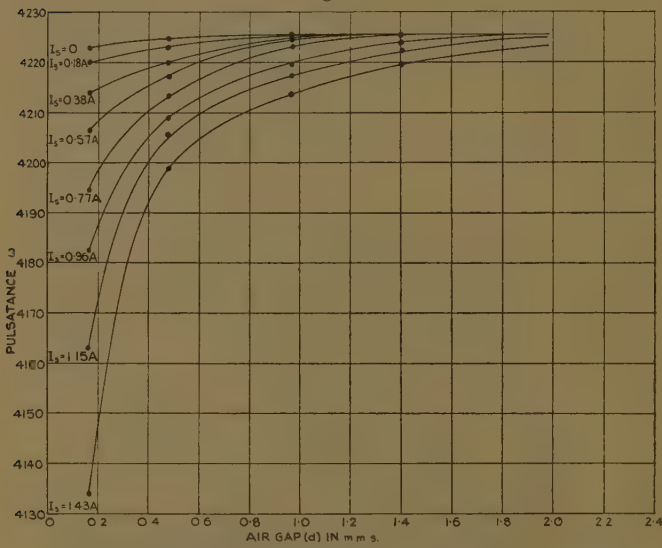

Graph of apparent resonance pulsatance (ω_r) against air gap (d).
Reed length= $2{\cdot}38_8$ cm.

(ii.) The pulsatance (ω_r) decreases with increasing I_m and I_s, and increases with increasing d.

These facts are also in agreement with the theory.

To find the true resonant pulsatance ω_0 from the observed apparent resonant pulsatance ω_r it is necessary to extrapolate to small values of I_m and I_s and to large values of d. This may be done as follows :—

(i.) The curves of fig. 11 are extrapolated to zero values of I_s—this gives the value of ω_r for different values of d and for zero I_s.

(ii.) The values of ω_r found in this way are then plotted against d, and the curve so obtained is the upper curve ($I_s=0$) of fig. 12. The last three points on this curve corresponding to $d=1{\cdot}07_1$ mm., $d=1{\cdot}40_8$ mm., and $d=2{\cdot}30$ mm. are seen to lie accurately on a horizontal line corresponding to $\omega_r=3640$, and this is taken to be the value of ω_0. Since the curves of figs. 11 and 12 become horizontal within the limits of experimental error for large values of d and for small values of I_s, the extrapolation can be carried out with good accuracy.

Fig. 14.

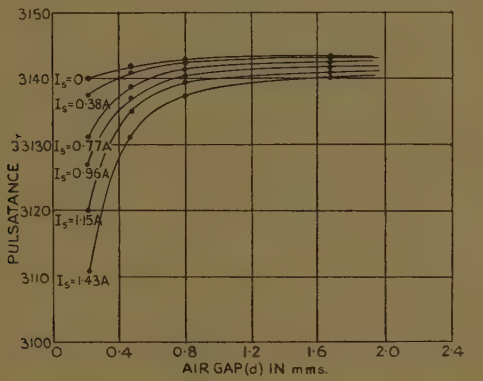

Graph of apparent resonance pulsatance (ω_r) against air gap (d).
Reed length$=2{\cdot}80_6$ cm.

The amplitude-pulsatance and the impedance-pulsatance resonance curves for the other two reed lengths taken, viz. $l_2=2{\cdot}38_9$ cm. and $l_3=2{\cdot}80_6$ cm., are not shown; the curves showing the apparent resonant pulsatance (ω_r) plotted against the air-gap, d, are, however, shown in figs. 13 and 14 respectively.

The main features of these curves are similar to those already described, and by extrapolation the values of ω_0 are found to be 4226 and 3143·5 respectively.

The resonance curves obtained with reed length $l=2{\cdot}38_9$ cm. and $I_s=1{\cdot}43$ a., $I_m=27$ m.a., and $d=0{\cdot}165$ mm., are of special interest, since they show the instability effects mentioned previously (*v.* Sec. I. *d*

of the preceding paper). The resistance-pulsatance, inductance-pulsatance, reactance-pulsatance, amplitude-pulsatance, and motional impedance-pulsatance curves are shown in figs. 15–19. The range of pulsatance lying between 4100 and 4140 is an unstable region, and in

Fig. 15.

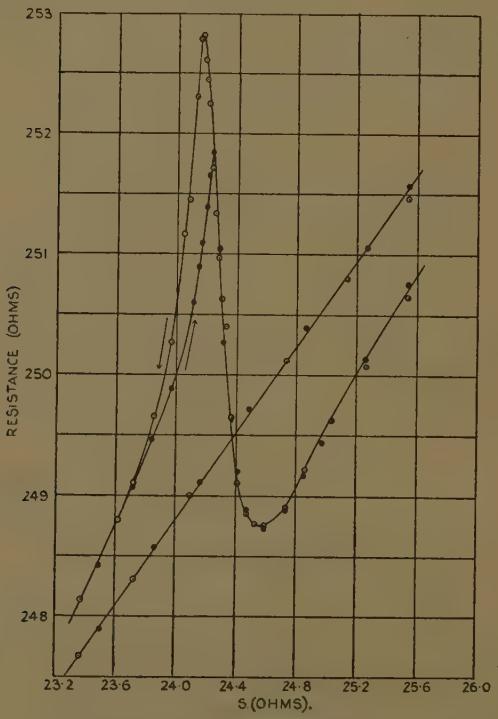

Curve showing instability effects.

this region the reed can vibrate with one of two amplitudes, each of which gives different values for the motional resistance, inductance, and impedance. If the pulsatance is initially less than 4100, and if it be gradually increased, the curves described are those marked with an arrow pointing upwards ; on the other hand, if the pulsatance is initially above 4140, and if it be gradually decreased,

the curves described are those marked with an arrow pointing downwards. The amplitude-pulsatance curves are of the same form as those previously observed by Appleton (*loc. cit.*) and Mallett (*loc. cit.*); the corresponding electrical curves do not appear to have been previously obtained.

Fig. 16.

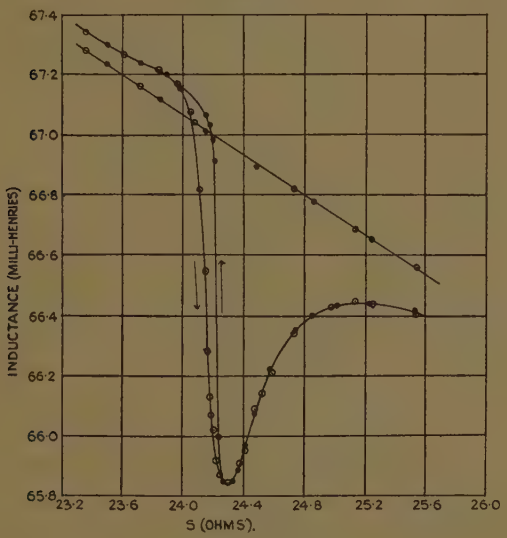

Curve showing instability effects.

V. Calculation of the Value of Young's Modulus.

The theory of the transverse oscillation of a thin rod clamped at one end and free at the other, and carrying a finite load W at the free end, is worked out by Prescott ('Applied Elasticity,' p. 213: Longmans, Green & Co., 1924).

Let

l=length of the reed.

w=weight per unit volume.

a=area of cross-section.

k=radius of gyration of a section of the reed about the axis through its centre of gravity perpendicular to the plane of motion.

E=value of Young's Modulus.

Fig. 17.

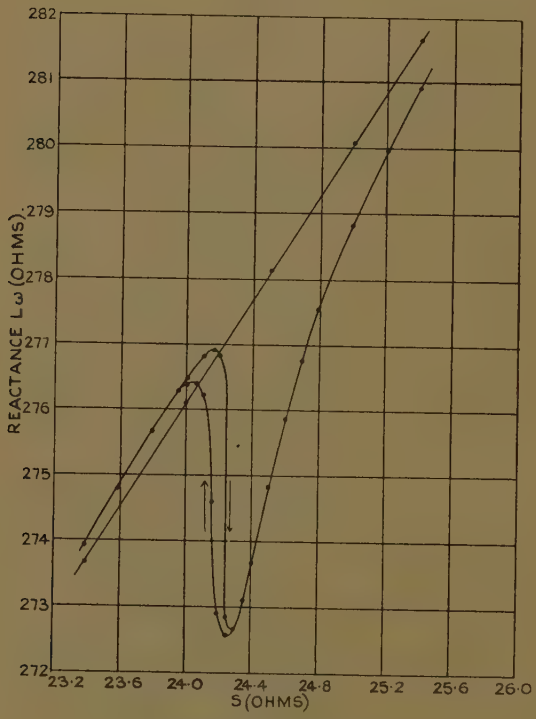

Curve showing instability effects.

Then the frequency n $\left(n=\frac{\omega_0}{2\pi}\right)$ of the fundamental mode of vibration of the bar is given by

$$\frac{k}{2\pi}\cdot\sqrt{\frac{g\mathrm{E}}{w}}=\frac{l^2n}{z^2}, \quad \ldots\ldots \quad (1)$$

Fig. 18.

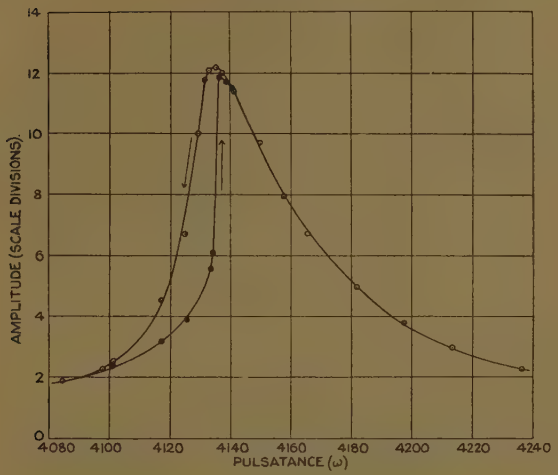

Amplitude-pulsatance curve showing instability effects.

Fig. 19.

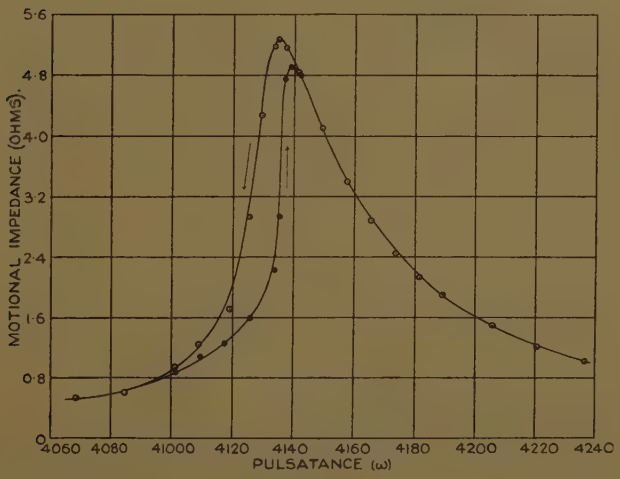

Motional impedance-amplitude curve showing instability effects.

where z is given by the equation

$$\frac{1+\cosh z \cos z}{\cosh z \sin z - \sinh z \cos z} = cz, \quad . \quad . \quad . \quad (2)$$

where $c = \frac{W}{alw}$; *i. e.*, the ratio of the weight W to the weight of the rod.

Equation (2) can be solved by plotting the curve

$$y_1 = \frac{1+\cosh z \cos z}{\cosh z \,.\, \sin z - \sinh z \cos z}$$

$$= \frac{\cos z + \operatorname{sech} z}{\sin z - \cos z \,.\, \tanh z},$$

and the straight line

$$y_2 = cz,$$

and finding the value of z at the intersection.

The natural pulsatance ω_0 has been determined for three different lengths of the bar. Let these lengths be l_1, l_2, l_3, and the corresponding natural frequencies be n_1, n_2 and n_3 respectively.

As $c = W/alw$, therefore for each length there will be a corresponding value of c, and therefore of z. Let these values be z_1, z_2, and z_3.

All the quantities on the left-hand side of equation (1) are constant for the bar; therefore the quantity l^2n/z^2 should be constant.

This quantity is determined, as shown below, for each length of the bar, and the mean value is taken to determine the value of Young's Modulus E.

Width of the bar $= 0{\cdot}60_7$ cm.

Thickness $= 0{\cdot}08_0$ cm.

Density w $= 8{\cdot}78_6$ gm./c.c.

Weight of the stalloy attachment plus solder $= W$

$= 0{\cdot}136$ gm.

Length of the bar $l_1 = 2{\cdot}38_9$ cm.

$l_2 = 2{\cdot}59_4$ cm.

$l_3 = 2{\cdot}80_6$ cm.

Solving equation (2), using these values of l_1, l_2, and l_3, the corresponding values of z are

$$z_1 = 1{\cdot}681_5.$$

$$z_2 = 1{\cdot}693_5.$$

$$z_3 = 1{\cdot}703_0.$$

The corresponding values of the natural frequencies n_1, n_2, and n_3 are

$$n_1 = 4226/2\pi = 672{\cdot}6_0 \text{ cycles per second.}$$

$$n_2 = 3640/2\pi = 579{\cdot}3_1 \quad ,, \quad ,, \quad ,,$$

$$n_3 = 3143{\cdot}5/2\pi = 500{\cdot}3_1 \quad ,, \quad ,, \quad ,,$$

We therefore have that if $A = l^2n/z^2$

$$\left.\begin{aligned} A_1 &= \frac{l_1^2 n_1}{z_1^2} = \frac{2{\cdot}38_9^2 \times 672{\cdot}60}{1{\cdot}681_5^2} = 1357{\cdot}8 \\ A_2 &= \frac{l_2^2 n_2}{z_2^2} = \frac{2{\cdot}59_4^2 \times 579{\cdot}31}{1{\cdot}693_5^2} = 1359{\cdot}1 \\ A_3 &= \frac{l_3^2 n_3}{z_3^2} = \frac{2{\cdot}80_6^2 \times 500{\cdot}31}{1{\cdot}703_0^2} = 1358{\cdot}2 \end{aligned}\right\}.$$

It is seen that these quantities are constant to about 1 in a 1000, which is the order of accuracy of the measurements.

The mean value $A = 1358{\cdot}4$.

The value of Young's Modulus (at 25° C.) is then given by

$$E = \frac{w}{g}\left(\frac{2\pi}{k} \cdot A\right)^2 \text{ gm./sq. cm.}$$

$$= w\left(\frac{2\pi}{k} \cdot A\right)^2 \text{ dynes/sq. cm.}$$

$$= 8{\cdot}78_6\left[\frac{2\pi \cdot \sqrt{3}}{0{\cdot}04} \cdot 1358{\cdot}4\right],$$

i. e., $$E = 11{\cdot}99_8 \times 10^{11} \text{ dynes/sq. cm.}$$

The value of Young's Modulus for phosphor bronze given by Kaye and Laby ('Physical Constants') is $E = 12{\cdot}0 \times 10^{11}$ dynes/sq. cm.

VI. Discussion of Results.

The three independent results obtained above for the value of Young's Modulus of the phosphor-bronze bar show that the method developed is capable of an accuracy of about 1 in 1000, and may therefore be used with confidence for the determination of the Young's Modulus of substances such as crystals, which are only available in the form of short bars.

In this connexion it must be remembered that the aim of the present work has been to explore the capabilities and limitations of the method, and that the number of readings actually necessary for the determination of Young's Modulus is much smaller than the number taken in the present work. It is clear, *e. g.*, that it is unnecessary to take resonance curves for large amplitudes of vibration, since the apparent resonant pulsatance at large amplitudes are unimportant when extrapolating to the limiting conditions of large separations between reed and pole-piece, and to small values of measuring and driving currents. Another obvious way of shortening the work is to utilize the fact that the pulsatance of maximum amplitude and maximum motional impedance coincide ; it is therefore sufficient to take either the amplitude-pulsatance curve or the impedance-pulsatance curve. From the standpoint of ease and simplicity of observation the method employing the amplitude-pulsatance curves is superior, but it may happen that conditions may arise when direct observation of the amplitude of vibration is difficult or impossible. Conditions of this nature may arise when the investigation deals with the temperature coefficient of Young's Modulus ; in investigations of this type the bar under test has to be enclosed in a vessel which has to be maintained at different temperatures, and it may be impossible to arrange matters so that the amplitude of vibration may be observed. In cases of this nature the electrical method of finding the apparent resonant pulsatance is available, since it does not require direct observation of the reed ; the upper temperature limit of the method is determined by factors such as the breakdown temperature of the insulation of the wire used in the coils and the Curie temperature of the coil cores.

It is interesting to compare the accuracy and convenience of the dynamical method of determining Young's

Modulus developed in this work with the statical methods generally employed when the only available specimens are in the form of short bars. In a statical method the bar is generally supported on two knife edges, loaded at the middle, and the deflexion of the mid-point observed; the deflexions obtained are usually very small, so that some method involving observation of interference fringes is necessary for determining these deflexions. At temperatures near room temperatures it is not very difficult to obtain good fringes and to carry out the necessary measurements with them; at temperatures which differ to any extent from room temperature it is, however, a matter of considerable difficulty to obtain fringes and to carry out the necessary measurements. This constitutes one grave disadvantage of the statical method when applied to the determination of Young's Modulus at temperatures differing to any appreciable extent from room temperature.

Another inherent disadvantage of the statical method, applying to all temperatures, is the uncertainty as to what happens at a knife edge. When the beam is loaded the knife edges must cut into the beam to some extent, and this will result in a displacement of the beam as a whole in the same direction as the deflexion due to bending; it follows that the measured deflexion at the mid-point of the beam will be the deflexion due to bending together with the deflexion due to the cutting in at the knife edges. This effect introduces considerable uncertainty into the results obtained by statical methods, and, although the knife edge effect can be estimated by finding the deflexion when using a thick bar which does not bend appreciably, the accuracy of the method is seriously limited on this account.

Taking into account all the difficulties associated with the statical method it may be estimated that the results obtained by its means will be accurate to about 0·5 per cent., which compares unfavourably with the accuracy actually obtained in the present work.

Apart from its application to the determination of Young's Modulus, the present work brings out very clearly, both theoretically and practically, the fact that the pulsatance of maximum amplitude and maximum impedance of an electrically driven reed depends not merely on the dimensions and material of the reed,

but also on the magnitude of the polarizing and driving fields and on the air-gap between reed and pole-piece. It may well happen that this effect may be of importance in connexion with reed-type frequency-meters; it is quite conceivable, *e.g.*, that the indications of a frequency-meter of the reed type may be accurate for small amplitudes of vibration and yet be inaccurate for larger amplitudes.

In conclusion, the authors desire to express their sincerest thanks to Professor Gwilym Owen for his constant interest and valuable suggestions, and also to Messrs. L. E. Sulston and D. Owen for their help in the construction of the apparatus. One of the authors (E. G. J.) is also indebted to the Council of the College for the award of a Sir Garrod Thomas Fellowship, which enabled the work to be carried out.

July 1934.

XCVIII. *X-Ray Levels and Atomic Constants.* *By* H. R. Robinson, *F.R.S., East London College (University of London)* †.

1. THE magnetic spectra of the photoelectrons expelled from a number of substances by two different primary X-radiations have recently been measured in the same apparatus—*i. e.*, under conditions particularly favourable to accurate comparison. The two radiations used were the K-radiations of copper ‡ and chromium §.

The kinetic energy of the photoelectrons in any group may be obtained from the measurements of the magnetic spectra ‖; the difference between this energy and that of a quantum ($h\nu$) of the primary X-rays gives the energy

† Communicated by the Author.

‡ Robinson, Andrews, and Irons, Proc. Roy. Soc. A, cxliii. p. 48 (1933). [Later quoted as reference (1).]

§ Robinson, Phys. Soc. Proc. xlvi. p. 693 (1934). [Later quoted as reference (2).]

‖ The energy is deduced from the product rH, where r is the radius of curvature of the path of the electron in a magnetic field H perpendicular to the plane of the path.

characteristic of the level of origin of the photoelectrons constituting this group. The following Tables, I. to VI., give a number of the X-ray levels of gold, platinum, tungsten, tin, silver, and copper, determined in this manner with copper $K\alpha_1$ and chromium $K\alpha_1$ respectively. Most of the results are based on data taken from references (1) and (2), but the results for copper K-rays with platinum and tin have not previously been published.

In calculating the photoelectron energies from magnetic spectra alone, it is necessary to assume values for the electronic charge and specific charge. Further, for comparison with X-ray data it is necessary either to express the electron energies as equivalent frequencies or to convert X-ray frequencies into equivalent energies by the Planck relation. Thus, in the course of the comparison values have to be assumed for e, e/m_0, and h, or, more strictly, for e/m_0 and e/h. In the paper of Robinson, Andrews, and Irons (reference 1), these values were taken :—$e=4{\cdot}770\times10^{-10}$ E.S.U., $h=6{\cdot}543\times10^{-27}$ erg sec., $e/m_0=1{\cdot}759\times10^{7}$ E.M.U. gm.$^{-1}$. In reference (2) I took what appear to be more appropriate values :—$e=4{\cdot}768\times10^{-10}$, $h=6{\cdot}547\times10^{-27}$, $e/m_0=1{\cdot}757\times10^{7}$. These latter values are retained here.

2. In the following tables all energies and frequencies are expressed in Rydberg units (ν/R) ; the results taken from reference (1) have been corrected for an error of 0·08 per cent.† in the magnetic field, and recomputed in terms of the second set of constants just quoted. The two primary frequencies are taken as : copper $K\alpha_1$, ν/R=592·7 ; chromium $K\alpha_1$, ν/R=398·8. The photoelectron energies are marked with an asterisk (ν^*/R) to distinguish them from less indirectly determined frequencies. The " Intensities " of the lines of the magnetic spectra are given on a 1–6 scale, 6 being the strongest. These are no more than rough visual estimates of relative intensities ; they are useful here as an indication of the accuracy to be expected—lines of intensity 5 or 6 can be much more easily and accurately measured than those of intensity 1 or 2. In the last column Siegbahn's ‡ level values are given for comparison.

† Robinson, ' Nature,' cxxxiv. p. 179 (1934).
‡ Siegbahn, ' Spektroskopie der Röntgenstrahlen,' 1931, pp. 346–348.

TABLE I.

79. Gold (metal).

Primary→ X-radiation.	$CuK\alpha_1$ (592·7).			$CrK\alpha_1$ (398·8).			Level value: Siegbahn.
Level	Intensity.	$\nu^*/R.$	Level value $592{\cdot}7-\nu^*/R.$	Intensity.	$\nu^*/R.$	Level value $398{\cdot}8-\nu^*/R.$	
M_I	2	340·8	251·9	2 (*i*)	146·5	252·3	252·2
M_{II}	2–3	361·4	231·3	3	167·1	231·7	231·8
M_{III}	6	391·3	201·4	5	197·0	201·8	201·9
M_{IV}	6	424·6	168·1	6	230·3	168·5	168·6
M_V	6	431·1	161·6	6	236·6	162·2	162·2
N_I	4	537·9	54·8	2	343·7	55·1	55·8
N_{II}	4	546·2	46·5	3	352·3	46·5	47·3
N_{III}	4–5	553·7	39·0	4	359·6	39·2	39·9
N_V	5	568·7	24·0	5	374·9	23·9	24·5

TABLE II.

78. Platinum (metal).

Primary→ X-radiation.	$CuK\alpha_1$ (592·7).			$CrK\alpha_1$ (398·8).			Level value: Siegbahn.
Level.	Intensity.	$\nu^*/R.$	Level value $592{\cdot}7-\nu^*/R.$	Intensity.	$\nu^*/R.$	Level value $398{\cdot}8-\nu^*/R.$	
M_I	3	350·7	242·0	1–2	156·3	242·5	242·0
M_{II}	4	370·7	222·0	3	176·4	222·4	221·9
M_{III}	6	398·8	193·9	5	204·4	194·4	193·9
M_{IV}	6	431·3	161·4	6	237·0	161·8	161·2
M_V	6	437·5	155·2	6	243·0	155·8	155·3
N_I	2	540·9	51·8	1–2	346·8	52·0	52·3
N_{II}	3	549·8	42·9	2–3	355·6	43·2	44·0
N_{III}	3–4	556·2	36·5	4	361·7	37·1	37·3
N_V	4	570·9	21·8	5	376·4	22·4	22·3

Table III.

74. Tungsten (oxide).

Primary→ X-radiation.	$CuK\alpha_1$ (592·7).			$CrK\alpha_1$ (398·8).			Level value: Siegbahn.
Level.	Intensity.	$\nu^*/R.$	Level value $592\cdot7-\nu^*/R.$	Intensity.	$\nu^*/R.$	Level value $398\cdot8-\nu^*/R.$	
M_I	4	385·5	207·2	2	191·6	207·2	207·3
M_{II}	4–5	403·6	189·1	3	209·8	189·0	189·3
M_{III}	6	425·3	167·4	6	231·2	167·6	167·5
M_{IV}	5–6	455·2	137·5	6	261·4	137·4	137·5
M_V	5–6	460·2	132·5	6	266·1	132·7	132·9
N_I	4	550·4	42·3	2	355·6	43·2	43·3
N_{II}	4	557·2	35·5	2	362·0	36·8	36·0
N_{III}	4–5	562·8	29·9	3–4	369·0	29·8	31.0
N_V	5	575·7	17·0	5	381·7	17·1	17·6

The N, and to a smaller extent the M, levels will be affected by the use of a target of oxide in place of the metal.

Table IV.

50. Tin (metal).

Primary→ X-radiation.	$CuK\alpha_1$ (592·7).			$CrK\alpha_1$ (398·8).			Level value: Siegbahn.
Level.	Intensity.	$\nu^*/R.$	Level value $592\cdot7-\nu^*/R.$	Intensity.	$\nu^*/R.$	Level value $398\cdot8-\nu^*/R.$	
L_I	4	264·4	328·3	1–2(?)	69·4	329·4	327·4
L_{II}	5	287·0	305·7	2–3	92·8	306·0	304·9
L_{III}	6	303·8	288·9	5	109·3	289·5	288·1
M_I	4	528·9	63·8	5	334·7	64·1	63·9
M_{III}	4	541·3	51·4	5–6	347·1	51·7	51·2
M_V	3	558·8	33·9	4	363·8	35·0	34·4

TABLE V.

47. Silver (metal).

Primary→ X-radiation.	$CuK\alpha_1$ (592·7).			$CrK\alpha_1$ (398·8).			Level value : Siegbahn.
Level.	Intensity.	ν^*/R.	Level value $592\cdot7-\nu^*/R$.	Intensity.	ν^*/R.	Level value $398\cdot8-\nu^*/R$.	
L_I	5	312·7	280·0	2–3	118·6	280·2	282·0
L_{II}	5	333·4	259·3	4	139·3	259·5	261·3
L_{III}	6	346·4	246·3	6	152·2	246·6	248·6
M_I	5	541·1	51·6	4	346·7	52·1	54·7
M_{III}	5	551·2	41·5	5	357·6	41·2	43·7
M_V	2–3	567·3	25·4	3–4	372·6	26·2	28·8

TABLE VI.

29. Copper (metal).

Primary→ X-radiation.	$CuK\alpha_1$ (592·7).			$CrK\alpha_1$ (398·8).			Level value : Siegbahn.
Level.	Intensity.	ν^*/R.	Level value $592\cdot7-\nu^*/R$.	Intensity.	ν^*/R.	Level value $398\cdot8-\nu^*/R$.	
L_I	6	512·4	80·3	6	318·3	80·5	81·0
L_{III}	4	524·6	68·1	6–	330·2	68·6	68·9

3. As the results of the experiments with copper K-rays on platinum and tin have not previously been published, they are given in full below.

$$Cu\ K\alpha_1,\ \nu/R=592\cdot7$$

$$Cu\ K\beta_1,\ \nu/R=655\cdot9$$

Table II a.

78. Platinum (metal).

Level values (Siegbahn) ν/R :—

M_I 242·0	N_I 52·3	O_I 6·4
M_{II} 221·9	N_{II} 44·0	$O_{II, III}$ 3·3
M_{III} 193·9	N_{III} 37·3	
M_{IV} 161·2	N_{IV} 23·4	
M_V 155·3	N_V 22·3	
	N_{VI} 4·5	
	N_{VII} 4·3	

Remarks.	Intensity.	rH cm. gauss.	ν^*/R.	Origin.
	3	$233{\cdot}0_5$	350·7	M_I : $CuK\alpha_1$—242·0
	4	$239{\cdot}6_5$	370·7	M_{II} : $CuK\alpha_1$—222·0
	6	248·6	398·8	M_{III} : $CuK\alpha_1$—193·9
	6	258·6	431·3	M_{IV} : $CuK\alpha_1$—161·4
	6–	$260{\cdot}4_5$	437·5	M_V : $CuK\alpha_1$—155·2
Inaccurate ...	2–	267·9	462·7	M_{III} : $CuK\beta_1$—193·2
Inaccurate ...	1–2	277·2	495·2	M_{IV} : $CuK\beta_1$—160·7
Inaccurate ...	1–2	278·9	501·3	M_V : $CuK\beta_1$—154·6
	2	289·8	540·9	N_I : $CuK\alpha_1$—51·8
	3	292·2	549·8	N_{II} : $CuK\alpha_1$—42·9
	3–4	293·9	556·2	N_{III} : $CuK\alpha_1$—36·5
Double, not resolved.	4	297·8	570·9	$N_{IV, V}$: $CuK\alpha_1$—21·8
Diffuse band ...	3	303·0	590·9	$N_{VI, VII}$, O : $CuK\alpha_1$—1·8
Inaccurate ...	1	310·4	619·9	N_{III} : $CuK\beta_1$—36·0
Inaccurate ...	1	314·4	635·8	$N_{IV, V}$: $CuK\beta_1$—20·1
Inaccurate ...	1	319·4	656·0	$N_{VI, VII}$, O : $CuK\beta_1$—(−0·1)
Inaccurate ...	0–1	323·5	672·9	?

TABLE IV A.

50. Tin (metal).

Level values (Siegbahn) ν/R :—

L_I 327·4	M_I 63·9	N_I 8·8	O_I (−1·2)
L_{II} 304·9	M_{II} 54·4	$N_{II, III}$ 5·3	
L_{III} 288·1	M_{III} 51·2	N_{IV}, 0·6	
	M_{IV} 35·1	N_V, 0·4	
	M_V 34·4		

Remarks.	Intensity.	ρH cm. gauss.	ν^*/R.	Origin.
	4	$202{\cdot}2_5$	264·4	L_I : $CuK\alpha_1$—328·3
	5	210·7	287·0	L_{II} : $CuK\alpha_1$—305·7
	6	$216{\cdot}8_5$	303·8	L_{III} : $CuK\alpha_1$—288·9
Inaccurate ...	0–1	225·5	328·4	L_I : $CuK\beta_1$—327·5
Inaccurate ...	0–1	233·1	350·8	L_{II} ; $CuK\beta_1$—305·1
	1	$238{\cdot}7_5$	367·9	L_{III} : $CuK\beta_1$—288·0
	4	$286{\cdot}5_5$	528·9	M_I : $CuK\alpha_1$ – 63·8
Double, not resolved.	4	289·9	541·3	$M_{II, III}$: $CuK\alpha_1$—51·4
Double, not resolved.	3	294·6	558·8	$M_{IV, V}$: $CuK\alpha_1$—33·9
	3–4	302·1	587·4	N : $CuK\alpha_1$—5·3
Inaccurate ...	1	303·4	592·5	N, O : $CuK\alpha_1$—0·2 M_I : $CuK\beta_1$—63·4
Inaccurate ...	1	306·7	605·3	$M_{II, III}$: $CuK\beta_1$—50·6

4. Returning now to the consideration of Tables I. to VI., the discussion will be confined entirely to the numerical aspect of the results, including their relation with the accepted values of the atomic constants. Practically all the results tabulated above refer to spectrum lines which were measured under quite favourable conditions—*i. e.*, in particular, strong lines on good plates and with ample separation between neighbouring lines. There are a few cases where, owing either to

difficulties in photography or to the overlapping of lines, the measurements are particularly difficult. Such cases are indicated by the letter "*i*" (="inaccurate") in the Intensity column. In all other cases the *relative* values of *r*H should be correct to 1 part in 2000, or the ν^*/R values to 1 part in 1000.

Purely as a matter of convenience in comparing the two series of results, the Tables have been formed by using the photoelectron energies, combined with the primary X-ray quantum, to deduce the X-ray levels of the various targets. For other purposes—*e. g.*, for deducing relations between the atomic constants—this is not the most suitable arrangement of the data. The arrangement adopted does, however, enable an immediate estimate to be made, by simple inspection of the Tables, of the *internal* consistency of the measurements made with the magnetic spectrometer. On the whole, it will be seen that this is highly satisfactory, especially with gold, platinum, and silver, where a great many beautiful photographs were obtained by the use of very thin and highly polished targets. It is a little less good in other cases, but it will be seen throughout that the tendency is for the work with copper K-rays to give *lower* values for the energy levels than the work with chromium K-rays. When considering the agreement, or disagreement, between different pairs of values, it is well to remember that the greatest errors are liable to occur with the levels of lowest (negative) energy. Thus, with silver L_I, an error of 0·05 per cent. in the measurement of *r*H produces a difference of 0·3 Rydberg unit in the level value when operating with copper $K\alpha_1$, and 0·1 Rydberg when operating with chromium $K\alpha_1$. If these are in opposite senses, the total discrepancy between the observed energy levels, due to this alone, will be 0·4 Rydberg. With silver M_V, however, the corresponding errors would be 0·6 and 0·4 Rydberg respectively, with a total of 1 unit. Considering this, the evidence for the systematic difference between the level values obtained with the two primary radiations is remarkably clear and definite.

5. The differences between the "photoelectric" and the "crystal" (Siegbahn) level values are far less systematic, and the results listed above clearly indicate a need for some revision of the X-ray data. The general

tendency is for the chromium series to give level values in close agreement with the crystal data—at all events in the case of the levels of moderately high energy—while the copper results are a little lower. The internal consistency of the photoelectric results with gold and platinum indicates that, if the M-levels listed by Siegbahn for gold are correct, those for platinum should be raised by about 0·5 Rydberg. The photoelectric results for tungsten are a little less consistent, probably owing to the less perfect target employed, but on the same basis of comparison there is excellent agreement for the M-levels.

With tin and silver there is marked disagreement with the values quoted by Siegbahn. Moreover, the discrepancies are in opposite senses, although with elements so close together in the periodic table any systematic errors in the photoelectric experiments would affect the results for both elements in almost identical ways. The most recent spectroscopic measurements on these elements, from Siegbahn's Laboratory are, however, in better accord with the photoelectric results. Inglestam and Ray † find, from measurement of the K-absorption edges and combination with $K\alpha_1$ and $K\alpha_2$:—

	L_{II}.	L_{III}.
Tin (metal)	305·51	288·77
Silver (bromide)	259·98	247·24

while the older direct measurements of L-absorption edges by Van Dyke and Lindsay ‡ gave :—

	L_{I}.	L_{II}.	L_{III}.
Tin (metal)	329·0	306·6	289·4
Silver (metal)	280·6	259·9	246·9

Here the accuracy of the photoelectric method does not compare at all unfavourably with that of the spectroscopic.

† Ingelstam and Ray, *Zs. Phys.* lxxxviii. p. 218 (1934).
‡ Van Dyke and Lindsay, Phys. Rev. xxx. p. 562 (1927).

The results with copper (Table VI.) call for no comment.

A less satisfactory feature of the photoelectric results appears on examination of the level values deduced from groups due to the conversion of the copper and chromium $K\beta_1$ radiations. These have not been entered in Tables I. to VI., as their inclusion would have made the Tables too unwieldy. Further, they are of a lower order of accuracy, as the lines are much fainter and somewhat less sharp than those due to the conversion of $K\alpha_1$. It is not possible to bring up these β-lines at all strongly without grossly over-exposing the α-lines, and veiling the whole plate by the effects of straggled and scattered radiations; the irregular or unsystematic errors will therefore always be appreciably greater for the β- than for the α-lines. Even allowing for the possibility of relatively large experimental errors in the measurement of these faint lines, it is evident throughout that the β-lines give definitely lower photoelectric level values than the α-lines—in other words, the corresponding photoelectron energies are all too high; the differences are as large as 0·5 or even 0·7 Rydberg, and they are just as marked in the chromium as in the copper results (*cf.* reference 2). A small difference of this sign would be expected as a consequence of the greater natural width of the β-line, but the observed difference is unexpectedly large.

6. A somewhat similar effect is observed in the higher velocity electron groups due to the $K\alpha_1$ lines: with elements for which the "photoelectrically" determined M-levels are in excellent agreement with the "crystal" values, the photoelectric values for the N-levels are appreciably lower than the crystal values. The effect is not large, and it occurs in the region where, as has been pointed out already, comparatively large errors are most likely to arise. The differences are, however, so persistent that they cannot fairly be explained away as accidental errors. Professor A. E. Ruark has suggested privately to me, in a somewhat different connexion, the "spread" of the lines on the photographic plate as a partial explanation. So far as my evidence goes, this will not adequately explain the whole effect, but it is hoped shortly to test this point by additional experiments. It is scarcely possible to place the onus

upon the spectroscopic values of the N-terms ; although these have not been measured directly, the values are pretty well substantiated by combinations between measurable levels and emission lines. The need for some revision of the values of the lower energy levels is indicated, and Ruark †, in particular, has indicated important improvements in the methods of computing the level values, but in the face of the available evidence it does not seem likely that all the levels can be adjusted to fit the photoelectric results, as the latter now stand.

7. Before leaving the question of the agreement (or otherwise) between the photoelectric and spectroscopic level values, it should be pointed out that some fairly recent and very careful direct determinations of M-absorption edges yield results which are very different from both the photoelectric values and those given in Siegbahn's Table. Thus, Lindberg ‡ gives :—

	$M_{III.}$	$M_{IV.}$	$M_{V.}$
Gold	202·2	171·0	164·8
Platinum	194·9	164·4	158·6
Tungsten	167·9	140·5	—

The problem of the measurement and interpretation of the X-ray levels is still far from being completely solved in all its details.

We may then sum up by saying that the photoelectric experiments are, on the whole, in good agreement with selected spectroscopic data, when we use the values quoted at the end of Paragraph 1 of this paper for the atomic constants, and when we retain the "crystal" wave-lengths for the X-ray data. The agreement is definitely less good if the "ruled grating" values are taken for the latter.

8. Considering, now, the results in their bearing on the problem of the fundamental constants, a better procedure is to ignore entirely all other values of the energy levels and to work, as far as possible, with the

† Ruark, Phys. Rev. xlv. p. 827 (June 1934).
‡ Lindberg, *Nova acta reg. soc. sci. ups.* ser. 4, vii. no. 7 (1931).

photoelectric results alone. We cannot dispense with the spectroscopic values for the frequencies of the primary X-rays, but these are known unambiguously and very accurately in terms of the conventional crystal spacing.

Now the frequency *difference* between the principal two radiations employed is $CuK\alpha_1 - CrK\alpha_1 = (592{\cdot}74 - 398{\cdot}80) = 193{\cdot}94$ Rydberg. In a perfect (and not over-elaborated) world this would also be the difference between the two photoelectron energies (expressed as ν^*/R) obtained when any selected atomic level is excited by these two primary radiations in turn. Tables I. to VI. contain 41 such pairs of ν^*/R values. Taking the differences between the members of each pair, and rejecting five obviously anomalous values, we get 36 values lying between 193·6 and 194·5, of which again 30 lie between 193·8 and 194·4. The mean value of the difference $(\nu^*/R)_{Cu} - (\nu^*/R)_{Cr}$ is $194{\cdot}1_8$; this is very nearly 1 part in 800 greater than the value deduced above from the ("crystal") frequencies of the two radiations.

This difference, of 1 part in 800, provides the simplest and most direct basis of comparison between the photoelectric and spectroscopic results. It will therefore be examined in some detail.

In the first place, it is admittedly a defect in the method of magnetic spectrometry that the quantity measured (rH) is very nearly proportional to the square root of the quantity required (*i. e.* the energy). Hence, any proportional error made in the measurement of rH is doubled in the calculation of ν^*/R. The difference between the photoelectric and the crystal values would therefore be annulled if the rH values could all be reduced by 1 part in 1600. From the mode in which this figure has been derived, it is obvious that this adjustment would on the average bring the level values, deduced in the two series with copper K and chromium K respectively, into exact agreement. It would also improve the general fit in the values obtained for the levels of lowest energy, which are very sensitive to slight errors of measurement or adjustments of the constants.

One part in 1600 is perhaps not a large error in the measurement of rH, but I am reluctant to admit this adjustment. On the other hand, if we can accept

Bearden's† latest value for the calcite grating space, which makes the X-unit very nearly $0{\cdot}99949 \times 10^{-11}$ cm., all the "spectroscopic" frequencies must be raised by 1 part in 2000, and the discrepancy between them and the photoelectric results is reduced to 1 part in 1350. The requisite adjustment in the rH values—1 part in 2700—becomes much more acceptable, and the general agreement may, indeed, be called highly satisfactory. Any change of the spectroscopic values in the opposite sense—*i. e.*, in the direction indicated by the ruled grating measurements—would obviously be unacceptable.

9. It only remains to consider one other possibility—that of still further adjusting the values of e/h and e/m_0. In the range covered by this work—*i. e.*, for comparatively slow electrons—to a very close approximation these quantities enter into the expression for ν^*/R in the form $e/h \times e/m_0$. The values taken for e and h were given very recently by Professor R. T. Birge. It seems unlikely that an appreciably lower value of e or higher value of h will be put forward in the near future.

The value of e/m_0 has recently been subject to many vicissitudes. The rather low value adopted here—$1{\cdot}757 \times 10^7$ E.M.U. gm.$^{-1}$—has been obtained by Kretschmar ‡ with the magnetic spectrometer, by Dunnington § in very ingenious new "direct" experiments, and, finally, by Gibbs and Williams ‖ from the spectra of H^1 and H^2. Kretschmar's work is of special interest in connexion with the present paper. It appears to have been very carefully conducted with particularly well-designed apparatus; further, the primary radiation used ($\mathrm{MoK}\alpha_1$) was of a frequency about 1000 Rydberg higher than those of the levels from which the photoelectrons were extracted, so that small uncertainties in the level values had very little influence on the final result.

There is, therefore, considerable authority for this low value of e/m_0; it is, however, difficult to understand the reasons for the appreciably higher values found in other recent experiments. On the whole, it is scarcely possible to judge from the history of the measurements

† *Cf.* Ruark, *loc. cit.*
‡ Kretschmar, Phys. Rev. xliii. p. 417 (1933).
§ Dunnington, Phys. Rev. xliii. p. 404 (1933).
‖ Gibbs and Williams, Phys. Rev. xliv. p. 977 (1933).

whether the value of e/m_0 is coming asymptotically to rest at a generally accepted value a little below $1{\cdot}757 \times 10^7$, or whether it is indulging in damped oscillations about some value which will ultimately turn out to be a little higher than this. Unless, however, there is some factor which has not yet been taken properly into account, but which may emerge from further study of the magnetic spectrometer, the photoelectric results speak definitely for the lowest authenticated values of e/h and e/m_0, and for the " crystal " values of the X-ray wave-lengths.

Summary.

A number of the X-ray levels of gold, platinum, tungsten, tin, silver, and copper have been investigated with the magnetic spectrometer, using copper Kα and chromium Kα radiations in turn. There are some anomalies which require closer examination, but on the whole the results are remarkably consistent, and they lead to fairly definite indications of the most probable values of the atomic constants and of X-ray wave-lengths.

I have much pleasure in acknowledging my indebtedness to the Department of Scientific and Industrial Research for a grant which enabled me to employ a full-time assistant for a considerable part of the work which is discussed in this paper.

East London College.

XCIX. *Deformation of Thin Cylindrical Shells subjected to Internal Loading.* *By* I. A. Wojtaszak *.

§1. *Introduction.*

In this paper two problems on deformation of thin cylindrical shells are discussed :—(1) a complete circular cylindrical shell freely supported at its edges and subjected to internal hydrostatic pressure; (2) a portion of a cylindrical shell cut out from a circular cylinder by two diametral sections and two cross-sections perpendicular to the axis of the cylinder. In both cases

* Communicated by Prof. S. Timoshenko.

trigonometric series for expressing displacements have been used *, and it was shown that the coefficients of these series rapidly diminish, so that only few terms are necessary to represent the deformation with sufficient accuracy. General equations were applied to numerical examples, and in the case of the portion of a cylindrical shell comparison of the deflexion of the curvilinear rectangle with that of a rectangular plate has been made, and it was shown that the rigidity of the curvilinear

Fig. 1.

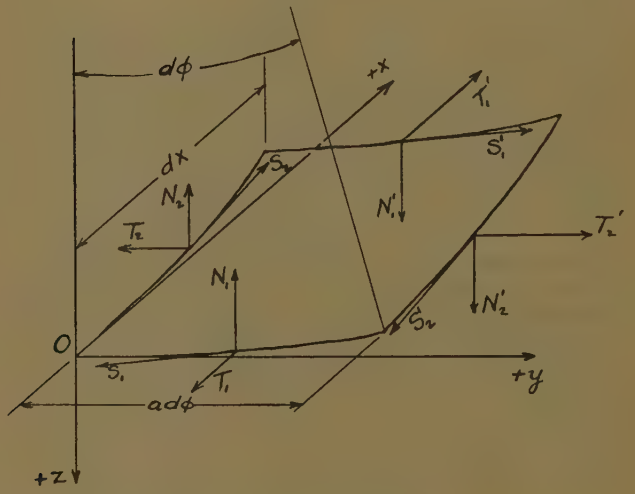

rectangle increases rapidly with the increase of the central angle which it subtends.

§ 2. *General Equations.*

Considering the condition of equilibrium of an element of the cylindrical shell cut out by two diametral sections and two cross-sections perpendicular to the axis of the cylindrical shell, and using for stress-resultants and stress-

* This method has been used previously by S. Timoshenko (see 'Theory of Elasticity,' ii. pp. 384–387, St. Petersburg (1916)). See also H. Reissner, *Zeit. f. ang. Math. u. Mech.* xiii. p. 133 (1933).

couples the notation indicated in fig. 1 *, where the vectors representing the stress-couples H_1 and G_1 have the same directions as T_1 and S_1 and the vectors representing the stress-couples H_2 and G_2 have the same directions as T_2 and S_2, the following equations of equilibrium are obtained :

$$\left.\begin{aligned} &a\frac{\partial T_1}{\partial x}-\frac{\partial S_2}{\partial \phi}=0\,; \quad a\frac{\partial H_1}{\partial x}-\frac{\partial G_2}{\partial \phi}+N_2 a=0\,; \\ &a\frac{\partial S_1}{\partial x}+\frac{\partial T_2}{\partial \phi}+N_2=0\,; \quad a\frac{\partial G_1}{\partial x}+\frac{\partial H_2}{\partial \phi}-N_1 a=0\,; \\ &a\frac{\partial N_1}{\partial x}+\frac{\partial N_2}{\partial \phi}-T_2+qa=0\,; \quad (S_1+S_2)a=0\,; \end{aligned}\right\} \quad . \quad (1)$$

where q is the load per unit area of the middle surface acting in the direction of the positive z-axis.

Eliminating N_1 and N_2 from equations (1), and using the relations

$$S_1=-S_2=S \quad \text{and} \quad H_1=-H_2=H,$$

we obtain the following equations of equilibrium :

$$\left.\begin{aligned} &a\frac{\partial T_1}{\partial x}+\frac{\partial S}{\partial \phi}=0, \\ &a\frac{\partial S}{\partial x}+\frac{\partial T_2}{\partial \phi}+\frac{\partial G_2}{a\partial \phi}-\frac{\partial H}{\partial x}=0, \\ &\frac{\partial^2 G_1}{\partial x^2}-\frac{2}{a}\frac{\partial^2 H}{\partial x\,\partial \phi}+\frac{1}{a^2}\frac{\partial^2 G_2}{\partial \phi^2}-\frac{T_2}{a}+q=0. \end{aligned}\right\} \quad . \quad . \quad (2)$$

Resolving the displacement of any point of the middle surface of the shell during deformation into three components—u along the generator, v along the tangent to the circular section, and w along the normal to the surface drawn outwards (see fig. 2)—the strain components and changes in curvature are †

$$\left.\begin{aligned} &\epsilon_1=\frac{\partial u}{\partial x}; \quad \epsilon_2=\frac{1}{a}\frac{\partial v}{\partial \phi}+\frac{w}{a}; \quad \omega=\frac{\partial v}{\partial x}+\frac{1}{a}\frac{\partial u}{\partial \phi}; \\ &k_1=\frac{\partial^2 w}{\partial x^2}; \quad k_2=\frac{1}{a^2}\frac{\partial^2 w}{\partial \phi^2}-\frac{1}{a^2}\frac{\partial v}{\partial \phi}; \quad \tau=\frac{1}{a}\frac{\partial^2 w}{\partial x\,\partial \phi}-\frac{1}{a}\frac{\partial v}{\partial x}. \end{aligned}\right\} \quad . \quad (3)$$

* See A. E. H. Love, 'The Mathematical Theory of Elasticity' (1927), pp. 534–536.

† See A. E. H. Love, *loc. cit. ante*, pp. 521, 524, & 568.

The stress-resultants and stress-couples are represented now by the following equations * :—

$$\left.\begin{aligned} T_1 &= \frac{2Eh}{1-\sigma^2}(\epsilon_1+\sigma\epsilon_2); \quad T_2 = \frac{2Eh}{1-\sigma^2}(\epsilon_2+\sigma\epsilon_1); \\ S &= \frac{Eh}{1+\sigma}\omega; \\ G_1 &= -D(k_1+\sigma k_2); \quad G_2 = -D(k_2+\sigma k_1); \\ H &= D(1-\sigma)\tau; \end{aligned}\right\} \quad . \quad (4)$$

where $2h$ is the thickness of the shell and

$$D = \frac{2}{3}\frac{Eh^3}{1-\sigma^2} = \text{Flexural Rigidity.}$$

Substituting this into (2), and neglecting $h^2/3a^2$ in comparison with 1/2 and 1 in the second equation, we obtain

$$\left.\begin{aligned} &\frac{\partial^2 u}{\partial x^2} + \frac{1-\sigma}{2a^2}\frac{\partial^2 u}{\partial \phi^2} + \frac{1+\sigma}{2a}\frac{\partial^2 v}{\partial x \partial \phi} + \frac{\sigma}{a}\frac{\partial w}{\partial x} = 0, \\ &\frac{1+\sigma}{2}\frac{\partial^2 u}{\partial x \partial \phi} + \frac{a(1-\sigma)}{2}\frac{\partial^2 v}{\partial x^2} + \frac{1}{a}\frac{\partial^2 v}{\partial \phi^2} + \frac{1}{a}\frac{\partial w}{\partial \phi} - \frac{h^2}{3a} \\ &\qquad \times\left(\frac{\partial^3 w}{\partial x^2 \partial \phi} + \frac{1}{a^2}\frac{\partial^3 w}{\partial \phi^3}\right) = 0, \\ &\sigma a\frac{\partial u}{\partial x} + \frac{\partial v}{\partial \phi} - \frac{h^2}{3}\left\{(2-\sigma)\frac{\partial^3 v}{\partial x^2 \partial \phi} + \frac{1}{a^2}\frac{\partial^3 v}{\partial \phi^3}\right\} + w \\ &\qquad + \frac{h^2}{3}\left\{a^2\frac{\partial^4 w}{\partial x^4} + \frac{2\partial^4 w}{\partial x^2 \partial \phi^2} + \frac{\partial^4 w}{a^2 \partial \phi^4}\right\} = -\frac{qa^2h^2}{3D}. \end{aligned}\right\} \quad . \quad (5)$$

These three equations will now be applied to particular cases.

§ 3. *Circular Cylindrical Shell under Internal Hydrostatic Pressure.*

In the case of a circular cylindrical shell freely supported at the edges, as shown in fig. 2, and submitted to the pressure of liquid within the cylindrical shell, we have the intensity of the load q represented by the following equations:

$$\left.\begin{aligned} q &= \gamma a(\cos\phi - \cos\alpha) \quad \text{when} \quad 0 \leqq \phi \leqq \alpha, \\ q &= 0 \qquad\qquad\qquad\quad \text{when} \quad \pi \geqq \phi \geqq \alpha, \end{aligned}\right\} \quad . \quad . \quad (6)$$

* See A. E. H. Love, *loc. cit. ante*, p. 530.

where γ is the weight of the liquid per unit volume and angles α and ϕ are shown in fig. 2. The conditions of symmetry and the conditions at the supports will be satisfied if we take the components of displacement in the form of the following series:

$$\left.\begin{aligned} u &= \Sigma\Sigma A_{mn} h \cos n\phi \cos\frac{m\pi x}{l}, \\ v &= \Sigma\Sigma B_{mn} h \sin n\phi \sin\frac{m\pi x}{l}, \\ w &= \Sigma\Sigma C_{mn} h \cos n\phi \sin\frac{m\pi x}{l}. \end{aligned}\right\} \quad . \quad . \quad . \quad . \quad (7)$$

Fig. 2.

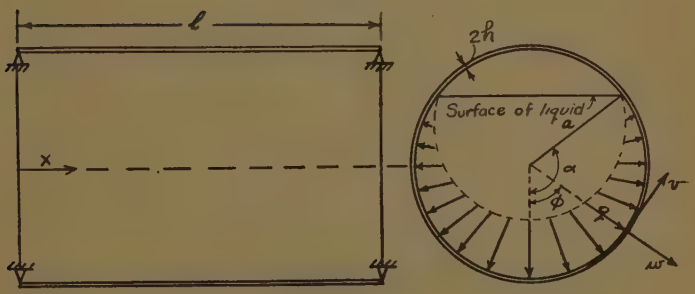

The load q also can be represented by the series

$$q = \Sigma\Sigma D_{mn} \cos n\phi \sin\frac{m\pi x}{l} \quad . \quad . \quad . \quad . \quad . \quad (8)$$

The coefficients D_{mn}, which can be readily calculated in the usual way from (6), are

$$D_{mn} = \frac{8\gamma a}{mn\pi^2(n^2-1)}[\cos\alpha \sin n\alpha - n \cos n\alpha \sin\alpha], \quad (9)$$

where $m = 1.3.5 \ldots .$, and $n = 2.3.4 \ldots .$, while

$$D_{mo} = \frac{4\gamma a}{m\pi^2}(\sin\alpha - \alpha\cos\alpha), \quad . \quad . \quad . \quad (10)$$

and

$$D_{m1} = \frac{2\gamma a}{m\pi^2}(2\alpha - \sin 2\alpha). \quad . \quad . \quad . \quad . \quad (11)$$

In the case of a cylindrical shell completely filled with liquid we denote by $z\gamma$ the pressure at the axis of the cylindrical shell (see fig. 3); then

$$q=\gamma(z+a\cos\phi), \quad . \quad . \quad . \quad . \quad . \quad (12)$$

and we obtain instead of (9), (10), (11):

$$\left.\begin{aligned} &D_{mn}=0,\\ &D_{mo}=\frac{4\gamma z}{m\pi},\\ &D_{m1}=\frac{4\gamma a.}{m\pi} \end{aligned}\right\} \quad . \quad . \quad . \quad . \quad . \quad (13)$$

Fig. 3.

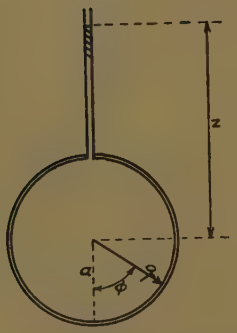

Substituting (7) and (8) into (5), and introducing the notation:

$$\lambda=\frac{l}{a}; \quad \eta=\frac{h}{l};$$

we obtain

$$\left.\begin{aligned} &A_{mn}[2m^2\pi^2+(1-\sigma)\lambda^2n^2]-B_{mn}(1+\sigma)\lambda mn\pi\\ &\qquad -C_{mn}2\sigma\lambda m\pi=0,\\ &A_{mn}3(1+\sigma)\lambda mn\pi-B_{mn}[3(1-\sigma)m^2\pi^2+6\lambda^2n^2]\\ &\qquad -C_{mn}2\lambda^2n[3+\eta^2(m^2\pi^2+\lambda^2n^2)]=0,\\ &A_{mn}3\sigma\lambda m\pi-B_{mn}\lambda^2n[3+\eta^2\{(2-\sigma)m^2\pi^2+\lambda^2n^2\}]\\ &\qquad -C_{mn}[3\lambda^2+\eta^2(m^2\pi^2+\lambda^2n^2)^2]=-\frac{D_{mn}l^2h}{D}. \end{aligned}\right\} \quad (14)$$

Since D_{mn} is known from equations (9), (10), (11), or (13), coefficients A_{mn}, B_{mn}, C_{mn} can be calculated in each particular case from (14) for any value of m and n, and therefore the stress-resultants, stress-couples, and components of displacement can be found for any point of the cylindrical shell by using equations (3), (4), and (7).

§ 4. *Numerical Examples.*

The above theoretical solution will now be applied to the case of a cylindrical shell full of liquid and pressure $a\gamma$ at the axis, and with the following numerical data :

$$a=50 \text{ cm.}; \quad l=25 \text{ cm.};$$

$$h=3{\cdot}5 \text{ cm.}; \quad \sigma={\cdot}3 \text{ cm.};$$

Then

$$\alpha=\pi;$$

$$\lambda=\frac{l}{a}={\cdot}5; \quad \lambda^2={\cdot}25;$$

$$\eta=\frac{h}{l}={\cdot}14; \quad \eta^2={\cdot}0196.$$

From (13) we obtain

$$D_{mo}=D_{m1}=\frac{4\gamma a}{m\pi}, \text{ where } m=1.3.5\ldots,$$

and $\quad D_{mn}=0, \quad \text{for } n>1.$

Beginning with the terms $n=0$; $m=1.3.5\ldots$ of the series (7), and using the notation

$$\Psi=\frac{4\cdot a}{\pi^2}\cdot\frac{l^2h}{D},$$

the solution of equations (14) is found to be

$$\left.\begin{aligned} A_{mo}&=\frac{\Psi\lambda\sigma}{3m^2\left[\lambda^2(1-\sigma^2)+\frac{\eta^2}{3}m^4\pi^4\right]},\\ B_{mo}&=0,\\ C_{mo}&=\frac{\Psi\pi}{3m\left[\lambda^2(1-\sigma^2)+\frac{\eta^2}{3}m^4\pi^4\right]}. \end{aligned}\right\} \quad \ldots \quad (15)$$

From equations (15) A_{mo}, B_{mo}, and C_{mo} may be found for any value of m. These values for $m=1$, 3, and 5 are compiled in Table I.

In order to find the coefficients A_{m1}, B_{m1}, C_{m1} we put $n=1$ in equations (14), and find, after letting $A'_{m1}=A_{m1}.m$, from the first of equations (14) that

$$C_{m1}=A'_{m1}\left[20{\cdot}94+{\cdot}1857\,\frac{1}{m^2}\right]-B_{m1}\,2{\cdot}167. \quad . \quad (16)$$

TABLE I.

$n=0$.

m.	$A_{mo}\psi^{-1}\times10^3$.	$B_{mo}\psi^{-1}\times10^3$.	$C_{mo}\psi^{-1}\times10^3$.	$A'_{mo}\psi^{-1}\times10$.
1 ...	57·88	0	1212	57·88
3 ...	·1073	0	6·742	·3219
5 ...	·005025	0	·5263	·0251

Eliminating C_{m1} from the last two of equations (14), and using the notation

$$\left.\begin{aligned} p_{m1}&=m^2(25{\cdot}36+2{\cdot}026\,m^2)+{\cdot}2790,\\ q_{m1}&=m^2(1{\cdot}755-20{\cdot}52\,m^2),\\ r_{m1}&=14{\cdot}29\,m^2+{\cdot}1393+({\cdot}4105\,m^2+{\cdot}003639)\\ &\qquad\times({\cdot}25+9{\cdot}870\,m^2)^2,\\ s_{m1}&=m^2[{\cdot}8738-{\cdot}08221\,m^2+{\cdot}04247({\cdot}25+9{\cdot}870\,m^2)^2], \end{aligned}\right\} \quad (17)$$

we find the following equations for calculating A'_{m1} and B_{m1}:

$$\left.\begin{aligned} A'_{m1}p_{m1}-B_{m1}q_{m1}&=0,\\ A'_{m1}r_{m1}-B_{m1}s_{m1}&=\Psi\pi m. \end{aligned}\right\} \quad . \quad . \quad . \quad . \quad (18)$$

For any value of m we may first calculate p_{m1}, q_{m1}, r_{m1}, s_{m1} from equations (17), and then the coefficients A'_{m1}, B_{m1} are found from (18), after which C_{m1} is found from (16). Values of $A'_{m1}\,\Psi^{-1}\times10^3$, $B_{m1}\,\Psi^{-1}\times10^3$, and $C_{m1}\,\Psi^{-1}\times10^3$, for $m=1$, 3, and 5 are compiled in Table II.

Having the coefficients A_{mo}, A_{m1} . . . . C_{m1}, the stress-resultants and stress-couples will be calculated as follows:

From equations (3), (4), and (7) it is seen that

$$\left.\begin{aligned} T_2 &= \frac{3D\Psi}{lh}\Sigma\Sigma T_{mn}\cos n\phi \sin\frac{m\pi x}{l} \\ \text{and} \\ G_2 &= \frac{Dh\Psi}{l^2}\Sigma\Sigma G_{mn}\cos n\phi \sin\frac{m\pi x}{l}, \end{aligned}\right\} \quad . \quad . \quad (19)$$

TABLE II.

$n=1$.

m.	p.	q.	r.	s.	πm.	$A'_{m1}\psi^{-1}\times10^3$.	$B_{m1}\psi^{-1}\times10^3$.	$C_{m1}\psi^{-1}\times10^3$.
1 ..	27·66	− 18·76	56·84	5·140	3·142	48·76	−71·90	1186
3 ..	392·6	− 1646	29470	3034	9·425	·3121	− ·07444	6·705
5 ..	1900	−12780	626600	64740	15·71	·02469	− ·003671	·5252

where

$$T_{mn}=\Psi^{-1}[-A_{mn}\sigma m\pi+B_{mn}\lambda n+C_{mn}\lambda],$$

$$G_{mn}=\Psi^{-1}[B_{mn}\lambda^2 n+C_{mn}(\sigma m^2\pi^2+\lambda^2 n^2)].$$

Values of $T_{mn}\times10^3$ and $G_{mn}\times10^3$, for $n=0$, 1, and $m=1$, 3, 5, are compiled in Table III.

TABLE III.

	$m=1$.		$m=3$.		$m=5$.	
n....	$T_{1n}\times10^3$	$G_{1n}\times10^3$	$T_{3n}\times10^3$	$G_{3n}\times10^3$	$T_{5n}\times10^3$	$G_{5n}\times10^3$
0....	551·5	3589	3·068	179·7	·2394	38·95
1....	511·2	3791	3·021	180·3	·2375	39·01

Maximum values of w, T_2, G_2, T_1, and G_1 occur at $x=l/2$, $\phi=0$, and will now be computed. Substituting in the third of equations (7)

$$x=\frac{l}{2},\ \phi=0,\ m=1,\ 3 \text{ and } 5, \text{ and } n=0,\ 1,$$

we obtain

$$w_{max.} = h(C_{10} + C_{11} - C_{30} - C_{31} + C_{50} + C_{51}).$$

Similarly from (19):

$$T_{2max.} = \frac{3D\Psi}{lh}(T_{10} + T_{11} - T_{30} - T_{31} + T_{50} + T_{51}),$$

and $$G_{2max.} = \frac{Dh\Psi}{l^2}(G_{10} + G_{11} - G_{30} - G_{31} + G_{50} + G_{51}).$$

In the same manner we obtain

$$G_1 = \frac{D\Psi h}{l^2} \Sigma\Sigma G'_{mn} \cos n\phi \sin \frac{m\pi x}{l},$$

$$T_1 = \frac{3D\Psi}{hl} \Sigma\Sigma T'_{mn} \cos n\phi \sin \frac{m\pi x}{l},$$

where $$G'_{mn} = \Psi^{-1}[B_{mn}\sigma\lambda^2 n + C_{mn}(m^2\pi^2 + \sigma\lambda^2 n^2)],$$

$$T'_{mn} = \Psi^{-1}[-A_{mn} m\pi + B_{mn}\sigma\lambda n + C_{mn}\sigma\lambda].$$

Values of G'_{mn} and T'_{mn}, for $n=0$, 1 and $m=1$, 3, 5, are given in Table IV.

TABLE IV.

	$m=1.$		$m=3.$		$m=5.$	
n....	$T'_{1n}\times 10^3$	$G'_{1n}\times 10^3$	$T'_{3n}\times 10^3$	$G'_{3n}\times 10^3$	$T'_{5n}\times 10^3$	$G'_{5n}\times 10.$
0....	0	11960	0	598·9	0	129·9
1....	13·93	11790	−1·946	596·1	−·309	129·7

With the aid of the above equations and Tables I. to IV. inclusive we find:

$$w_{max.} = 11{,}790 \cdot \frac{\gamma}{E} \text{ cm.}; \quad T_{2max.} = 1.607\gamma \text{ kg./cm.};$$

$$G_{2max.} = 1.762\gamma \text{ kg.}; \quad T_{1max.} = .02367\gamma \text{ kg./cm.}$$

$$G_{1max.} = 5.663\gamma \text{ kg.}$$

$$\text{Max. circum. stress} = \frac{T_{2max.}}{2h} + \frac{3}{2}\frac{G_{2max.}}{h^2} = .4453\gamma \text{ kg./cm}^2.$$

$$\text{Max. long. stress} = \frac{T_{1\,max.}}{2h} + \frac{3}{2}\frac{G_{1\,max.}}{h^2} = .6968\gamma \text{ kg./cm}^2.$$

It is seen that for the cylindrical shell chosen the resulting maximum stresses for the case of the cylindrical

shell full of liquid are negligible from the practical point of view. Due to the comparatively large value of $G_{1max.}$ the maximum longitudinal stress is greater than the maximum circumferential stress.

If the cylindrical shell full of liquid is subjected to a pressure $z\gamma$ at its axis (see fig. 3), then from equations (13)

$$D_{m_0}=\frac{4\gamma z}{m\pi}; \quad D_{m_1}=\frac{4\gamma a}{m\pi};$$

while $D_{mn}=0$ for $n>1$.

Since the value of D_{m1} for this case is the same as the value of D_{m1} for the case of the cylindrical shell full of liquid and pressure $a\gamma$ at its axis, we may use Table II. to obtain the coefficients $A_{m1}\times\Psi^{-1}\times 10^3$, $B_{m1}\Psi^{-1}\times 10^3$, $C_{m1}\times\Psi^{-1}\times 10^3$.

Also, since $D_{mo}=\frac{4\gamma z}{m\pi}=\frac{z}{a}\cdot\frac{4\gamma a}{m\pi}$, we may use Table I. to obtain the coefficients

$$A_{mo}\left(\frac{z}{a}\Psi\right)^{-1}\times 10^3,\ B_{mo}\left(\frac{z}{a}\Psi\right)^{-1}\times 10^3,$$

and

$$C_{mo}\left(\frac{z}{a}\Psi\right)^{-1}\times 10^3.$$

It is seen that the coefficients $A_{mo}\psi^{-1}\times 10^3$ and $C_{mo}\psi^{-1}\times 10^3$ for this case will be z/a times those given in Table I. Also the coefficients $T_{mo}\times 10^3$ and $G_{mo}\times 10^3$ will be z/a times those given in Table III., while $T_{m1}\times 10^3$ and $G_{m_1}\times 10^3$ will remain the same as those given in Table III.

The maximum values of T_2, G_2, T_1, and G_1 occur at $x=l/2$ and $\phi=0$. For the case where $z/a=100$ they are

$$T_{2max.}=84{\cdot}17\gamma \text{ kg./cm.}; \quad G_{2max.}=86{\cdot}49\gamma \text{ kg.};$$

$$T_{1max.}={\cdot}02367\gamma \text{ kg./cm.}; \quad G_{1max.}=288\gamma \text{ kg.}$$

From which the maximum stresses are found to be

$$\text{Max. circum. stress} = 22{\cdot}61\ \gamma \text{ kg./cm.}^2.$$

$$\text{Max. long. stress} = 35{\cdot}27\ \gamma \text{ kg./cm.}^2.$$

It is seen that the maximum longitudinal stress is also the maximum stress in the cylindrical shell which we are considering.

In examining Tables I. to IV. inclusive it is observed that the coefficients A_{mn} . . . . G_{mn} diminish rapidly, so

that the series representing the stress-resultant, stress-couples, and components of displacement evaluated on the basis of $n=0$, 1 and $m=1$, 3, 5 give fairly accurate results. However, in the case of a long, thin, cylindrical shell having, say, $\lambda=8$ and $\eta=1/800$, it is found that the coefficients A_{mn} . . . . G_{mn} diminish rather slowly, so that it is necessary to compute a somewhat large number of coefficients in order that the series representing the stress-resultants, stress-couples, and components of displacement when evaluated will yield results of sufficient accuracy.

As a second example * we take the case of a cylindrical shell freely supported at its edges, loaded as shown in fig. 4. The data for this cylindrical shell is

$a=48$ cm. ; $l=27{\cdot}6$ cm. ;
$h=3{\cdot}4$ cm. ; $\sigma={\cdot}3$ cm. ;
$E=2{\cdot}2\times10^6$kg./cm.^{2} ; $Z=160$ kg./cm.^{2}.

Fig. 4.

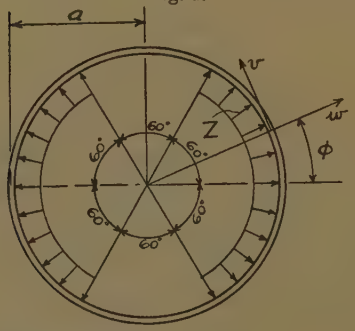

Equations (17) for this case become

$$\left.\begin{aligned}
p_{mn}&=n^2[m^2(869+53{\cdot}89m^2+9{\cdot}749n^2)\\
&\qquad+n^2(50{\cdot}63+{\cdot}3387n^2)],\\
q_{mn}&=m^2[m^2(12{\cdot}82n^2-309{\cdot}6)+n^2(138{\cdot}3\\
&\qquad+1{\cdot}718n^2)],\\
r_{mn}&=16{\cdot}44m^2+{\cdot}8472n^2+{\cdot}0280(9{\cdot}870m^2\\
&\qquad+{\cdot}4629n^2)\times(1{\cdot}323n^2+9{\cdot}870m^2)^2,\\
s_{mn}&=m^2[2{\cdot}314+10^{-2}\{6{\cdot}576(1{\cdot}323n^2+9{\cdot}870m^2)^2\\
&\qquad-1{\cdot}327n^2-16{\cdot}84m^2\}],
\end{aligned}\right\}\quad . \quad (17')$$

* This example was discussed by H. Reissner in *Zeit. f. ang. Math. u. Mech.* xiii. p. 136–138 (1933).

while equations (18) become

$$\left.\begin{aligned} -\alpha'_{mn}\, p_{mn}+\beta'_{mn}\, q_{mn}&=0,\\ \alpha'_{mn}\, r_{mn}-\beta'_{mn}\, s_{mn}&=\Phi\,\frac{3m}{n}\sin\left(\frac{2\pi n}{3}\right),\end{aligned}\right\} \quad . \quad . \quad (18')$$

where $\alpha'_{mn}=a_{mn}.m$ and $\beta'_{mn}=\beta_{mn}.n$ and $\Phi=1{\cdot}10\ Z\times 10^{-5}$. Tables computed on the basis of the above equations and data follow (see Tables V., VI., VII., and VIII.).

TABLE V.

$n=0$.

m.	$\alpha'_{mo}\Phi^{-1}$.	$\gamma_{mo}\Phi^{-1}$.
1.....	·07245	1·320
3.....	·0004766	·00868
5.....	·00003731	·000679

By using these tables we find

$$x=\frac{l}{2}\begin{cases}\phi=0;\ \dfrac{w}{\Phi\bar{h}}=2{\cdot}000;\ \dfrac{w}{Z}=7{\cdot}512\times10^{-5};\\ \phi=\dfrac{\pi}{2};\ \dfrac{w}{\phi\bar{h}}={\cdot}02362;\ \dfrac{w}{Z}={\cdot}08871\times10^{-5};\end{cases}$$

$$x=\frac{l}{2}\begin{cases}\phi=0;\ \mathrm{P}_2=\dfrac{3C\Phi}{lh}1{\cdot}021;\ \dfrac{\mathrm{P}_2}{Z}=22{\cdot}84;\\ \phi=\dfrac{\pi}{2};\ \mathrm{P}_2=\dfrac{3C\Phi}{lh}{\cdot}2164;\ \dfrac{\mathrm{P}_2}{Z}=4{\cdot}840;\end{cases}$$

$$x=\frac{l}{2}\begin{cases}\phi=0;\ \mathrm{G}_2=\dfrac{Ch\Phi}{l^2}(-5{\cdot}492);\ \dfrac{\mathrm{G}_2}{Z}=-17{\cdot}15;\\ \phi=\dfrac{\pi}{2};\ \mathrm{G}_2=\dfrac{Ch\Phi}{l^2}1{\cdot}362;\ \dfrac{\mathrm{G}_2}{Z}=4{\cdot}254.\end{cases}$$

From which

$\mathrm{P}_{2\max.}=3655$ kg./cm. ; $\mathrm{G}_{2\max.}=-2745$ kg. at $\phi=0$;

$\sigma_{\max.}=893{\cdot}7$ kg./cm.^{2} *.

* These results are different from those calculated by Reissner. The difference comes from the numerical mistake made by him in calculating the coefficients of α'_{mn} and β'_{mn} in equations (18').

TABLE VI.

$m=1$.

n.	p.	q.	r.	s.	$\frac{3}{n}\sin\frac{2\pi n}{3}$.	$\alpha'_{1n}\Phi^{-1}\times 10^3$.	$\beta'_{1n}\Phi^{-1}\times 10^3$.	$\gamma_{1n}\Phi^{-1}\times 10^3$.
1	983·6	− 156·8	53·53	10·37	2·598	21·91	−137·4	1013
2	4679	322·4	95·26	17·21	−1·299	8·409	122·1	− 347·0
4	31610	2548	495·8	65·25	·6495	− 2·071	− 25·69	45·30
5	66100	4543	1144	123·0	− ·5196	·8046	11·71	− 18·90

TABLE VII.

$m=3$.

n.	p.	q.	r.	s.	$\frac{9}{n}\sin\frac{2\pi n}{3}$.	$\alpha'_{3n}\Phi^{-1}\times 10^4$.	$\beta'_{3n}\Phi^{-1}\times 10^4$.	$\gamma_{3n}\Phi^{-1}\times 10^4$.
1	12330	−22780	20470	4817	7·794	3·378	−1·827	69·76
2	50980	−15700	22640	5249	−3·897	− ·9819	3·188	−32·07
4	231800	15410	32760	7165	1·949	− ·2598	−3·908	11·81
5	396400	41670	41940	8797	−1·559	·3733	3·552	− 7·706

TABLE VIII.

	$m=1$.		$m=3$.		$m=5$.	
n..	$P_{1n}\times10^3$	$G_{1n}\times10^3$	$P_{3n}\times10^4$	$G_{3n}\times10^4$	$P_{5n}\times10^4$	$G_{5n}\times10^4$
0..	690·4	3907	45·42	2313	3·555	502·9
1..	403·9	4250	34·83	1950		
2..	−67·11	−2873	−13·85	−1022		
3..	0	0	0	0		
4..	− 1·543	1076	2·540	561·9		
5..	1·838	− 673·1	− ·6983	− 457·8		

The above value of $\sigma_{max.}$ gives the maximum circumferential stress. In order to find the maximum longitudinal stress we write P_1 and G_1 in the following forms :

$$P_1=\frac{3C\Phi}{lh}\,\Sigma\Sigma\,P'_{mn}\cos 2n\phi\sin\frac{m\pi x}{l},$$

$$G_1=\frac{Ch\Phi}{l^2}\,\Sigma\Sigma\,G'_{mn}\cos 2n\phi\sin\frac{m\pi x}{l},$$

where values of P'_{mn} and G'_{mn} are compiled in Table IX. for different values of m and n.

TABLE IX.

	$m=1$.		$m=3$.		$m=5$.	
n..	$P'_{1n}\times10^3$	$G'_{1n}\times10^3$	$P'_{3n}\times10^3$	$G'_{3n}\times10^3$	$P'_{5n}\times10^3$	$G'_{5n}\times10^3$
0..	0	12990	0	765	0	166
1..	58·5	10370	·08	622·5		
2..	−44·1	−3950	−·135	−290		
3..	0	0	0	0		
4..	5·46	730	·15	112·3		
5..	− 1·75	− 371·7	−·1277	− 76		

From the above equations for P_1 and G_1 we find, with the aid of Table IX., that the maximum values of these quantities occur at $x=l/2$ and $\phi=0$. They are

$$P_{1max.}=64\cdot4\text{ kg./cm. ; }G_{1max.}=9325\text{ kg.;}$$

and therefore

$$\text{Max. long. stress}=\frac{P_{1max.}}{2h}+\frac{3}{2}\frac{G_{1max}}{h^2}$$

$$=1219\text{ kg./cm.}^2,$$

which is also the maximum stress in the cylindrical shell under consideration.

§ 5. *Deflexion of Portion of Cylindrical Shell* *.

Equations (5) will now be applied to the case of a plate in the form of a curvilinear rectangle (see fig. 5) cut out by two diametral planes and two cross-sections perpendicular to the axis of the portion of the cylindrical shell. This curvilinear plate is supported along its four edges, and is acted upon by a uniform intensity of internal pressure q.

Fig. 5.

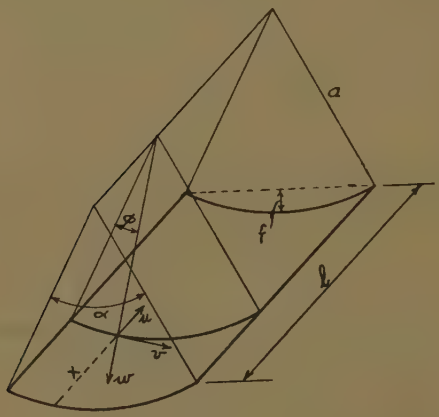

The components of displacement will be represented in the form of the following series :—

$$\left.\begin{aligned} u &= \Sigma\Sigma A_{mn} \sin\frac{n\pi\phi}{\alpha}\cos\frac{m\pi x}{l}, \\ v &= \Sigma\Sigma B_{mn} \cos\frac{n\pi\phi}{\alpha}\sin\frac{m\pi x}{l}, \\ w &= \Sigma\Sigma C_{mn} \sin\frac{n\pi\phi}{\alpha}\sin\frac{m\pi x}{l}, \end{aligned}\right\} \quad . \quad . \quad . \quad . \quad (20)$$

* See S. Timoshenko, 'Theory of Elasticity,' ii. pp. 386–387 (St. Petersburg, 1916).

and q in the case of uniformly distributed load is

$$q=\Sigma\Sigma\, D_{mn}\sin\frac{n\pi\phi}{\alpha}\sin\frac{m\pi x}{l}, \quad . \quad . \quad . \quad (21)$$

where

$$D_{mn}=\frac{16q}{\pi^2}\cdot\frac{1}{mn}, \quad . \quad . \quad . \quad . \quad . \quad . \quad (22)$$

$$m=1.3.5.... \quad \text{and} \quad n=1.3.5....$$

It is seen from equations (3), (4), and (20) that along the edges cut out by the cross-sections, *i. e.*, the curved edges of the plate,

$$w=0\,; \quad v=0\,; \quad T_1=0\,; \quad G_1=0,$$

while along the edges cut out by the diametral planes, *i. e.*, the straight edges of the plate,

$$w=0\,; \quad u=0\,; \quad T_2=0\,; \quad G_2=0.$$

Thus conditions on the simply supported edges are satisfied. Substituting equations (20) and (21) into equations (5), we obtain

$$\left.\begin{aligned}
&A_{mn}\pi\left[\left(\frac{am}{l}\right)^2+\frac{1-\sigma}{2}\left(\frac{n}{\alpha}\right)^2\right]+B_{mn}\pi\cdot\frac{1+\sigma}{2}\cdot\frac{am}{l}\cdot\frac{n}{\alpha}\\
&\qquad -C_{mn}\sigma\cdot\frac{am}{l}=0,\\
&A_{mn}\pi\frac{am}{l}\cdot\frac{n}{\alpha}\cdot\frac{1+\sigma}{2}+B_{mn}\pi\left[\frac{1-\sigma}{2}\left(\frac{am}{l}\right)^2+\left(\frac{n}{\alpha}\right)^2\right]\\
&\qquad -C_{mn}\frac{n}{\alpha}\left[1+\frac{\pi^2h^2}{3a^2}\left\{\left(\frac{am}{l}\right)^2+\left(\frac{n}{\alpha}\right)^2\right\}\right]=0,\\
&A_{mn}\sigma\pi\frac{am}{l}+B_{mn}\frac{n\pi}{\alpha}\left[1+\frac{\pi^2h^2}{3a^2}\left\{(2-\sigma)\left(\frac{am}{l}\right)^2\right.\right.\\
&\qquad \left.\left.+\left(\frac{n}{\alpha}\right)^2\right\}\right]-C_{mn}\left[1+\frac{\pi^4h^2}{3a^2}\left\{\left(\frac{am}{l}\right)^2+\left(\frac{n}{\alpha}\right)^2\right\}^2\right]\\
&\qquad =-\frac{D_{mn}a^2(1-\sigma^2)}{2Eh}.
\end{aligned}\right\} \quad . \quad (23)$$

With D_{mn} known from (22) the coefficients A_{mn}, B_{mn}, and C_{mn} may be found from equations (23) for any value of m and n. Then the stress-resultants, stress-couples, and components of displacement may be found at any point of the curvilinear plate under consideration from (3), (4), and (20).

If α is a small angle and $\alpha a=l$, then if we let $\mu=f/h$, where f is the sag (see fig. 5) of the curvilinear plate, we may compile Table X.

The maximum deflexion of this small plate is at $x=l/2$, $\phi=\alpha/2$. From equations (20)

$$w_{\max.}=\Sigma\Sigma C_{mn}\sin\frac{n\pi}{2}\sin\frac{m\pi}{2};$$

putting $m=1.3.5$ and $n=1.3.5$,

$$w_{\max.}=C_{11}-C_{13}+C_{15}-C_{31}+C_{33}-C_{35}+C_{51}-C_{53}+C_{55}. \quad (24)$$

The magnitude of the maximum deflexion we put in the following form:

$$w_{\max.}=\beta\frac{ql^4}{D},$$

TABLE X.

μ.	0.	·5.	1.	2.	4.	7.	12.
$C_{11}\times\left(\frac{ql^4}{D}\right)^{-1}\times10^5$	416·0646	404·7218	374·1236	287·2545	148·9311	64·0777	24·2702
C_{13} " "	5·5475	5·5473	5·5465	5·5436	5·5317	5·4992	5·4078
C_{31} " "	5·5475	5·5275	5·4681	5·2428	4·5012	3·2406	1·7941
C_{33} " "	·5707	·5705	·5699	·5676	·5584	·5345	·4759
C_{15} " "	·4924	·4924	·4924	·4924	·4924	·4923	·4921
C_{51} " "	·4924	·4921	·4912	·4876	·4738	·4395	·3639
C_{35} " "	·0960	·0960	·0960	·0959	·0958	·0955	·0945
C_{53} " "	·0960	·0960	·0959	·0957	·0947	·0922	·0856
C_{55} " "	·0266	·0266	·0266	·0266	·0266	·0264	·0260

where β is a numerical value depending on the ratio $\mu=f/h$. The values of β calculated from (24) to five decimal places are given in Table XI.

TABLE XI.

μ.	0.	·5.	1·0.	2·0.	4·0.	7·0.	12·0.
$\beta\times10^5$ ..	406	395	364	278	140	57	18

Table XI. indicates that the deflexion of the curvilinear plate decreases rapidly as α increases until, when the ratio of the sag f to the half-thickness h of the plate is 12, the maximum deflexion of the curvilinear plate is only ·044 times as great as that of a flat plate of the same size.

C. *The Clean-up of various Gases by Magnesium, Calcium, and Barium.* *By* A. L. Reimann, *B.Sc., Ph.D., F.Inst.P.** (Communication from the Research Staff of the M.O. Valve Co., Ltd., at Wembley.)

Introduction.

IT is well known that electropositive metals, such as magnesium, calcium, barium, and sodium may, in certain circumstances, absorb or "clean up" various gases to which they are exposed, and that by the proper use of such metal "getters" the residual gas pressures in vacuum vessels may be greatly reduced. The phenomena have already been described in some detail, and their physical nature explained, in the case of the getter magnesium and the gas nitrogen †, and also in that of magnesium and hydrogen ‡. In the present paper experiments with other getter-gas pairs will be discussed, the getters used having been magnesium, calcium, and barium, and the gases oxygen, nitrogen, hydrogen, carbon monoxide, and carbon dioxide.

The clean-up of a gas may be brought about in various ways. The metal getter is usually volatilized, or "dispersed," from a small piece on to the walls of the vacuum vessel, and if gas is present in the vessel at this stage, its pressure may be found to be less after the dispersal than before. After deposition the getter may be observed to continue to clean up gas by mere contact action. Generally, however, the rate of clean-up is greatly accelerated if an electric discharge of sufficient energy is maintained in the gas.

In one or two exceptional cases, *e.g.*, that of magnesium and nitrogen, it appears that dispersal gettering is due to a trapping of the molecules of the gas in the condensing getter. The amount of clean-up accompanying dispersal varies so enormously with the nature of the getter and gas, however, that it would be difficult, in general, to attribute an important part of it to a purely mechanical action of this kind. In none of the experiments to be discussed in this paper was there any evidence of dispersal

* Communicated by C. C. Paterson, M.I.E.E.
† P. I. Lukirsky and S. W. Ptizyn, *Z. Phys.* lxxi. p. 339 (1931).
‡ A. L. Reimann, Phil. Mag. (7) xvi. p. 673 (1933).

gettering being anything but contact gettering by a series of freshly formed getter surfaces. It will therefore not be considered here as a separate phenomenon.

For the convenient quantitative study of electric-discharge gettering it is necessary that ordinary contact gettering shall not be sufficiently rapid to change the order of magnitude of the pressure during the time occupied by the experiments. This condition is fulfilled with magnesium and nitrogen, magnesium and hydrogen, and magnesium and carbon monoxide, but not with any other getter-gas pair here considered. The first two cases have already been dealt with by Lukirsky and Ptizyn * and by the author †. The case of magnesium and carbon monoxide will be discussed in the present paper.

Finally, a few cases of the reliberation of an already cleaned-up gas, in addition to that of hydrogen from magnesium previously reported by the author, have been observed.

Method used for measuring Contact Gettering.

A bulb containing the getter attached to a previously outgassed stout nickel wire was connected by glass tubing to a mercury condensation pump, evacuated, and baked at 400° C. Between the bulb and the pump was a magnetically operated mercury cut-off, and on the bulb side of this was attached a Pirani manometer, sensitive down to about 10^{-3} mm. of mercury, and in addition whatever device was necessary for admitting to the system successive small doses of the gas to be used.

For the supply of oxygen, nitrogen, or carbon dioxide, a horizontal glass tube was used, closed at one end and provided with a plug of glass wool near the other, and containing a small quantity of finely divided potassium permanganate, barium azide, or magnesium carbonate, respectively. By suitably tapping this tube it was possible to distribute the material within it as desired, and so to " bake " in stages the whole of it without heating any of the enclosed particles. The latter were subsequently heated to just below the temperature at which they decomposed, in order to drive off volatile con-

* P. I. Lukirsky and S. W. Ptizyn, *loc. cit.*
† A. L. Reimann, *loc. cit.*

taminations, such as moisture or adsorbed gas. Finally, successive small doses of gas were liberated as desired, by first suitably distributing the material along the tube and then heating with a flame one or a few of the particles nearest the plug.

For the supply of carbon monoxide a number of small glass reservoirs filled to known pressures with this gas were attached to the pump system. Each of these reservoirs had a thin-walled and fragile projection within the wide tubing which joined it to the pump system, and on this projection was mounted a soft-iron armature. The contents of a reservoir were released when desired by pulling the armature to one side and so breaking off the projection by means of an electro-magnet. The carbon monoxide with which the reservoirs were originally filled was obtained from carbon dioxide in which a tungsten filament was burned, any residue of the dioxide having been frozen out by liquid air before the reservoir was sealed off.

Hydrogen was obtained from the reducing part of a coal-gas flame and admitted by diffusion through a palladium tube to which the flame was applied.

In cases where the gas to be admitted to contact with the getter was carbon dioxide the mercury trap was cooled by freezing acetone. In all other cases it was cooled by liquid air. The reason why liquid air was not used in the experiments with carbon dioxide is that this gas condenses at liquid-air temperatures.

The magnesium and calcium getter used were cut from lengths of very pure ribbon (the calcium ribbon was specially prepared in these Laboratories), which had previously been given prolonged heat treatments in a vacuum to outgas them, the gas in question being mainly hydrogen. The cut pieces were then welded to the outgassed nickel wire carrier. In the case of calcium the piece was scraped clean after welding and immediately given a protective coating of paraffin wax. The wax was subsequently all driven by the bake into the cooler parts of the pump tubing, where its presence was not objectionable.

The barium was obtained from barium azide (BaN_6), with which the nickel wire was coated by repeated dipping into an aqueous suspension and drying in a current of warm air between dips. The bulb containing the azide-

coated wire was given a preliminary bake at 120° C. on the pump for about 10 minutes to thoroughly dry out the azide, and the temperature was then gradually increased until the azide began to decompose, which it did at an appreciable rate at about 160° C. After completion of the decomposition the oven temperature was raised to 400° C. for a further 10 minutes. This left the wire with a black deposit of finely divided barium metal. This still contained an important quantity of occluded nitrogen however. Most of this was driven out, without the loss of much barium from the wire, by heating the wire to dull redness for a few seconds. During this operation the barium could be seen to melt.

In order to obtain a rough measure of contact-gettering power in any given case the following procedure was adopted :—First, with the cut-off open, the nickel wire supporting the getter was heated by a current until a good film of the metal was deposited all over the walls of the bulb. The cut-off was then closed, a puff of gas admitted, and the fall of pressure with time due to contact gettering observed by means of the Pirani manometer, pressures being measured as deflexions of the Pirani galvanometer. Over a sufficient range the relationship between galvanometer deflexion and pressure was linear. If most of the first dose of gas was eventually gettered, successive further doses were admitted and their clean-up also observed.

The total volume enclosed on the pump system was equivalent to 900 c.c. at room temperature when the mercury trap was cooled by liquid air, and 750 c.c. when it was cooled by freezing acetone.

The apparent surface area of the getter film was about 80 cm.^{2}. A monatomic covering of this by a gas, in the sense that each surface atom of getter holds one atom of gas, would mean, therefore, the adsorption of about 10^{17} atoms of gas, or, if the gas was diatomic, 5×10^{16} molecules. It so happened that this number of molecules in a volume of $\binom{400}{750}$ c.c. corresponded to a galvanometer deflexion, for all gases except hydrogen, of $\binom{1{\cdot}0}{1{\cdot}2}$ divisions. For hydrogen it corresponded to $\binom{1{\cdot}8}{2{\cdot}1}$ divisions. Since

5×10^{16} molecules is only very roughly the quantity of gas corresponding to a monatomic layer and we are in any case concerned only with orders of magnitude, we may take 2 and 1 divisions as corresponding, sufficiently accurately, to an apparent monatomic layer of hydrogen and of other gases respectively.

Before proceeding to discuss the results obtained, it is necessary to point out the imperfections and limitations of the method. The Pirani had an important time lag, which, bearing in mind the possible accuracy of reading pressures, may be taken as 5 to 10 seconds. The Pirani readings did not, therefore, correspond to true instantaneous pressures except when the rate of change of pressure was sufficiently slow. Consequently Pirani reading/time curves are not a true measure, but only serve as a more or less rough indication of pressure/time changes. Also the quantities of gas admitted were generally measured only after admission, by the peak of the Pirani reading. Since absorption must have been going on from the moment of admission, and the maximum Pirani reading did not occur until, perhaps, 4 or 5 seconds after admission, the actual quantity admitted must always have exceeded that corresponding to the maximum Pirani reading. On the assumption that the initial unobserved rate of gettering did not greatly exceed that corresponding to the greatest negative slope of the Pirani reading/time curve, however, the former was in every case sufficiently slow to make the actual and apparent quantities of gas agree within about 30 per cent., and generally the agreement was much closer than this. It will be clear that the method was not suitable for measuring the rate of adsorption of the first monomolecular layer or two of gas. All that can definitely be asserted is that this must have been at least as great as corresponded to the apparent initial rate of clean-up. From the fact that the initial observed pressure fall was nearly always exponential with time, however, it may, perhaps, also be inferred that the surface initially kept itself nearly clean by diffusion of adsorbed gas into the interior of the getter film, and that the unobserved initial rate of clean-up was therefore *not much greater* than the apparent initial rate.

Contact-gettering Results.

The relative contact-gettering powers for the various getter-gas pairs are best shown by curves of pressure variation with time. Such curves are given in figs. 1–5.

Fig. 1.

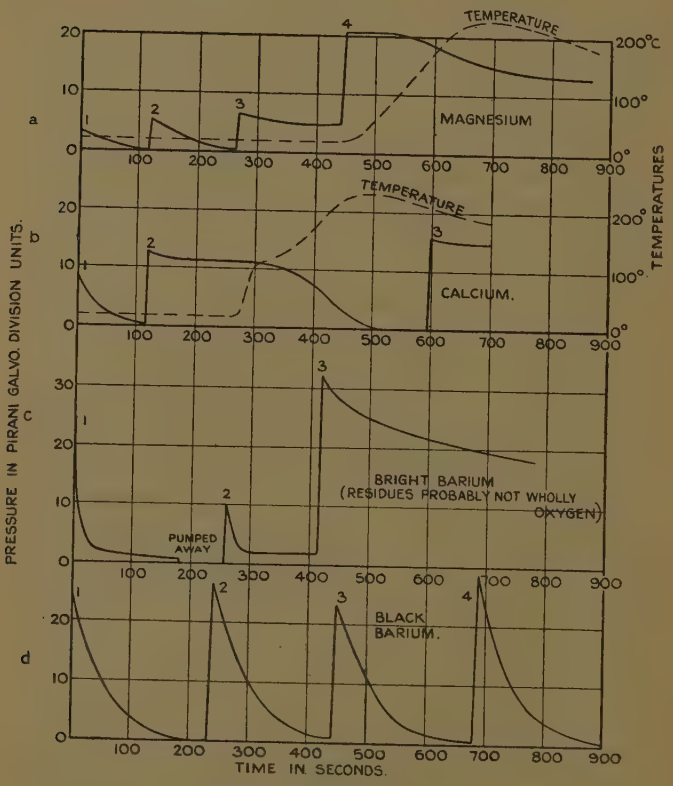

Contact gettering of oxygen.

Each diagram is concerned with one gas and up to four getters, these being magnesium, calcium, bright barium, and black barium. If the getter bulb, containing barium, was attached to the pump by wide tubing, and the dispersal carried out with extreme slowness, a bright

metallic-looking deposit of barium was always formed. If, on the other hand, narrow tubing was used and the getter was dispersed rapidly, so that the gas (nitrogen) pressure in the bulb during dispersal was relatively high,

Fig. 2.

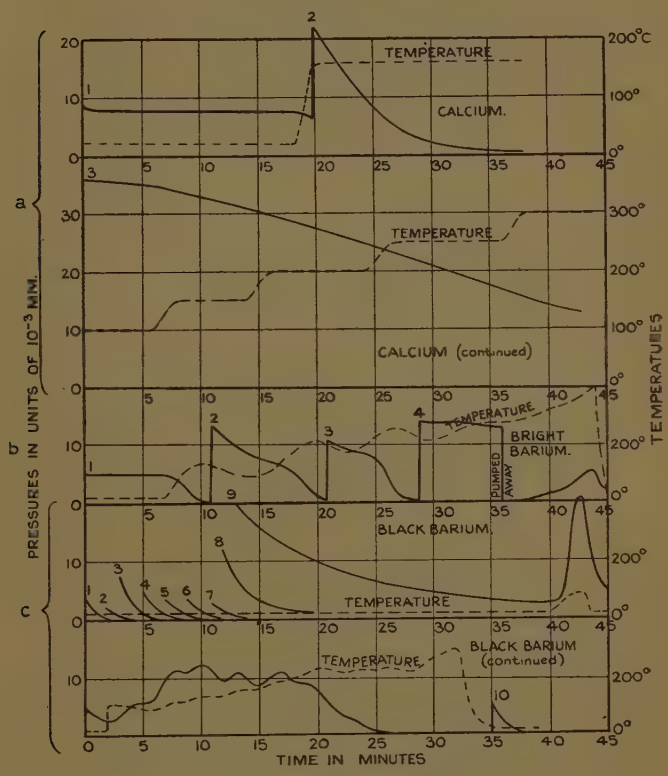

Contact gettering of nitrogen.

a black deposit was formed on the walls. It has been necessary to distinguish between the two cases, owing to the quite different gettering powers exhibited by the deposits, the black deposit being much superior in this respect to the bright one. There can be little doubt that both deposits consist essentially of barium metal,

but the appearance of the black deposit suggests that in it the barium is in a fine state of division. The

Fig. 3.

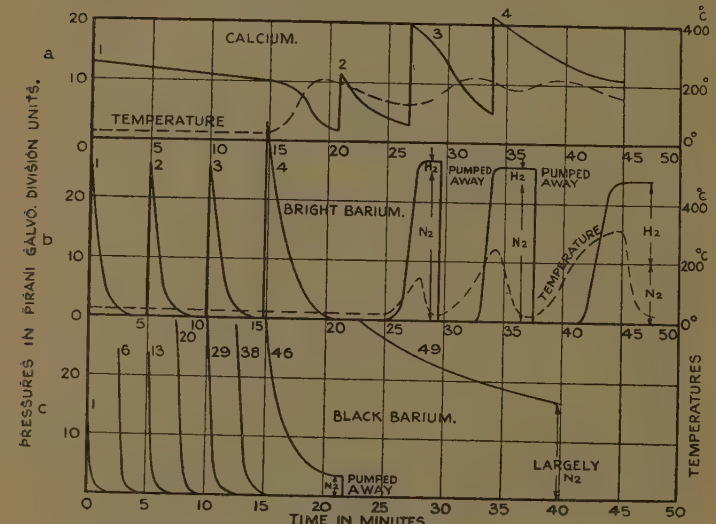

Contact gettering of hydrogen.

Fig. 4.

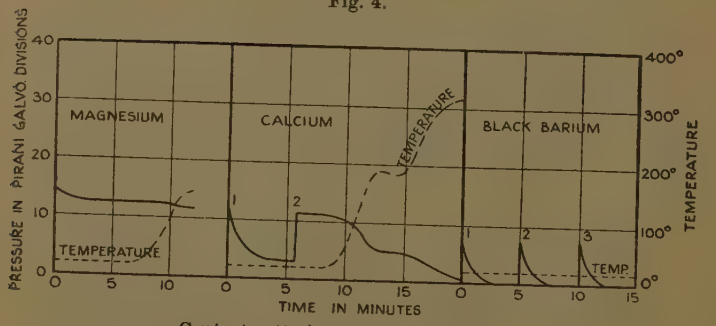

Contact gettering of carbon monoxide.

superiority of its gettering power is possibly due simply to the surface presented by it being many times that presented by the bright deposit.

In some cases, where several doses of a gas were admitted and allowed to clean up, it has been necessary to shift the time-zero for the later curves in the diagrams, in order to accommodate them. Such curves are always numbered in the order in which they were taken. In one case, that of black barium and hydrogen, only a few representative curves have been given. The amounts of gas admitted corresponding to the missing curves were of the same order as those shown.

Fig. 5.

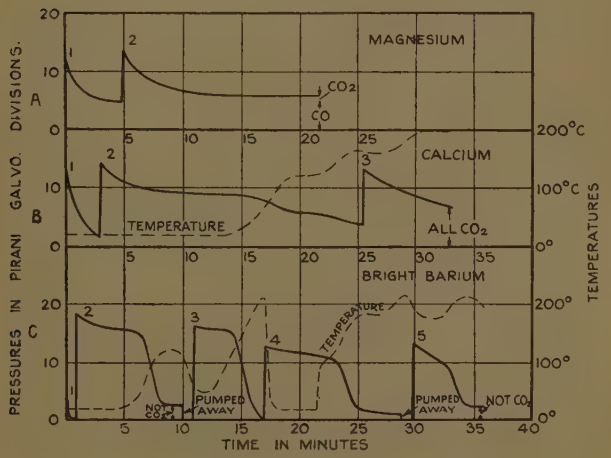

Contact gettering of carbon dioxide.

In every case the curves show the absorption of much more gas than could be accommodated in a single molecular layer on the surface of the getter deposit—at least on anything of the order of the *apparent* surface. We should expect the presence of such an adsorbed layer to have a profound effect on the condensation of any further gas, reducing its rate to a much lower order. Yet the relative rate of fall of pressure, $-\frac{1}{p}\frac{dp}{dt}$, does not generally change in order of magnitude until after several molecular layers of gas have been cleaned up. From this it seems only reasonable to infer that either (1) the condensed

gas diffuses through the getter, (2) it diffuses through a film of a chemical compound it forms with the getter at the surface, or (3) such a compound diffuses into the getter as it is formed. In any case the process can come to an end only when the most deep-seated parts of the getter have been reached, and when this happens must depend on the thickness of the deposit. In the present experiments observations were generally discontinued long before this stage had been reached.

Since diffusion enters into the phenomona, it is hardly surprising to find that they depend to quite an important degree on the temperature. Where no indication is given to the contrary, the experiments were carried out simply at room temperature. In many cases, however, the temperature was varied and interesting effects on the rate of clean-up observed. In general, the clean-up was greatly accelerated by a rise in temperature, indicating that, by helping diffusion of condensed gas to more deep-seated parts of the deposit, it tended to keep the surface of the getter clean. In some cases, however, where a large quantity of gas had already been gettered, a rise in temperature had the opposite effect, reliberating some of the already cleaned-up gas. Sometimes this was followed by a re-absorption and the final establishment of a much lower pressure than before the temperature was raised. Obviously this is due to the fact that besides liberating some gas from the surface layers of the deposit, where its concentration was high, the rise in temperature lowered this concentration by promoting diffusion into the interior. The effect of these two processes taking place simultaneously is shown beautifully, for example, in fig. 2, *c*.

In a few cases gas residues left in the bulb at various stages of the experiments were found not to be of the same nature as the gas originally admitted. This has been indicated in the diagrams. Thus a large quantity of hydrogen has been found to displace nitrogen from barium. This nitrogen undoubtedly remained occluded in the barium on the nickel wire after decomposition of the azide and was taken up by the deposit as it was formed. That the gas displaced really was nitrogen was shown by a spectroscopic test. Incidentally, in this case it appears likely that barium hydride was formed, for after the absorption of sufficient hydrogen the origin-

ally opaque deposit on the walls of the bulb became quite transparent, the only trace of it still remaining being a play of interference colours. In the case of one calcium bulb in which the calcium deposit was first made to take up a considerable quantity of hydrogen and then exposed to oxygen, some of the hydrogen was observed to be re-evolved during the absorption of oxygen at 250° C. Probably the displacement of one gas from a getter by another occurs in other cases besides these two.

A rather different phenomenon, in which also a gas residue was left which differed from that admitted, was exhibited in the case of magnesium and carbon dioxide. In addition to cleaning up some of the carbon dioxide admitted, the magnesium reduced the remainder of it to the monoxide.

The nature of the residue left after the absorption of carbon dioxide by bright barium (see fig. 5, C) was not determined. The fact that it did not condense at liquid-air temperature showed that it was not carbon dioxide. It may have been either carbon monoxide reduced from the dioxide or nitrogen displaced from the barium.

Electric-discharge Gettering of Carbon Monoxide by Magnesium.

The apparatus used for this was a simplified version of that previously employed by the author for observing the clean-up of hydrogen by magnesium. A previously outgassed nickel disk, to the centre of which was welded a small piece of outgassed magnesium, was mounted about 1·5 cm. from the top of a small bulb with the magnesium facing the glass, and behind this was an oxide-coated filament. A wire was fused through the wall of the bulb opposite the disk, and ground flush with the surface of the glass on the inside to make contact with the magnesium film later to be deposited. The bulb was attached by wide tubing to a sensitive Pirani manometer. Carbon monoxide could be admitted to the system in given doses from small glass reservoirs, communication with which was established as required by means of magnetic glass-breaking devices.

After the apparatus had been baked at 400° C. on the pump, the filament was lit to break down the carbonates

in the coating to oxides, and a light deposit of magnesium was brought down by induction heating of the disk. The apparatus was then sealed off. Next, the filament was activated by passing an electron current from it to the disk, and finally the disk was bombarded sufficiently heavily to bring down more magnesium. When a thick deposit had been formed on the glass in this way the apparatus was ready for use.

A little carbon monoxide was now admitted to the apparatus by establishing communication with one of the reservoirs, and the rate of contact gettering observed. After about $0{\cdot}25/\rho$ of a monomolecular layer of the gas had been cleaned up non-electrically, where ρ was the ratio of true to apparent surface area of the magnesium film, a discharge was passed with the disk held at 22 volts positive and the getter film at 5 volts negative to the centre of the filament, and the increase in the rate of disappearance of the gas noted. The corresponding current in the getter circuit was such as to show that something like four ions were taken up by the getter out of every five neutralized at its surface. The discharge was continued under the same conditions until a total of about $0{\cdot}4/\rho$ of a monomolecular layer of gas had been cleaned up. The potential of the disk with respect to the filament was then increased from $+22$ to $+100$ volts, and the efficiency of discharge clean-up again determined. It was now found that about two out of every three ions reaching the getter surface were held by it. Thus in both cases the number of ions electrically cleaned up was of the same order as the number that reached the getter surface. That the former was somewhat less than the latter can be plausibly attributed to the already existing contamination of the magnesium film. There is no indication of a dependence of the efficiency of discharge clean-up on the anode potential.

In view of the observation of Lukirsky and Ptizyn that with nitrogen a current begins to flow in the getter circuit when the potential of the anode relative to the filament is only about half the ionization potential of the gas, this being associated with the formation of metastable molecules, an analogous phenomenon was looked for in this case. In order to make the test more sensitive, another dose of carbon monoxide, about five times as great as the previous one, was first admitted.

It was then found that a current in the getter circuit first became noticeable when the anode potential was only 11 volts, *i. e.*, 3 volts less than the ionization potential of carbon monoxide, although considerably greater than that necessary to form metastable CO molecules. As the anode voltage was increased beyond 11, the getter current rose fairly rapidly and showed an abnormally large increase at about 18 volts. This is 4 volts above the ionization potential. The apparatus was, however, hardly suitable for finding critical potentials with any great accuracy, and in view of this it seems probable that the critical potentials found corresponded to, although they were by no means equal to, that necessary for excitation of the molecules to the metastable state and for ionization respectively. Incidentally, in a later test, using the same apparatus with *nitrogen*, a current in the getter circuit was first observed at 12 volts anode potential, as against 8 volts found by Lukirsky and Ptizyn. The appearance of a getter current at a voltage below the ionization potential of carbon monoxide is undoubtedly due to the same effect as in the case of nitrogen, viz., the liberation of electrons from the magnesium by incident metastable molecules.

It was not possible to test for the absorption of metastable CO molecules by the getter, owing to the masking effect of the contact absorption of ordinary CO. An acceleration in the rate of clean-up due to the discharge was first detectable with certainty at an anode potential of 20 volts.

Liberation of cleaned-up Gas by Electron Bombardment.

Gettered carbon monoxide was found to be knocked off from magnesium by electrons in the same way as hydrogen. A quite appreciable effect was noted with impinging electrons as slow as 6 volts.

A similar effect was tried for in the case of nitrogen which had been cleaned up on to magnesium by means of an ionizing discharge. No effect was observed, however, even at 100 volts. This is not surprising, since, as Lukirsky and Ptizyn have found, nitrogen cleaned up by an ionizing discharge combines with magnesium, forming the nitride, Mg_3N_2. One would not expect such a compound to be dissociated, even

by quite fast electrons. Nitrogen has not been found to be gettered by magnesium appreciably except by an electric discharge, so there is practically no adsorbed or dissolved nitrogen to be dislodged.

We have seen, however, that nitrogen is freely contact-gettered by barium, and that subsequently it may either be driven off thermally or displaced by another gas. From this it may be inferred that nitrogen contact-gettered by barium does not combine with it, but is merely adsorbed and then goes into solution. It might be expected, therefore, that impinging electrons of sufficient energy would dislodge such of the gas as is still on the surface.

The results of experiments with a valve having a barium getter, derived from azide, and therefore containing nitrogen, seem to fulfil this expectation.

In a valve in operation there may be either one or two possible stable potentials for an electrically floating getter film. One such potential is always very near that of the cathode. But if the anode potential is high enough there will also be a possible stable potential of the getter film somewhere between that of the cathode and that of the anode—in general rather nearer the latter. The existence of this upper stable potential depends primarily on secondary electron emission. Its exact value will depend not only on the condition of the getter surface and the electrode potentials, but also on the geometry of the valve and the distribution of space charge within it, and it may be affected to some extent also by conditions of illumination. When it is established, the rate at which stray electrons are absorbed by the getter film is exactly balanced by the rate at which secondary electrons plus photo-electrons permanently leave it and are collected by the anode. Which of the two getter potentials is established, supposing them both to be possible, depends on the way the operation of the valve is started. If the anode is switched on first and the valve is exposed to ordinary illumination, the getter film will quickly acquire a potential practically equal to that of the anode, in virtue of photoelectric emission from it, and then, when the cathode is switched on, the potential of the getter will sink to its upper stable operating value. If, on the other hand, the cathode is switched on first, the getter film will take up a potential near that of the cathode, but then, when

the anode is switched on, the electrostatically induced potential on the getter film may still be sufficiently high for it to swing over to its upper stable value. The only certain way to prevent the upper potential from being established is to switch on first the cathode, and then the anode *at a sufficiently low potential*, after which the anode potential is raised *continuously* to its desired value.

These phenomena were made use of with the valve in question. By switching on the cathode first and then sliding the anode potentiometer up from zero, the valve was set in operation with the getter potential near that of the cathode, so that it could not collect electrons of any appreciable energy. The residual gas pressure in the valve was then found from the ratio of the positive-ion current collected by the grid to the electron current flowing to the anode. Next, the cathode was switched off for a sufficient length of time for it to grow cold, and then on again. This must have caused the upper stable getter potential to be established, for it was found that the vacuum immediately began to deteriorate. On now sliding the anode potentiometer down and up again, so as to re-establish the lower getter potential, the vacuum ceased to deteriorate and began to improve by clean-up. By alternately establishing the upper and lower getter potential in this way the vacuum could be made to deteriorate and improve correspondingly several times. The deterioration associated with the upper getter potential can only have been due to the liberation of gas from the getter by impinging electrons, and there is every reason to believe that this gas was nitrogen.

General Conclusions.

From the results obtained in the present work, together with those obtained with magnesium and nitrogen by Lukirsky and Ptizyn, and with magnesium and hydrogen by the author, it seems safe to make the following generalizations :—

(1) Both speed and capacity in the contact gettering of a given gas generally increase in the order : magnesium, calcium, bright barium (deposited under good vacuum conditions), and black barium (deposited under relatively gassy conditions).

(2) In most cases of contact gettering the getter takes up much more gas than would cover its apparent surface with a monomolecular layer before showing signs of "fatigue." The gas may either combine chemically with the getter or be adsorbed on its surface. Adsorption is usually followed by diffusion into the interior of the getter deposit.

(3) In general, a rise in temperature accelerates the absorption of further gas, probably by promoting diffusion.

(4) A gas which has been absorbed by a getter without forming a chemical compound with it may be reliberated (*a*) by virtue of its "vapour-pressure," which increases strongly with both concentration and temperature, (*b*) by being displaced by another gas which combines with the getter, (*c*) by impinging electrons (even quite slow ones), or (*d*) by positive ions.

(5) Electric-discharge gettering may be regarded as the contact gettering of particles which are a direct or indirect product of the discharge, and which differ from the ordinary molecules of the gas. Examples of such particles are positive ions, metastable molecules, and single atoms. In some cases the products of the discharge form with the getter a stable chemical compound, where none would be formed by mere contact gettering of the ordinary molecules.

The author desires to tender his acknowledgment to the General Electric Company and the Marconiphone Company, on whose behalf the work was done which has led to this publication.

CI. *Triangle—Probability Problem in Integers.*

By L. Silberstein, *Ph.D.**

A GIVEN integer n is split haphazardly into three integers x, y, z, all supposed to differ from zero. To find the probability p that a triangle with sides proportional to x, y, z can be constructed, *i. e.*, that

$$x \leqq y+z, \quad y \leqq z+x, \quad z \leqq x+y \quad . \quad . \quad . \quad (1)$$

* Communicated by the Author.

This is the arithmetization * of a famous problem. For continuous x, y, z the probability of a triangle, obtained by the well-known geometrical method (which, however, is not free from obvious objections), is $p=\frac{1}{4}$.

It has seemed interesting to find p for whole numbers n, x, etc., and, *inter alia*, to determine its limit for $n\to\infty$.

Let $P(n)$ be the number of all possible partitions of n and $Q(n)$ the number of " favourable " ones, with $n\geqq 3$ of course. Then $p=Q(n)/P(n)$.

Now it is not difficult to see that

$$P(n)=1+2+3+\ldots.+(n-2)=\tfrac{1}{2}(n-1)(n-2). \quad . \quad (2)$$

It remains to find $Q(n)$. Its expression will differ according as n is odd or even. Whatever n, the inequalities (1) are equivalent to

$$x\leqq\frac{n}{2},\quad y\leqq\frac{n}{2},\quad z\leqq\frac{n}{2}. \quad . \quad . \quad . \quad . \quad (1a)$$

Thus, for $n=2m+1$,

$$x\leqq m,\quad y\leqq m,\quad z\leqq m,$$

so that we have the following triangular triplets, *i. e.*, favourable partitions (and only these) :

$$\left.\begin{matrix}1,\ m,\ m\ ;\\ \left.\begin{matrix}2,\ m-1,\ m\\ 2,\ m,\ m-1\end{matrix}\right\},\end{matrix}\quad \left.\begin{matrix}3,\ m-2,\ m\\ 3,\ m-1,\ m-1\\ 3,\ m,\ m-2\end{matrix}\right\}, \text{ etc. ;}$$

thus $$Q(2m+1)=1+2+3+\ldots+m=\tfrac{1}{2}m(m+1). \quad . \quad (3a)$$

Again, for $n=2m$ the table of triangular triplets is

$$\left.\begin{matrix}1,\ m-1,\ m\\ \left.\begin{matrix}1,\ m,\ m-1\end{matrix}\right\},\end{matrix}\quad \left.\begin{matrix}2,\ m-2,\ m\\ 2,\ m-1,\ m-1\\ 2,\ m,\ m-2\end{matrix}\right\} \text{ etc. ;}\quad \left.\begin{matrix}m,\ 1,\ m-1\\ m,\ 2,\ m-2\\ \ldots\ldots\\ \ldots\ldots\\ \ldots\ldots\\ m,\ m-1,\ 1\end{matrix}\right\}.$$

Thus

$$Q(2m)=2+3+\ldots.+(m-1)$$
$$+m+(m-1)=\tfrac{1}{2}m(m+3)-2. \quad . \quad . \quad (3b)$$

Consequently, by (2) and (3 *a*) or (3 *b*), the required probability is, for n even,

$$p_{2m}=\frac{m(m+3)-4}{2(2m-1)(m-1)},\quad m\geqq 2, \quad . \quad . \quad . \quad (4a)$$

* One might almost say " quantization."

and for n odd,

$$p_{2m+1}=\frac{m+1}{2(2m-1)}, \quad m\geqq 1. \quad . \quad . \quad . \quad (4b)$$

Both start from $p=1$ ($p_3=p_4=1$) and decrease with increasing n. For $m\to\infty$ both expressions tend to

$$p_\infty=\tfrac{1}{4},$$

agreeing with (and serving as a rigorous corroboration of) the familiar solution of the continuous problem.

Rochester, N.Y.
August 17, 1934.

CII. *On the Emission Spectra of the Vapours of the Sodium and Potassium Halides.* *By* H. HAMADA*. (*From the Laboratory of Physics, Sendai, Japan.*)

[Plate XVIII.]

Introduction.

FROM the thorough investigation, theoretical as well as experimental, made by J. Franck, H. Kuhn, G. Rollefson, K. Sommermeyer, H. D. Schmidt-Ott, and others it is now well known that a molecule of the alkali halides in the normal state is firmly held together by Coulomb forces, while in the excited states it is loosely held together by the polarization forces. Moreover, from the correspondence between the distances between the maxima of the continuous absorption bands †, which appear in the vapour at moderate temperature, and the differences in the excitation energies of the dissociation products, each of these continuous maxima was identified with each pair of the resulting dissociation products. This identification was also confirmed by the experimental results of the excitation of the atomic line-

* Communicated by Prof. J. Okubo.

† L. A. Müller, *Ann. d. Phys.* lxxxii. p. 39 (1927); J. Franck, H. Kuhn, and G. Rollefson, *Zeits. f. Phys.* xliii. p. 155 (1927); K. Sommermeyer, *Zeits. f. Phys.* lvi. p. 548 (1929); H. Kuhn, *Zeits. f. Phys.* lxiii. p. 458 (1930); H. D. Schmidt-Ott, *Zeits. f. Phys.* lxix. p. 724 (1931); H. Beutler and H. Levi, *Zeits. f. Elektrochemie*, xxxviii. p. 589 (1932); M. S. Desai, *Zeits. f. Phys.* lxxxv. p. 360 (1933).

fluorescence *, which occurs when the vapour is illuminated by the radiations corresponding to these continuous absorption-maxima. Numbering these continuous maxima in the order of wave-length—*i. e.*, the continuous maximum with the longest wave-length as the first, and so on—it was ascertained that the first, second, and third continuous maxima are due to the transitions from the normal state (fig. 1, 0) to the excited states, dissociating into a normal alkali atom and a halogen atom in the normal $^2P_2$ as well as in the excited $^2P_1$ state, and into a normal halogen atom and an excited alkali atom in the lowest ^2P state respectively (fig. 1, 1, 2, 3).

Fig. 1.

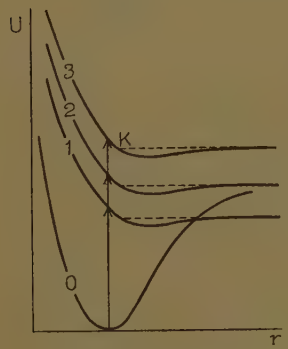

Fig. 2.

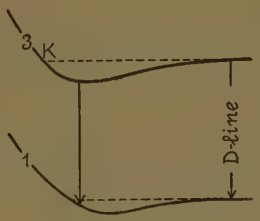

The successively numbered continuous maxima are also accounted for in each case as due to the transition to the excited state, the dissociation products of which are a normal halogen atom and an excited alkali atom in one of the higher levels.

But closer examination shows that the frequency difference between the first and the third continuous maxima above mentioned is nearly but not strictly equal to the frequency difference between the horizontal parts of the potential curves 1 and 3—that is, the frequency of the resonance line of the alkali metal—and the latter is always slightly greater than the former. Of

* A. Terenin, *Zeits. f. Phys.* xliv. p. 713 (1927); K. Butkow and A. Terenin, *Zeits. f. Phys.* xlix. p. 865 (1928); G. H. Visser, 'Physica,' ix. p. 115 (1929); A. C. S. van Heel and G. H. Visser, *Zeits. f. Phys.* lxx. p. 605 (1931); lxxxvi. p. 694 (1933).

course the accurate determination of the wave-lengths, corresponding to the absorption maxima, may be difficult, but the small difference above mentioned is always beyond the limit of experimental error. For example, the values of the former in cæsium iodide, cæsium chloride, rubidium iodide, and sodium iodide are measured as 10,900, 11,000, 11,200, and 16,300 cm.$^{-1}$ respectively, while the values of the latter are 11,450, 12,700, and 16,950 cm.$^{-1}$ respectively in these three metals. Therefore it is considered that the potential curves of the first and the third excited states are so relatively situated that the minimum of the latter is deeper and has a smaller nuclear distance than that of the former. Moreover, taking into account the fact that the frequency of the third absorption maximum is slightly greater than the sum of the dissociation energy, thermochemically determined, and the frequency of the resonance line, and also the fact that the dissociation energy given by the thermochemical data is approximately in accordance with the value obtained from the frequency of the longest wave-length limit (this is not sharply defined) of the light capable of exciting the resonance lines in the fluorescence of alkali halide vapour, it is clearly conceivable that the nuclear distance, corresponding to the intersecting point K of the potential curve 3 with its horizontal asymptote, does not differ much from the nuclear separation in the non-vibrating state of the normal molecule. Hence, in consequence of the absorbing light or of the electron collisions, the main part of the non-vibrating and some part of the vibrating molecules in the normal state are probably excited to the unstable states above the horizontal asymptote of the potential curve 3, and are dissociated into a normal halogen atom and an excited alkali atom in the lowest ^{2}P state, and these afterwards emit the resonance lines, while one part of the vibrating molecules in the normal state is also capable of being excited to the discrete and stable levels below the asymptote of the same potential curve, and therefore emits the radiations when they return to the normal state or to the first excited state 1. In the case of the latter transition it is to be expected that the apparently continuous spectrum in the longer wave-length side of the resonance lines of the alkali metal, having an intensity maximum at these lines, should be emitted, and also that it should

sometimes have a structure in the neighbourhood of these lines. In this communication it is desired to report the results obtained by the experiment recently carried out on the emission spectra of the alkali halide vapours to ascertain the correctness of this assumption.

Experimental Results.

In this experiment the same apparatus was used as in the previous experiment on the continuous spectrum of sodium*. A suitable quantity of alkali halide under test was placed in a hollow iron cathode, the material in this being vaporized by heating. The spectrum in question is well observed at a low vapour pressure, even at one much lower than 0·1 mm. Hg., and the intensity increases with the increase of the vapour pressure; but the observations in this case were made under a vapour pressure of about 1 mm. The intensity distribution of the spectrogram was approximately measured with the help of Dorgelo's stepped reducer. The materials tested were the chlorides, bromides, and iodides of sodium and of potassium.

The spectrograms and their intensity distribution in the cases of the vapours of sodium salts are shown in Pl. XVIII. and in fig. 3. It will be seen that the D-lines are intensely and sharply excited in all the cases, and from them an apparently continuous spectrum, having a maximum intensity in the immediate neighbourhood of the lines, extends towards the longer wave-length side, diminishing at first, and then, after passing through the region of almost constant intensity, gradually fading away without showing a sharp edge. In the case of sodium chloride it was known that the spectrum extends beyond the region at 8500 Å., but not beyond the region at about 8200 Å. in the cases of the bromide as well as of the iodide of sodium. The lack of sensibility in the photographic plate used, together with the superposition of temperature radiations from the hot cathode, made it difficult to measure the intensity distribution in the infra-red region (>7000 Å.), and the intensity distribution in fig. 3 is merely qualitative in this region of wave-lengths. Apparently a continuous spectrum is also seen in the short wave-length side of the D-lines. This branch

* H. Hamada, Phil. Mag. xv. p. 574 (1933).

Fig. 3.

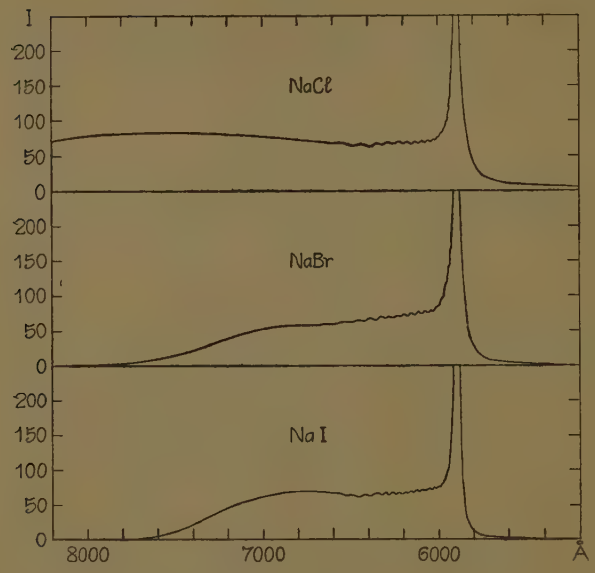

TABLE I.

NaCl.			NaBr.			NaI.		
λ.	ν.	Δν.	λ.	ν.	Δν.	λ.	ν.	Δν.
6545	15275	268	6529	15312	183	6570	15217	173
6432	15543	208	6452	15495	165	6496	15390	167
6347	15751	171	6384	15660	143	6426	15557	189
6279	15922	146	6326	15803	124	6349	15746	133
6222	16068	143	6277	15927	110	6296	15879	91
6167	16211	111	6234	16037	98	6260	15970	100
6125	16322	107	6196	16135	113	6221	16070	88
6085	16429	95	6153?	16248	111	6187	16158	82
6050	16524	74	6111	16359	92	6156?	16240	82
6023	16598	67	6077	16451	112	6125	16322	105
5999	16665	61	6036	16563	74	6086	16427	86
5977	16726	45	6009	16637	78	6054	16513	80
5961	16771	34	5981	16715	59	6025	16593	69
5949	16805	25	5960	16774	48	6000	16662	47
5940	16830	23	5943	16822	31	5983	16709	37
5932	16853	20	5932	16853	29	5970	16746	34
5925	16873	14	5922	16882		5958	16780	33
5920	16887					5946	16813	

of the spectrum has a much smaller intensity and extension compared with the branch appearing in the longer wave-length side of the same lines, and the intensity of this spectrum gradually decreases towards the shorter wave-length side, showing no sharp edge. The extension of this latter spectrum is greatest in the chloride and least in the iodide.

In every case of the spectra of three sodium halides the structure of a diffused nature was found on the longer wave-length side of the D-lines, and the wave-lengths of the intensity maxima, together with the corresponding wave-numbers ν and the wave-number differences $\Delta\nu$, were measured and are tabulated in Table I. By plotting the values of $\Delta\nu$ against those of

Fig. 4.

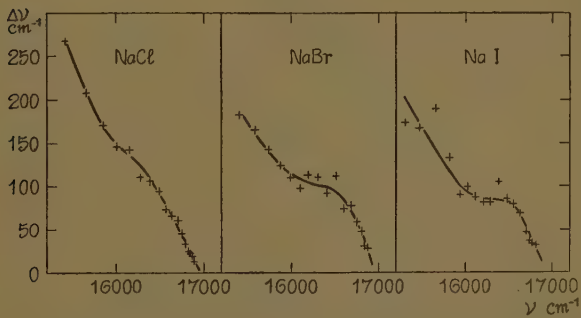

ν, as shown in fig. 4, it is found that the convergence limit is the frequency of the D-lines. In the case of chloride the series of maxima is regular in the whole region of the spectrum, and in bromide the middle part of the series is somewhat irregular, while in iodide the regularity of the series almost disappears. It may be considered that the spectrum in the longer wave-length region is really a continuous one, as no structure was found at all in that region.

The increase of vapour pressure intensifies the spectrum as a whole, but does not modify the intensity distribution. In the condition in which the vapour pressure and the exciting current are unaltered the intensities of the molecular spectra and also their relative intensities to the D-line are nearly the same in the case of all three

kinds of molecules. When the pressure is increased to about a few mm. the D-lines begin to widen out, and this is probably due to the emission of the quasi-molecules, though this emission is very faint compared with that in the case of pure sodium vapour.

Similarly to the sodium halides the apparently continuous spectrum appears in the potassium halides in the longer wave-length side of the resonance lines at 7699–7665 Å., and extends to the region beyond 8800 Å. in all the three halides. It was impossible to observe any structure of this continuous spectrum, on account of the development of many atomic lines.

Discussion of the Results.

Evidently the spectrum here observed differs from that due to the alkali molecules (Na_2, K_2) or to the halogen molecules (Cl_2, Br_2, I_2), and is certainly due to the diatomic alkali-halogen molecules (NaCl, NaBr, NaI, etc.), and its intensity distribution may be explained by the relative positions of the potential curves of the responsible molecule. As the representative one of alkali halide molecules it is convenient to study the intensity distribution of the spectrum due to the sodium halide molecules.

As the potential curve of the upper excited molecular state 3 may be assumed to have a deeper minimum at a smaller nuclear distance than that of the lower excited state 1—as already shown in fig. 2,—and also as the transitions to the higher vibrational levels of the upper state 3 from the normal state 0 take place more frequently in comparison with the transitions to the lower vibrational levels of the same state, and, in addition, as the probability of electronic transition with the emission of light is greater at the attractive branch than that at the repulsive branch of the potential curve 3, the molecular spectrum will gradually fade away towards the longer wave-length side from the maximum at the resonance lines, and the structure will be found in the part nearer to the lines in the spectrum and the continuous region without any structure in the part remote from those lines. It is natural to consider that the average vibration frequency in the upper excited state 3 is greater than that of the lower excited state 1, as in

the former state the two atoms are more firmly combined in comparison with the atoms in the latter state. In the case of sodium chloride, ω'' is probably much smaller than ω', and a regular series of maxima may be emitted. In sodium bromide the difference between ω'' and ω' may not be so great as in chloride, and therefore some perturbations may be observed at the middle part of the series corresponding to the lower vibrational states of the potential curve 1. In the case of sodium iodide the difference between ω'' and ω' is considered to be small, the favourable condition for the formation of the regular series of " fluted bands " may not be satisfied, and the regularity of the intensity distribution may almost disappear in the whole series. Provided a spectrograph of higher dispersion together with the stronger light source were used, the spectrum above described would be resolved into the individual bands having rotational structures.

In considering the intensity distribution of the spectrum above mentioned, in which almost all the maxima may probably be emitted by the transitions to the stable levels of the lower state 1, it is known that the dissociation energy of the upper state 3 is about 0·1 volts in the order of magnitude in all the three sodium halides, and also that the dissociation energy of the lower state 1 will be less than 0·1 volts in all the three, among which the dissociation energy of chloride is the least and that of iodide is the greatest.

The reason why the spectrum covers the widest region in the chloride and the narrowest region in the iodide is well understood by considering that the minimum of the potential curve of the lower state 1 is more displaced in the chloride than in the iodide relatively to that of the upper state 3 with respect to the nuclear separation. From the measurement of the relative intensities of the spectra of the three sodium halides with respect to each other, observed under the same experimental conditions, and also from the measurement of their relative intensities to the accompanying D-line, it is found that the potential curves of the upper state 3 and of the normal state 0 are similarly situated in relative positions in all halides of sodium, and it is concluded that the displacement of the minimum of the lower potential curve 1 relative to the potential minimum of the curve 0 is greatest in

the chloride and least in the iodide. This consideration serves to account for the regularity of the series of the intensity maxima above mentioned and also for the experimental fact observed in the absorption.

It was not easy to determine whether the narrow and apparently continuous spectrum faintly developed on the shorter wave-length side of the D-lines is emitted by the transitions between other molecular states or not.

Polarization-molecule and Quasi-molecule.

It is very interesting to compare the spectrum here observed in the vapour of sodium halide with the continuous spectrum of the pure sodium vapour *. Although both of these spectra appear in the vicinity of the D-lines, the halide spectrum is emitted by the quantized molecules loosely held together by the polarization forces, while the sodium spectrum is emitted mainly by the quasi-molecules, and therefore it is naturally considered that there should be a marked distinction between these two kinds of spectrum †.

In the first place it is easily found that there are diffused intensity fluctuations in the halide spectrum observed with a glass prism spectrograph, and finer structure due to the nuclear rotation should be expected if the observations were made under a higher dispersion. However, the continuous spectrum of pure sodium shows no structure at all, even when the second-order spectrum of the concave grating, 21·5 ft. in focal length, is observed.

Next, let us examine the intensity distribution of the spectra. The ratio of the intensity of the molecular spectrum at 6200 Å. to that of the atomic D_2-line is measured as about 1 : 400 in all three halides from the spectrograms taken with a glass prism spectrograph under a vapour pressure of $\sim$1 mm., while the ratio of the intensity of the sodium spectrum at 5500 Å. to that of the D_2-line is about $1 : 10^4$ under a vapour pressure of $\sim$2 mm. and in a temperature of $\sim 950°$ C. Although the appearance of the D-line taken with a small spectrograph is apparently not very different in the case of pure sodium from that in the case of sodium halide the

* H. Hamada, *loc. cit.*

† The writer is much indebted to Dr. H. Kuhn for the helpful advice that he has given in connexion with this point.

D_2-line observed in the spectrum of halide vapour in a high dispersion is very narrow, and shows no sign of self-reversal, while in the spectrum of pure sodium the self-reversal, with a width of about 0·2 or 0·3 Å., is observed in the same D_2-line. This fact suggests that the partial pressure of sodium vapour in the sodium halide vapour is small, in consequence of the small degree of the dissociation of the vapour, and that the relative intensity of the molecular spectrum, estimated from the ratio above obtained, is too large for the halide spectrum to be attributed to the emission of quasi-molecules. In contrast to the case of the halides the value $1 : 10^4$ obtained in the case of pure sodium is merely the ratio of intensity of the molecular spectrum (5500 Å.) relative to the wing of the D_2-line. Since the breadth (half-value width) of this line, due to the atomic collisions, is calculated as about $5 \cdot 10^{-3}$ Å. at 2 mm. and 950° C., the breadth of the line will be mainly due to the Doppler breadth of about $3 \cdot 10^{-2}$ Å., and therefore the above ratio will be extremely small if the self-absorption of the D-lines by the vapour itself did not occur, and the molecular spectrum is not too intense to be considered as due to the emission of the quasi-molecules.

It is also known that the halide spectrum clearly appears under very low vapour pressure, even in the case of far less than 0·1 mm. Hg. However, the continuous spectrum of sodium appears only at the high pressure of more than 1 or 2 mm. Hg, and it is understood that the emission of the latter depends on the average duration of the free path relatively to the lifetime of the excited sodium atom, while the former does not directly depend on this condition.

Finally, by mixing neon at a pressure of 10 mm. Hg with the sodium vapour it was observed that the total intensity of the glow was reduced and that the intensity reduction was greater in the continuous spectrum, while it was less in the discrete band spectrum. This confirmed the conclusion that the relative intensity between the continuous and the discrete band spectrum is modified just as might be expected, but it is not definitely certain whether this effect is actually due to the relative increase of triple collisions or not, as the mechanism of light emission in the case in which a hollow cathode is used is much more complicated in comparison with that

in the case of fluorescence. The halide spectrum was not sensibly affected by the introduction of neon gas.

In conclusion, the writer wishes to express his sincere thanks to Prof. J. Okubo, under whose direction this work has been done.

Sendai, Japan.
May 1934.

CIII. *Hyperfine-Structure of Spectrum Lines of Manganese Arc in Vacuum.*—Part I. *By* Wali Mohammad, *M.A.* (*Punjab*), *B.A.* (*Cantab.*), *Ph.D.* (*Göttingen*), *Professor of Physics, Lucknow University, Lucknow, and* Prem Nath Sharma, *M.Sc., Research Scholar, Lucknow University* *.

Introduction.

THE following is an extension of the work on the Hyperfine-structure of Spectrum Lines that the authors have undertaken. Lines from the arcs of zinc[1], lead[2], silver[3], and bismuth[4] have already been investigated and their results published.

Janicki[5] and Wali Mohammad[6] have worked on manganese spectrum, but their investigations have been confined to the visible region of the spectrum. White and Ritschl[7] have recently examined the hyperfine-structure of some 40 lines of manganese arc, but they too have not extended their work beyond the visible. This paper deals with the investigation in the visible region only. The results of the work in the ultra-violet region will be communicated later on. It will, however, be found from what follows that the authors' results are more in conformity with those of Janicki and Wali Mohammad than with the results of White and Ritschl.

Experimental Procedure.

Hilger's E_1 spectrograph with quartz optical system was used in conjunction with quartz Lummer-Gehrcke

* Communicated by the Authors.

plates of the following dimensions to photograph the hyperfine-structure patterns :—

Plate No. 1 .. Length 195 mm., thickness 3·65 mm.
Plate No. 2 .. Length 200 mm., thickness 4·75 mm.
Plate No. 3 .. Length 130 mm., thickness 4·597 mm.

The source of light was similar to the one used in previous investigations by the authors. It consists of a platinum cathode coated with oxides of barium and strontium which can be heated to any desired temperature by passing a current through it from a set of secondary cells. The anode is formed by putting manganese powder inside a small tube of fused silica on a nickel rod. The whole is encased in a Pyrex-glass tube, the upper end of which is closed by a plano-convex lens of quartz cut perpendicular to the optic axis. The lower end of the tube is sealed by means of vacuum sealing wax and the space inside the lamp is evacuated by means of a Cenco Hyvac pump. A pressure of the order of 0·1 mm. of mercury is found to be quite sufficient for the purpose. The Pyrex-glass tube is surrounded by a metal jacket through which water circulates.

A current of 15 to 18 amp. was required to heat the cathode, and the arc was struck up by applying a voltage of 220 from the mains through suitable resistances to the anode. An emission current of 1·5 amp. was found to be the most suitable. The colour of the Mn arc was faint green.

A source of the type of Schuler's hollow cathode discharge-tube would have been an ideal arrangement, but for want of liquid air and rare gases this source could not be used. The lamp used by the authors worked fairly satisfactorily, and an exposure of between 5 and 30 minutes was required for photographing the Lummer patterns according to the intensity of the lines.

Calculation of Wave-length.

Von Baeyer's formula

$$\Delta\lambda_{\max} = \frac{n\lambda^2}{n^2\lambda - 4t^2\mu\,\frac{d\mu}{d\lambda}}$$

has been employed for calculating the distance between

two successive fringes. The position and wave-length of the satellites have been found as in previous cases.

Results.

6016·86.

Janicki finds this line simple. The authors find that this possesses two satellites. Wali Mohammad found only one. This line has been found to possess the following structure :—

0·000
−0·051
−0·102 (?)

6013·48.

Janicki finds this line simple. Wali Mohammad found one satellite having the wave-length −0·035. The authors have found the following structure for this line :—

0·000
−0·034

5849·33.

This line is found to possess the following structure :—

0·000
−0·109

5537·962.

Janicki found that this line possesses two or three weak satellites, but he did not measure their wave-lengths. The authors' results, together with those of Wali Mohammad, are given below :—

Wali Mohammad.	Authors.
0·000	0·000
−0·046	−0·047
−0·104	−0·106

5516·977.

Janicki, Wali Mohammad, and White and Ritschl have all found this line to possess two satellites.

Janicki.	Wali Mohammad.	White & Ritschl.	Authors.
0·000	0·000	0·0000	0·000
−0·073	−0·070	−0·0498	−0·050
−0·118	−0·120	−0·0748	−0·075

5506·099.

The authors' results, together with those found by other workers, are given below :—

Janicki.	Wali Mohammad.	White & Ritschl.	Authors.
0·000	0·000	0·0000	0·000
−0·047	−0·047	0·0413	−0·047
−0·089	−0·088	−0·0484	−0·087

5481·607.

Janicki and Wali Mohammad found two satellites to this line. White and Ritschl have found three. The authors find only two satellites for this line :—

Janicki.	Wali Mohammad.	White & Ritschl.	Authors.
0·000	0·000	0·0000	0·000
−0·065	−0·062	−0·0365	−0·062
−0·122	−0·115	−0·0512	−0·112
		−0·0662	

5413·913.

This line is found to possess the following structure :—

0·000
−0·050

5407·616.

This line is found to have two satellites :—

Janicki.	Wali Mohammad.	White & Ritschl.	Authors.
0·000	0·000	0·0000	0·000
−0·057	−0·054	−0·0445	−0·055
−0·105	−0·104	−0·0552	−0·148

5341·178.

This line has four satellites. White and Ritschl found five satellites to this line :—

Janicki.	Wali Mohammad.	White & Ritschl.	Authors.
0·000	0·000	0·0000	0·000
−0·057	−0·058	−0·0232	−0·046
−0·108	−0·107	−0·0342	−0·088
−0·149	−0·149	−0·0438	−0·122
−0·183	−0·190	−0·0530	−0·151
		−0·0628	

The following lines are found sharp and simple. Wali Mohammad and Janicki also found them simple :—

5196·748	4854·809
5151·14	4823·688
5118·113	4783·614
5074·758	

4727·662.

Janicki and Wali Mohammad found this line to be simple. White and Ritschl found one satellite for this line. The authors, too, find that this line possesses one satellite :—

White & Ritschl.	Authors.
0·0000	0·000
−0·0152	−0·060

4709·911.

This line is also found to have one satellite, while Janicki and Wali Mohammad found this to be simple :—

White & Ritschl.	Authors.
0·0000	0·000
−0·0133	−0·090

4502·399.

This line has one satellite. Janicki and Wali Mohammad found it to be simple :—

White & Ritschl.	Authors.
0·0000	0·000
−0·0244	−0·033

4499·096.

Janicki, Wali Mohammad, and White and Ritschl found this line to be simple. The authors also find that this line is simple.

4490·271.

Janicki and Wali Mohammad found this line to be simple. The authors find it to be double :—

White & Ritschl.	Authors.
0·0000	0·000
−0·0235	−0·022

4464·864.

This line has one satellite :—

White & Ritschl.	Authors.
0·0000	0·000
−0·0236	−0·030

4415·002.

Janicki and Wali Mohammad found this line to be simple. The authors find it to be double :—

White & Ritschl.	Authors.
+0·0264 (?)	0·000
0·0000	−0·036

4312·735.

This line is found to have one satellite :—

+0·064
0·000

4281·287.

Janicki and Wali Mohammad found it to be simple. The authors also find it to be simple.

The following lines are also found to be simple. Janicki and Wali Mohammad also found them sharp and simple.

4266·076	4070·419
4239·88	

4041·546.

Janicki found this line to possess two satellites. White and Ritschl find it to have five satellites, while the authors find only two :—

Janicki.	White & Ritschl.	Authors.
0·000	0·0000	0·000
−0·032	−0·0165	−0·032
−0·045	−0·0140	−0·046
	−0·0116	
	−0·0093	
	−0·0060	

NOTE.—The results of the investigation of the ultra-violet lines of Mn-arc will be communicated later.

References.

(1) Wali Mohammad and Sharma, Phil. Mag. x. p. 916 (1930).
(2) Wali Mohammad and Sharma, *ibid.* xii. p. 1106 (1931).
(3) Wali Mohammad and Sharma, Ind. J. Phys. vi. p. 75 (1931).
(4) Wali Mohammad and Sharma, Phil. Mag. xiv. p. 1143 (1932).
(5) Janicki, *Ann. der Phys.* xxxi. p. 845 (1909).
(6) Wali Mohammad, Astrophys. Journ. xxxix. p. 200 (1914).
(7) White and Ritschl, Phys. Rev. xxxv. p. 1147 (1930).

Department of Physics,
Lucknow University.
May 1934.

CIV. *On the Concept of Force in Wave Mechanics.* *By* R. L. ROSENBERG, *M.A., Ph.D., D.I.C.* (*Beit Scientific Research Fellow, Imperial College of Science*) *.

§1. A COLLISION between two bodies in classical mechanics entails a change of momentum of each body. This change of momentum determines the impulse of the one body on the other. In the scattering of a current of particles by a force centre (this force centre being due to the presence of another body, "the scatterer") we have a redistribution of the current throughout space. There is a change of momentum of the scattered particles, which in this case can be expressed as a rate of change of momentum. To complete the analogy with classical theory one would inquire what is this rate of change of momentum, or the force exerted on the scatterer by the current of particles. We shall therefore attempt to formulate the idea of force in wave mechanics as it arises out of this scattering problem. We shall, however, find general formulæ which will be applicable also to the case of electrons in discrete negative energy states, *i. e.*, corresponding to the periodic motions of classical mechanics. Further, we shall discuss properties of the force in stationary and non-stationary states in which the effect of a perturbation causing transitions will be found. In finding the force exerted by a current of particles on a scatterer characterized by a field of force, we shall be guided by the correspondence between wave mechanics and the wave theory of light; and the method will be similar to the calculations for the pressure of light on a body. A particular case of this has already been considered by the author †, and the force expressed in terms of an effective cross-section of the scatterer.

§2. We approach the problem from the point of view of a field theory, and shall define the force-density as the four-dimensional divergence of the energy-momentum tensor of the material field.

* Communicated by the Author.

† R. L. Rosenberg, *Ann. der Physik*, (5) xv. p. 757 (1932).

In classical mechanics the energy-momentum tensor is defined by the scheme

$$\left.\begin{array}{llll} \mathrm{T}_{\mu\nu}=\rho u^2, & \rho vu, & \rho wu, & \rho u, \\ \rho uv, & \rho v^2, & \rho wv, & \rho v, \\ \rho uw, & \rho vw, & \rho w^2, & \rho w, \\ \rho u, & \rho v, & \rho w, & \rho, \end{array}\right\} \quad . \quad . \quad (1)$$

where ρ is the density and u, v, w the components of velocity.

Then the force density is

$$\mathrm{F}_\nu=\sum_{\mu=1}^{4}\frac{\partial \mathrm{T}_{\mu\nu}}{\partial x_\mu}, \quad . \quad . \quad . \quad . \quad . \quad (2)$$

with x_1, x_2, $x_3=x$, y, z, and $x_4=t$; since the right-hand side of (2) is the rate of change of momentum in the ν direction.

For example, $\nu=1$ gives, using the equation of continuity,

$$\sum_\mu \frac{\partial \mathrm{T}_{1\mu}}{\partial x_\mu}=u\left(\frac{\partial(\rho u)}{\partial x}+\frac{\partial(\rho v)}{\partial y}+\frac{\partial(\rho w)}{\partial z}+\frac{\partial \rho}{\partial t}\right)$$
$$+\rho\left(u\frac{\partial u}{\partial x}+v\frac{\partial u}{\partial y}+w\frac{\partial u}{\partial z}+\frac{\partial u}{\partial t}\right)=\rho\frac{\mathrm{D}u}{\mathrm{D}t}.$$

We shall restrict ourselves throughout to a non-relativistic treatment. Schrödinger * has deduced the corresponding energy-momentum tensor in wave mechanics, taking as his basis the Gordon relativistic wave equation. We shall form a purely non-relativistic tensor by taking Schrödinger's tensor and neglecting all terms involving inverse powers of c greater than the first.

Then the wave equation is

$$\Delta\psi+\frac{4\pi i}{h}\left\{\frac{e}{c}(\mathfrak{A}\ \mathrm{grad}\ \psi)-m\frac{\partial\psi}{\partial t}\right\}-\frac{8\pi^2 m}{h^2}\mathrm{V}\psi=0, \quad (3)$$

where $\mathfrak{A}$ is the vector potential and V the scalar potential of any field which may be present.

Schrödinger finds the tensor in the form

$$-\frac{\partial \mathrm{T}_{\rho\sigma}}{\partial x_\sigma}=\frac{\partial \mathrm{L}_m}{\partial x_\rho}-\frac{\partial}{\partial x_\sigma}\left(\bar{\psi}_\rho\frac{\partial \mathrm{L}_m}{\partial \bar{\psi}_\sigma}+\psi_\rho\frac{\partial \mathrm{L}_m}{\partial \psi_\sigma}+\phi_\rho\frac{\partial \mathrm{L}_m}{\partial \phi_\sigma}\right), \quad (4)$$

* E. Schrödinger, *Ann. der Physik*, (4) lxxxii. p. 265 (1927).

where L_m is the Lagrangian function and

$$\psi_\rho = \frac{\partial \psi}{\partial x_\rho} \; ; \quad \phi_\rho = \frac{2\pi e}{hc} \mathfrak{A}_\rho \; ;$$

and the bar denotes the conjugate complex.

Further, he shows that

$$\frac{\partial}{\partial x_\alpha}\left(\bar{\psi}\frac{\partial L_m}{\partial \bar{\psi}_\alpha}\right) = L_m \; ; \quad \frac{\partial}{\partial x_\alpha}\left(\psi \frac{\partial L_m}{\partial \psi_\alpha}\right) = L_m \; ;$$

and hence

$$L_m = \tfrac{1}{2}\frac{\partial}{\partial x_\alpha}\left(\bar{\psi}\frac{\partial L_m}{\partial \bar{\psi}_\alpha} + \psi \frac{\partial L_m}{\partial \psi_\alpha}\right).$$

Hence

$$\frac{\partial L_m}{\partial x_\rho} = \tfrac{1}{2} \cdot \frac{\partial}{\partial x_\alpha} \cdot \frac{\partial}{\partial x_\rho}\left(\bar{\psi}\frac{\partial L_m}{\partial \psi_\alpha} + \psi \frac{\partial L_m}{\partial \psi_\alpha}\right). \quad . \quad . \quad (5)$$

Changing the dummy suffix α to σ we get, substituting (5) in (4),

$$-\frac{\partial T_{\rho\sigma}}{\partial x_\sigma} = -\frac{\partial}{\partial x_\sigma}\Big(\tfrac{1}{2}\bar{\psi}_\rho \frac{\partial L_m}{\partial \bar{\psi}_\sigma} + \tfrac{1}{2}\psi_\rho \frac{\partial L_m}{\partial \psi_\sigma} + \phi_\rho \frac{\partial L_m}{\partial \phi_\sigma} - \tfrac{1}{2}\bar{\psi}\frac{\partial}{\partial x_\rho}\frac{\partial L_m}{\partial \bar{\psi}_\sigma} - \tfrac{1}{2}\psi \frac{\partial}{\partial x_\rho}\frac{\partial L_m}{\partial \psi_\sigma}\Big),$$

and hence

$$T_{\rho\sigma} = \tfrac{1}{2}\Big[\bar{\psi}_\rho \frac{\partial L_m}{\partial \psi_\sigma} + \psi_\rho \frac{\partial L_m}{\partial \bar{\psi}_\sigma} - \bar{\psi}\frac{\partial}{\partial x_\rho}\frac{\partial L_m}{\partial \bar{\psi}_\sigma} - \psi \frac{\partial}{\partial x_\rho}\frac{\partial L_m}{\partial \psi_\sigma} + 2\phi_\rho \frac{\partial L_m}{\partial \phi_\sigma}\Big].$$

With the Lagrangian given by Schrödinger as

$$L_m = (\psi_\alpha + i\phi_\alpha \psi)(\bar{\psi}_\alpha - i\phi_\alpha \bar{\psi}) + k^2 \psi \bar{\psi},$$

we get to the first order in c, for $\rho, \sigma = 1, 2, 3$.

$$T_{\rho\sigma} = \tfrac{1}{2}[\psi_\rho \bar{\psi}_\sigma + \psi_\sigma \bar{\psi}_\rho - \psi \bar{\psi}_{\rho\sigma} - \bar{\psi}\psi_{\rho\sigma}] + i\phi_\sigma(\bar{\psi}_\rho \psi - \psi_\rho \bar{\psi}) + i\phi_\rho(\bar{\psi}_\sigma \psi - \psi_\sigma \bar{\psi}). \quad . \quad (6)$$

For ρ or $\sigma = 4$ we have

$$T_{\rho 4} = -\frac{2\pi i m}{h}[\bar{\psi}_\rho \psi - \bar{\psi}\psi_\rho - 2i\phi_\rho \psi\bar{\psi}], \quad . \quad . \quad (6a)$$

$$T_{44} = \frac{8\pi^2 m}{h^2}\psi\bar{\psi}.$$

We note that (6 *a*) is the usual current vector, and corresponds completely to the form of (1).

(6) and (6 *a*) define the energy-momentum tensor completely in the non-relativistic case. Comparison with (1) determines a dimensional factor $\frac{h^2}{8\pi^2 m}$, with which every element of the tensor must be multiplied.

According to (2) we define the force density *

$$\mathrm{F}_\rho = \sum_{\sigma=1}^{3} \frac{\partial \mathrm{T}_{\rho\sigma}}{\partial x_\sigma} + \frac{\partial \mathrm{T}_{\rho 4}}{\partial t}. \quad . \quad . \quad . \quad . \quad (7)$$

We obtain the total force by integrating over the whole space τ

$$\mathrm{K}_\rho = \int \sum_{\sigma=1}^{3} \frac{\partial \mathrm{T}_{\rho\sigma}}{\partial x_\sigma} d\tau + \int \frac{\partial \mathrm{T}_{\rho 4}}{\partial t} d\tau. \quad . \quad . \quad (7\,a)$$

As in electromagnetic theory, the total force can be represented as an integral of surface stress over the surface of the total volume. If n be the unit normal vector outwards from the bounding surface f, then

$$\int \sum_{\sigma=1}^{3} \frac{\partial \mathrm{T}_{\rho\sigma}}{\partial x_\sigma} d\tau = \int \sum_{\sigma} \mathrm{T}_{\rho\sigma} \cos(n, \sigma)\, df.$$

Using (6) and relations such as

$$\sum_{\sigma} \psi_\sigma \cos(n, \sigma) = \psi_n = \frac{\partial \psi}{\partial n},$$

$$\sum_{\sigma} \psi_{\rho\sigma} \cos(n, \sigma) = \frac{\partial}{\partial n} \psi_\rho,$$

we get

$$\sum_{\sigma=1}^{3} \mathrm{T}_{\rho\sigma} \cos(n, \sigma) = \tfrac{1}{2}\Big[\bar{\psi}_\rho \psi_n + \psi_\rho \bar{\psi}_n - \bar{\psi} \frac{\partial}{\partial n} \psi_\rho - \psi \frac{\partial}{\partial n} \bar{\psi}_\rho\Big]$$
$$+ i\phi_n(\bar{\psi}_\rho \psi - \psi_\rho \bar{\psi}) + i\phi_\rho(\psi \bar{\psi}_n - \bar{\psi}\psi_n) \equiv \mathrm{P}_\rho. \quad . \quad (8)$$

If we define the surface stress P_ρ as in (8), then

$$\mathrm{K}_\rho = \frac{h^2}{8\pi^2 m} \int \mathrm{P}_\rho df + \int \frac{\partial \mathrm{T}_{\rho 4}}{\partial t} d\tau. \quad . \quad . \quad . \quad (9)$$

* If we were to carry out the differentiation in (7) we would naturally find

$$\mathrm{F}_\rho = \psi\Big(\frac{\partial \mathrm{V}}{\partial x_\rho} - \frac{h}{2\pi} \frac{\partial \phi_\rho}{\partial t}\Big) \bar{\psi} + \frac{h^2}{8\pi^2 m} \sum_{\sigma=1}^{3} (\bar{\psi}_\sigma \psi - \psi_\sigma \bar{\psi}) \Big(i \frac{\partial \phi_\rho}{\partial x_\sigma} - i \frac{\partial \phi_\sigma}{\partial x_\rho}\Big)$$

which corresponds to the classical expression for the force in an electromagnetic field.

If ψ depends on the time only through a factor $e^{-\frac{2\pi i}{h}Et}$ and ϕ_ρ is independent of the time, or is a very rapidly oscillating function, then $\frac{\partial T_{\rho 4}}{\partial t}=0$, and we are left only with the first part of (9).

Assuming this, we have

$$K_\rho=\frac{h^2}{8\pi^2 m}\int P_\rho df. \quad . \quad . \quad . \quad . \quad . \quad (9a)$$

If ψ represents a system in a discrete energy state, corresponding to a closed orbit in classical mechanics, then ψ tends to zero very rapidly on the infinite boundary (more rapid than $1/r$). Hence

$$k_\rho=\int F_\rho\, d\tau=0 \quad . \quad . \quad . \quad . \quad . \quad (10)$$

for a system in a stationary state, corresponding to the classical theorem for a periodic system: that there is no average resultant force in any direction. For a non-stationary state the dependence of ψ on the time is not of the form $e^{-\frac{2\pi i}{h}Et}$, and the term $\int\frac{\partial T_{\rho 4}}{\partial t}d\tau$ may give a contribution to K_ρ.

For states with a positive continuous eigenwert ψ only tends to zero as $1/r$ on the infinite boundary, and K_ρ may have a finite value. By replacing ψ by its eigen-differential we may still obtain (10). If, however, as in the scattering problem, ψ must be normalized that at the infinite boundary it should represent a finite current of particles, then we obtain a finite value for K_ρ which represents the total force exerted by the current of particles on the scattering centre. A case of this has been considered in detail, and the result expressed as an effective cross-section of the scatterer (*cf.* § 1).

§ 3. Let $\psi^\nu e^{-\frac{2\pi i}{h}E_\nu t}$ be the orthogonal normalized solutions of (3). Then the wave function ψ for the system in any state can be expressed as

$$\psi=\sum_\nu a_\nu\psi_\nu e^{-\frac{2\pi i}{h}E_\nu t} \quad . \quad . \quad . \quad . \quad . \quad (11)$$

Substituting this in (6), we shall obtain for $T_{\rho\sigma}$ terms such as

$$\sum_{\mu\nu} \bar{a}_\nu a_\mu \frac{\partial \psi_\nu}{\partial x_\rho} \cdot \frac{\partial \psi^\mu}{dx_\sigma} e^{\frac{2\pi i}{h}(E_\nu - E_\mu)t} \text{ etc.}$$

For $\nu \neq \mu$ and $E_\nu \neq E_\mu$ we get a rapidly oscillating contribution so that the time average of such terms is zero. We need only keep those terms for which $E_\nu = E_\mu$ (with no degeneracy, those for which $\nu = \mu$). Then

$$T_{\rho\sigma} = \sum_\nu a_\nu \bar{a}_\nu T^\nu_{\rho\sigma},$$

where $T^\nu_{\rho\sigma}$ is the tensor evaluated for the νth state. Further, with the form (11) $T_{\rho 4}$ is independent of the time, and hence

$$\begin{aligned} F_\rho &= \sum_\nu \sum_{\sigma=1}^{3} \frac{\partial T^\nu_{\rho\sigma}}{\partial x_\sigma} a_\nu \bar{a}_\nu \\ &= \sum_\nu a_\nu \bar{a}_\nu F^\nu_\rho, \quad \ldots \ldots \quad (12) \end{aligned}$$

i. e., for a system in a state given by (11) the forces for the separate states are additive; their sum, when each is multiplied by the probability of the respective state, gives the total force. Suppose that on a system given by (11) we now have the perturbation H acting, which causes certain transitions of the given states to other states. Then the a_ν are functions of the time determined by the equations

$$\left.\begin{aligned} \frac{\partial a_\nu}{\partial t} &= -\frac{2\pi i}{h} \sum_\lambda H_{\nu\lambda} a_\lambda e^{\frac{2\pi i}{h}(E_\nu - E_\mu)t}, \\ H_{\nu\lambda} &= \int \bar{\psi}_\lambda H \psi_\lambda d\tau. \end{aligned}\right\} \quad \ldots \quad (13)$$

We form a set of tensors $T^{\mu\nu}_{\rho\sigma}$ according to (6) by giving the barred terms the index μ and the unbarred the index ν. Then each element of the tensor $T^{\mu\nu}_{\rho\sigma}$ has a time factor $e^{-\frac{2\pi i}{h}(E_\nu - E_\mu)t}$ when $T^{\mu\nu}_{\rho\sigma}$ contains only the spatial part of the wave function.

Then

$$\begin{aligned} F_\rho = \sum_{\sigma=1}^{3} \sum_{\mu\nu} \bar{a}_\mu a_\nu \frac{\partial T^{\mu\nu}_{\rho\sigma}}{\partial x_\sigma} e^{-\frac{2\pi i}{h}(E_\nu - E_\mu)t} \\ + \sum_{\mu\nu} \frac{\partial}{\partial t}\left(T^{\mu\nu}_{\rho 4} \bar{a}_\mu a_\nu e^{-\frac{2\pi i}{h}(E_\nu - E_\mu)t} \right). \quad \ldots \quad (14) \end{aligned}$$

We take the time average of (14) thus :

$$[F_\rho]=\sum_{\sigma=1}^{3}\sum_{\mu\nu}\left[\bar{a}_\mu a_\nu e^{-\frac{2\pi i}{h}(E_\nu-E_\mu)t}\right]\frac{\partial T^{\mu\nu}_{\rho\sigma}}{\partial x_\sigma}$$
$$+\sum_{\mu\nu}\left[\frac{\partial}{\partial t}\left(\bar{a}_\mu a_\nu e^{-\frac{2\pi i}{h}(E_\nu-E_\mu)t}\right)\right]T^{\mu\nu}_{\rho 4}, \quad . \quad (14\,a,$$

where the [ ] denote the time average. Compared with (12) we notice that the cross-terms $\mu\neq\nu$ give contributions now which are the parts of the force due to the transitions from the one state to the other. If we were to find K_ρ, the total force integral, according to (7 *a*), and if the states are all discrete with negative energy, then, as before, the first part of (14 *a*) vanishes when integrated. We then have

$$K_\rho=\int\left[\frac{\partial}{\partial t}\left(\bar{a}_\mu a_\nu e^{-\frac{2\pi i}{h}(E_\nu-E_\mu)t}\right)\right]T^{\mu\nu}_{\rho 4}\,d\tau, \quad . \quad (15)$$

which gives the total resultant force due to the perturbation. Suppose, for simplicity, that the vector potential ϕ_1, ϕ_2, ϕ_3 is zero; if we carry out the differentiations in (14 *a*), and using the wave equation, we get

$$[F_\rho]=\sum_{\mu\nu}\left[\bar{a}_\mu a_\nu e^{-\frac{2\pi i}{h}(E_\nu-F_\mu)t}\right]\bar{\psi}^\mu\frac{\partial V}{\partial x_\rho}\psi^\nu$$
$$+\left[e^{-\frac{2\pi i}{h}(E_\nu-E_\mu)t}\frac{\partial}{\partial t}(\bar{a}_\mu a_\nu)\right]T^{\mu\nu}_{\rho 4}$$

which clearly shows the contributions to the force due to the dependence of the a_ν on the time.

We can express the additional terms by means of the perturbation H to a first approximation. Let us suppose that initially the system is in only one state $\nu=0$; so that at $t=0$, $a_0=1$, $a_1=a_2=\ldots=0$.

Using this as a zero approximation we can solve (13) to a first approximation :

$$a_0=e^{-\frac{2\pi i}{h}H_{00}t} \quad \text{and} \quad a_\nu=\frac{e^{\frac{2\pi i}{h}(E_\nu-E_0)t}-1}{E_0-E_\nu}H_{\nu 0}, \quad \nu\geq 1.$$

Then

$$\bar{a}_0 a_0=e^{-\frac{2\pi i}{h}(H_{00}-\bar{H}_{00})t};$$

$$\nu\neq 0 : a_\nu\bar{a}_\nu=\frac{2\left(1-\cos\frac{2\pi}{h}(E_\nu-E_0)t\right)}{(E_0-E_\nu)^2}|H_{\nu 0}|^2;$$

$$\mu\neq\nu\neq 0: \left[\bar{a}_\mu a_\nu e^{-\frac{2\pi i}{h}(E_\nu - E_\mu)t}\right] = \frac{1}{(E_0-E_\nu)(E_0-E_\mu)}\bar{H}_{\mu_0}H_{\nu_0};$$

$$\left[a_0 a_\mu e^{-\frac{2\pi i}{h}(E_0-E_\mu)t}\right] = \frac{\bar{H}_{\mu_0}}{E_0-E_\mu}\left[e^{-\frac{2\pi i}{h}H_{00}t}\right].$$

The value of $\left[e^{-\frac{2\pi i}{h}H_{00}t}\right]$ is not necessarily zero, as H_{00} may be imaginary or complex. Hence from (14 *a*)

$$[F_\rho] = \left[e^{-\frac{2\pi i}{h}(H_{00}-\bar{H}_{00})t}\right]\frac{\partial T^{00}_{\rho\sigma}}{\partial x_\sigma}$$
$$+\left[-\frac{2\pi i}{h}(H_{00}-\bar{H}_{00})\,e^{-\frac{2\pi i}{h}(H_{00}-\bar{H}_{00})t}\right]T_{\rho 4}$$
$$+\sum_{\mu\neq 0} 2\,|\,\Re\,|\left\{\left[e^{-\frac{2\pi i}{h}H_{00}t}\right]\frac{\bar{H}_{\mu 0}}{E_0-E_\mu}\frac{\partial T^{\mu 0}_{\rho\sigma}}{\partial x_\sigma}\right.$$
$$\left.+\left[-\frac{2\pi i}{h}H_{00}e^{-\frac{2\pi i}{h}H_{00}t}\right]\frac{\bar{H}_{\mu 0}}{E_0-E_\mu}T_{\rho 4}\right\}$$
$$+\sum_{\mu\neq\nu}\frac{\bar{H}_{\mu 0}H_{\nu 0}}{(E_0-E_\nu)(E_0-E_\mu)}\frac{\partial T^{\mu\nu}_{\rho\sigma}}{\partial x_\sigma}$$
$$+\sum_{\mu}\frac{2}{(E_0-E_\mu)^2}|H_{\mu 0}|^2\cdot\frac{\partial T^{\mu\mu}_{\rho\sigma}}{\partial x_\sigma}. \quad . \quad . \quad . \quad . \quad . \quad (16)$$

If H_{00} is real, then we get (if the time average is over a sufficiently long period, depending on the value of H_{00})

$$[F_\rho] = \frac{\partial T^{00}_{\rho\sigma}}{\partial x_\sigma} + \sum_{0\neq\mu\leq\nu} 2\,|\,\Re\,|\frac{\bar{H}_{\mu 0}-H_{\nu 0}}{(E_0-E_\nu)(E_0-E_\mu)}\frac{\partial T^{\mu\nu}_{\rho\sigma}}{\partial x_\sigma}, \quad (16\,a)$$

the first term being the force density for the unperturbed system. To obtain the total force we can make the transformation (9 *a*). Then to this approximation we again get, if the system is only capable of discrete negative energy states,

$$K_\rho = \int [F_\rho]\,d\tau = 0.$$

For the problem of inelastic scattering, however, the integral of (16 *a*) gives a finite result; thus (using (8))

$$K_\rho = \frac{h^2}{8\pi^2 m}\int P^{00}_\rho\,df + \sum_{\nu\leq\mu\neq 0}\frac{h^2}{8\pi^2 m}\int (b_{\mu\nu}P^{\mu\nu}_\rho + b_{\nu\mu}P^{\nu\mu}_\rho)\,df, \quad (17)$$

where $b_{\mu\nu}$ is a transition probability

$$b_{\mu\nu} = \frac{H_{\mu 0} H_{\nu 0}}{(E_0 - E_\nu)(E_0 - E_\mu)}.$$

If the system be a bound electron and the perturbation such as to ionize the atom, then the second part of (17) will still give a certain finite value due to the force exerted by the ejected electron on the atom. We must, however, remember that (16 *a*) and (17) hold only if H_{00} is real. If it is imaginary then the additional terms in (16) must be taken into account.

In general we see that we can form a force matrix $F_\rho^{\mu\nu}$, and that the total force is the sum of the forces due to the various states and the transition forces $F_\rho^{\mu\nu}$, each multiplied by their respective probabilities.

In conclusion, I would wish to express my sincere thanks to Dr. F. Möglich for the many discussions he has given me on this subject.

CV. *On some definite Integrals involving Legendre Functions.* *By* N. G. Shabde, *Research Student, Mathematical Department, Edinburgh University* *.

Introduction.

In a recent paper †, the author has obtained some definite integrals involving Legendre functions. The object of the present note is to generalize some of the results given in this paper Also use is made of a theorem of MacRobert ‡ to evaluate an integral, the integration being with respect to the degree of the Legendre functions. Such integrals with respect to the degrees of the Legendre functions have been a subject of study in a recent paper § by MacRobert. As little is known regarding such integrals, it will be worth while studying such integrals.

* Communicated by the Author.

† Proc. Edin. Math. Soc. ser. 2, iv. part i. pp. 41–46. This paper will be referred to as (P. 1) in this note. I take this opportunity of stating that (3.3) of (P. 1) is also valid if $n > p+q+m$.

‡ Proc. Roy. Soc. Edin. li. part ii. (no. 16), pp. 116–126. This paper will be referred to as (P. 2). The theorem is given on p. 123.

§ Proc. Roy. Soc. Edin. liv. part ii. (no. 13), pp. 135–144.

§ 1.

If p and q are positive integers or zero, $\mathrm{R}(n)>0$, such that $p+q>0$, $p \geq q$, and $\mathrm{R}(n)<p-q$ or $>p+q$, then we have

$$\int_{-1}^{1} \mathrm{P}_p(\mu).\mathrm{P}_q(\mu).\mathrm{Q}_n(\mu)\,d\mu$$

$$= \sum_{r=0}^{q} \frac{\mathrm{A}_{p-r}.\mathrm{A}_r.\mathrm{A}_{q-r}}{\mathrm{A}_{p+q-r}}\left(\frac{2p+2q-4r+1}{2p+2q-2r+1}\right) \times \int_{-1}^{1} \mathrm{P}_{p+q-2r}(\mu).\mathrm{Q}_n(\mu)\,d\mu$$

$$= \sum_{r=0}^{q} \frac{\mathrm{A}_{p-r}.\mathrm{A}_r.\mathrm{A}_{q-r}}{\mathrm{A}_{p+q-r}}\left(\frac{2p+2q-4r+1}{2p+2q-2r+1}\right) \times \left[\frac{-1+\cos(n-p-q+2r)\pi}{(n-p-q+2r)(n+p+q-2r+1)}\right] \quad . \quad (1.1)$$

by means (5.1) of (P. 1). Here $\mathrm{A}_r = \dfrac{2^r(\frac{1}{2})_r}{r!}$, as in (P. 1).

Similarly, with the same restrictions on p, q, and n as in (1.1), we have

$$\int_{0}^{1} \mathrm{P}_p(\mu).\mathrm{P}_q(\mu).\mathrm{Q}_n(\mu)\,d\mu$$

$$= \sum_{r=0}^{q} \frac{\mathrm{A}_{p-r}.\mathrm{A}_r.\mathrm{A}_{q-r}}{\mathrm{A}_{p+q-r}}\left(\frac{2p+2q-4r+1}{2p+2q-2r+1}\right)\int_{0}^{1} \mathrm{P}_{p+q-2r}(\mu).\mathrm{Q}_n(\mu)\,d\mu$$

$$= \sum_{r=0}^{q} \frac{\mathrm{A}_{p-r}.\mathrm{A}_r.\mathrm{A}_{q-r}}{\mathrm{A}_{p+q-r}}\left(\frac{2p+2q-4r+1}{2p+2q-2r+1}\right) \times \frac{1}{(n-p-q+2r)(n+p+q-2r+1)} \times \left[-1+\frac{\Pi\left(\frac{p+q-2r}{2}\right)\Pi\left(\frac{n-1}{2}\right)}{\Pi\left(\frac{p+q-2r-1}{2}\right)\Pi\left(\frac{n}{2}\right)}\cos\left(\frac{p+q-2r-n}{2}\right)\pi\right] \quad . \quad . \quad . \quad . \quad (1.2)$$

by means of (5.3) of (P. 1).

§ 2.

MacRobert's Fourier-Legendre integral theorem in (P. 2) states that

"if $F(\lambda)=\int_p^q f(\phi).P_{\lambda-\frac{1}{2}}(\cos\phi)\sqrt{\sin\phi}\,d\phi,\ 0\leq p<q\leq\pi,$

then

$$2\int_0^\infty F(\lambda).\lambda.\sin(\pi\lambda).P_{\lambda-\frac{1}{2}}(-\cos\theta)\sqrt{\sin\theta}.d\lambda$$

$$=\begin{Bmatrix}\frac{1}{2}\{f(\theta+0)+f(\theta-0)\}. & p<\theta<q \\ 0\qquad\qquad , & 0<\theta<p \text{ or } q<\theta<\pi\end{Bmatrix}."$$

We use this theorem with the integral

$$\int_{-1}^1 P_m(\mu).P_n(\mu)\,d\mu=\frac{-1}{(m-n)(m+n+1)}$$

$$\times\left[\frac{4}{\pi^2}\sin m\pi.\sin n\pi\{\psi(m+1)-\psi(n+1)\}+\frac{2}{\pi}\sin(n-m)\pi\right]. \quad . \quad . \quad . \quad (2.1)^*$$

This result is valid if $m\neq n$ and $m+n+1\neq 0$. Putting $n=\lambda-\frac{1}{2}$ and taking m such that $-\frac{1}{2}<m<0$, we have

$$\int_{-1}^1 P_m(\mu).P_{\lambda-\frac{1}{2}}(\mu)\,d\mu=\frac{+1}{(m-\lambda+\frac{1}{2})(m+\lambda+\frac{1}{2})}$$

$$\times\left[\frac{4}{\pi^2}\sin m\pi\cos\lambda\pi\{\psi(m+1)-\psi(\lambda+\tfrac{1}{2})\}+\frac{2}{\pi}\cos(\lambda-m)\pi\right]. \quad . \quad . \quad . \quad (2.2)$$

Using the theorem stated above, we get

$$\int_0^\infty \lambda\sin\lambda\pi.P_{\lambda-\frac{1}{2}}(-\cos\theta)$$

$$\times\left[\frac{2}{(m-\lambda+\frac{1}{2})(m+\lambda+\frac{1}{2})}\left\{\frac{4}{\pi^2}\sin m\pi\cos\lambda\pi\right.\right.$$

$$\left.\left.\times\{\psi(m+1)-\psi(\lambda+\tfrac{1}{2})\}+\frac{2}{\pi}\cos(\lambda-m)\pi\right\}d\lambda\right]$$

$$=P_m(\cos\theta);\quad -<m<0 \text{ and } 0<\theta<\pi. \quad . \quad (2.3)$$

* Ganesh Prasad, "On Non-orthogonal System of Legendre Functions," Proc. Benares Math. Soc. xii. pp. 33–42 (1930).

CVI. *Notices respecting New Books.*

Ocean Waves and kindred Geophysical Phenomena. By Vaughan Cornish, D.Sc. With Additional Notes by Harold Jeffreys, M.A., D.Sc., F.R.S. [Pp. xvi+164.] (Cambridge University Press. 10*s.* net.)

As Dr. Vaughan Cornish explains in the preface to this work, some thirty years have had to elapse before a generation of mathematicians has arisen which is sufficiently free from the domination of classical hydrodynamics to warrant the publication of this volume of observational work on wave-forms. These researches, conducted with great patience, acumen, and open-mindedness follow, after a great lapse of time, the famous observations of John Scott Russell. In the interval little observational work seems to have been done, except for a few remarks by Kelvin on the formation of capillary waves and, fairly recently, the observations of Dr. H. Jeffreys on the generation of water-waves by wind and the experimental formation of the "Roll-wave." These last two topics are discussed in the present volume: the recognition of the roll-wave is, in fact, due to Dr. Cornish.

A large variety of wave-forms is dealt with. Nearly one-third of the book is devoted to observations of sea-waves, and the author's enjoyment of an Atlantic gale is an excellent illustration of Sir W. S. Gilbert's lines

> "But to him who's scientific
> There's nothing that's terrific . . ."

The second chapter deals with snow-waves and sand-waves. The former phenomenon is rather infrequently observed, but considering how familiar a sight sand-ripples are it is surprising that scientists have not devoted portions of their summer holidays to measuring the size and movement of these interesting corrugations.

The third and final chapter deals with the discharge of a progressive wave from a standing wave in the rapids of Niagara, the roll-waves formed in shallow regular rectangular channels, and tidal bores. The last-named comes in for a more thorough treatment than it has hitherto received; Dr. Cornish has been able to observe the *eagre* on the Trent progressively by using a motor-car to outstrip the bore between successive observation posts. He makes a strong plea for team-work, by a party of undergraduates for instance, in the systematic study of this phenomenon.

The volume is nicely rounded off with a set of notes by Dr. Jeffreys of a mathematical and physical character. These

are written in his usual lucid style, and it is most fitting that this task should have been entrusted to one who has done more than any one else to bridge the gap between classical wave-theory and modern observations.

Dr. Cornish's excellent literary style makes for pleasant reading, and the typographical set-out of the book reaches the high level that one has come to expect from the Cambridge University Press. The twenty-six beautiful photographs are so admirably reproduced that by themselves they would be worth the cost of the book. If this treatise did no more than to appeal mainly to the æsthetic sense of the scientist and the general reader its publication would be justified. The collection in one volume of such a wealth of observational material is a valuable service to science.

A Comprehensive Treatise on Inorganic and Theoretical Chemistry. By J. W. Mellor. [Vol. XIII. Fe (Part II.), pp. viii+948.] (Longmans, Green & Co. Price 63*s*.)

Volume XII. of Mellor's monumental work was largely devoted to iron: Volume XIII., entirely devoted to that element, has now appeared. A large part of it deals with the physical and mechanical properties of iron and iron-carbon alloys, including such matters as the stress-strain relationship and general tensile properties, the Brinell hardness and the effect of cold-work; the thermal properties, such as expansion and conductivity; the electrical properties, including the behaviour of the solid metal and of iron salts in solution; the spectral properties; and the magnetic properties. In addition, the interesting phenomenon of passivity is discussed in detail, as are the colloidal properties of sols and gels of hydrated ferric oxide, while a considerable section is devoted to the chemical properties of iron.

One is staggered by the mass of references, which, with the index, take up some 200 pages in this volume of 950 pages. There must be getting on for 20,000 papers cited. We are frequently confronted by the statement that such and such a property has been discussed by—here follows a string of seventy or a hundred names, followed in its turn by brief disconnected notes of what certain of these workers have done. There is relatively little guidance as to which work is sound and which is important. To expect a balanced discussion of details might well be asking too much, but we feel that a brief critical statement of the present position in each particular section would not be impossible, and would be very valuable to the reader trying to orient himself in a part of the subject with which he has not expert acquaintance.

The value of the book as a work of reference, however,

remains undoubted. Here is a systematized record of practically everything that has been published on the subjects in question. Even if some of the references, such as "Doktorarbeits" of German students, are inaccessible to the average worker, it is well that they should all be collected. By the time the reader has looked up the latest and most accessible papers he will probably, from references in them, have a fair idea of the contents of the remainder. Every physicist who has had recourse to "Mellor" in the past, and this must mean nearly all physicists, will welcome this latest step on the way to completion. We suppose that by the time the last volume appears the distinguished editor will be issuing a new edition of Volume I., on hydrogen and oxygen. There are certainly plenty of new things to say about hydrogen!

Analytical Geometry of Three Dimensions. By Professor D. M. Y. Sommerville, M.A., D.Sc., F.N.Z. Inst. [416 pp.] (Price 18*s.* net.)

It is a melancholy task that faces the reviewer of the above treatise, inasmuch as its talented author was cut off with tragic unexpectedness in his early fifties, at the height of his powers as an original investigator and lucid expositor. It is given to few to excel in both these domains, and this, his last book, was completed just before his lamented death.

The object of the treatise is not merely to present the standardized ground-work of Analytical Geometry of Three Dimensions from the standpoint of recognized examinations. Sommerville was deeply influenced by the newer work of the Italian geometers, and he attempts to introduce its spirit and some of its content to students. For this reason he not only deals with planes and quadrics, but with cubic surfaces and some types of quartic surfaces as well. He also gives the elementary properties of twisted cubics and of the two types of quartic curves in space of three dimensions. A long chapter is devoted to Line Geometry based on Plücker's Coordinates.

A good deal of the later chapters of the book is devoted to the geometry of hyperspace. Thus straight lines in ordinary space are represented as points on the intersection of a quadric with the absolute quadric in space of five dimensions. The surface of Veronese is also discussed.

It ought to be mentioned, however, that the avowed intention of the author is to deal only with Algebraic Geometry and not with Differential Geometry. These two subjects have usually been combined in the same book in the traditional elementary text-books on Solid Geometry.

Throughout the book Sommerville's treatment is full and lucid, and the student has ample opportunity of gaining glimpses of the peaks beyond. A good collection of examples is also provided.

Atomic Theory and the Description of Nature. By NIELS BOHR. [119 pp.] (Cambridge University Press. Price 6*s*.)

THIS book contains four essays, together with an introductory survey on the subject dear to Professor Bohr's heart.

The first essay is an elaboration of a lecture delivered at the Scandinavian Mathematical Congress at Copenhagen in August 1925, and surveys the development of the quantum theory up to and including the first developments of Heisenberg.

The second essay is the substance of a paper read to the Volta Centenary Meeting at Como in September 1927. It is entitled "The Quantum Postulate and Recent Development of Atomic Theory," and its main purpose is to show that the "feature of complementarity is essential for a consistent interpretation of the quantum-theoretical methods."

The third essay, on "The Quantum of Action and the Description of Nature," was contained in the jubilee pamphlet published in June 1929, in celebration of the fiftieth anniversary of Planck's doctorate. The distinguished author in this article discusses in some detail the general philosophical aspects of the quantum theory, including even those epistemological and psychological questions which naturally arise but are ordinarily regarded as being outside the purview of physics.

The fourth, and final, short essay is in essence a lecture given to the Scandinavian Meeting of Natural Scientists in 1929, and is entitled "Atomic Theory and the Fundamental Principles underlying the Description of Nature."

The new prospects opened up in regard to living organisms by the discovery of the quantum of action are here mentioned. The bulk of the essay, however, deals with various aspects of the now rather familiar replacement of the continuous causal description by a statistical mode.

Non-mathematical and general in treatment, Bohr's clarity and terseness of expression fill every page—an important little book.

[*The Editors do not hold themselves responsible for the views expressed by their correspondents.*]

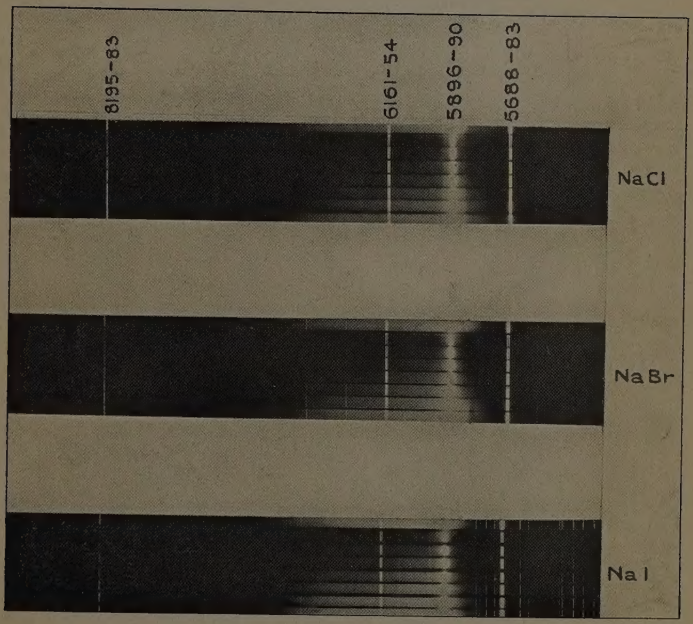

Emission spectra of the vapours of sodium halides.